NOVEL TREATMENT STRATEGIES FOR BREAST, LUNG AND CERVICAL CANCER

By
Mogammad Baahith Hamid

Thesis presented in fulfilment of the requirements for the degree of Doctor of Philosophy (Radiobiology) in the Faculty of Medicine and Health Sciences at Stellenbosch University

Supervisor: Professor John M Akudugu
Co-supervisor: Dr Antonio M Serafin

The financial assistance of the National Research Foundation (NRF) towards this research is hereby acknowledged. Opinions expressed and conclusions arrived at, are those of the author and are not necessarily to be attributed to the NRF.

December 2019

DECLARATION

By submitting this thesis electronically, I declare that the entirety of the work contained therein is my own, original work, that I am the authorship owner thereof (unless to the extent explicitly otherwise stated) and that I have not previously in its entirety or in part submitted it for obtaining any qualification.

Mogammad Baahith Hamid December 2019

Signature …….. Date ……

ABSTRACT

Cancer continues to be a global health burden, especially in the economically developing regions. The complex nature of this cancer contributes to a range of clinical challenges. Breast, lung and cervical cancer are known to have the highest incidence and mortality rates globally. Although many therapeutic options are available to treat cancer, the efficacy of most therapies is hindered due to normal tissue toxicity and tumour resistance. Novel treatment strategies are thus warranted to address clinical challenges and significantly improve patient outcomes. More than 50% of cancer patients receive radiotherapy throughout their illness. DNA damage resulting in cell death, as a consequence of ionising radiation exposure, has assisted in clinical tumour management. However, inherent and acquired resistance as well as the manipulation of essential pathways, like cell metabolism, have aided cancer cells to evade the toxic effects of radiotherapy. Increasing the therapeutic window of this treatment modality may benefit a large number of patients. There is evidence to suggest that ionising radiation may activate cell survival signalling pathways. Targeting the components of these pathways may modify cell metabolism and significantly radiosensitise cancer cells. Therefore, combining targeted therapy and ionising radiation may be a viable therapeutic strategy.

The objective of this study was to inhibit molecular targets of key pathways which regulate cell survival, and expose breast, lung, cervical cancer and normal cell lines to doses of radiation, so as to establish potential therapeutic targets that may be

amenable to combined modality therapy, and formulate a cocktail of inhibitors to evaluate its radiosensitising capability and effect on cellular metabolic activity.

In this study, clonogenic assays were performed to determine the relative sensitivity of 6 cell lines (cancer: MDA-MB-231 (breast), MCF-7 (breast), HeLa (cervix) and A549 (lung); apparently normal: L132 (lung) and MCF-12A (breast)) to ionising radiation and inhibitor therapy. Mathematic modelling was used to determine the mode of interaction between EGFR, PI3K/mTOR, and BcL-2 inhibitors, as well as, the modifying effects of inhibitors on the radiosensitivity and metabolic activity of the cell lines.

This study found that potential therapeutic benefit might be obtained by treating MDA-MB-231, MCF-7, HeLa and A549 cells with X-rays. The MCF-7 cell line showed the highest potential of therapeutic benefit with a greater than 2-fold higher radiosensitivity, relative to the normal MCF-12A cells. The A549 cell line showed the lowest potential for therapeutic benefit, when compared with the L132 cell line. Inhibition of PI3K and mTOR with NVP-BEZ235 resulted in a significant therapeutic benefit for the lung and cervical cancer cell lines, minor therapeutic benefit in the MCF-7 cell line, and no benefit for the MDA-MB-231 cell line. Bcl-2 inhibition with ABT-263 had either no effect on the MDA-MB-231 and A549 cell lines or resulted in potential therapeutic benefits for MCF-7 and HeLa cell lines. Pre-treatment of breast (MDA-MB-231 and MCF-7) and lung (A549) cancer cell lines with a cocktail of an EGFR (AG-1478), PI3K/mTOR (NVP-BEZ235), or Bcl-2 (ABT-263) inhibitors had an enhancing effect on radiosensitivity and cellular metabolic activity. The same

treatment provided radioprotection, and reduced the metabolic activity of the cervical cancer cell line, HeLa.

These findings suggest that concurrent inhibition of EGFR, PI3K, mTOR, and Bcl-2 during radiotherapy might improve the treatment response of breast and lung cancer in patients. Future studies validating these findings for lower inhibitor concentrations might be more relevant in the clinical setting, as systemic toxicity is a major concern. A study exposing cells to fractionated radiotherapy, after inhibitor pre-treatment, may further reveal the therapeutic potential of the inhibitors used in this study. Evaluating the effect of inhibitor pre-treatment and radiofrequency field, which have been shown to exhibit radiomodulatory effects on cancer and normal cell lines, may provide insight into the development of a novel therapeutic strategy.

OPSOMMING

Kanker is steeds 'n wêreldwye gesondheidslas, veral in die ekonomies ontwikkelende streke. Die ingewikkelde aard van kanker dra by tot 'n verskeidenheid kliniese uitdagings. Dit is bekend dat bors-, long- en servikale kanker wêreldwyd die hoogste voorkoms en sterftesyfers het. Alhoewel daar baie terapeutiese opsies beskikbaar is om kanker te behandel, word die doeltreffendheid van die meeste terapieë ingeboet weens normale weefseltoksisiteit en gewasweerstand. Nuwe behandelingsstrategieë sal dus in alle waarskynlikheid kliniese uitdagings aanspreek en pasiëntuitkomste beduidend verbeter. Meer as 50% van kankerpasiënte ontvang radioterapie regdeur hul siekte. DNA-skade as gevolg van blootstelling aan ioniserende bestraling, wat lei tot seldood, het gehelp met die beheer van kliniese gewasse. Inherente en verworwe weerstand en die manipulering van noodsaaklike paaie, soos selmetabolisme, het kankerselle egter gehelp om die giftige effekte van radioterapie te ontduik. Die vergroting van die terapeutiese venster van hierdie behandelingsmodaliteit kan moontlik 'n groot aantal pasiënte bevoordeel. Daar is bewyse wat daarop dui dat ioniserende bestraling selle se oorlewingseingewingpaaie kan aktiveer. Die teikening van die komponente van hierdie paaie kan selmetabolisme moontlik verander en kankerselle beduidend sensitiseer vir radioterapie. Daarom kan die kombinasie van geteikende terapie en ioniserende bestraling 'n haalbare terapeutiese strategie wees.

Die doel van hierdie studie was om molekulêre teikens van sleutelpaaie wat seloorlewing reguleer, te inhibeer, en bors-, long-, servikale kanker en normale

sellyne bloot te stel aan dosisse bestraling, om moontlike terapeutiese teikens daar te stel wat geskik is vir gekombineerde modaliteitsterapie, en 'n mengsel van inhibeerders te formuleer om die radiosensitiserende-vermoë en effek daarvan op sellulêre metaboliese aktiwiteit te evalueer.

In hierdie studie is klonogene ondersoeke uitgevoer om die relatiewe sensitiwiteit van 6 sellyne (kanker: MDA-MB-231 (bors), MCF-7 (bors), HeLa (serviks) en A549 (long) te bepaal; blykbaar normaal: L132 (long) en MCF-12A (bors)) tot ioniserende bestraling en inhibitorterapie. Wiskundige modellering is gebruik om die interaksiemodus tussen EGFR, PI3K / mTOR en BcL-2-inhibitors te bepaal, sowel as die modifiserende effekte van inhibitors op die radiosensitiwiteit en metaboliese aktiwiteit van die sellyne.

Hierdie studie het bevind dat potensiële terapeutiese voordele verkry kan word deur MDA-MB-231, MCF-7, HeLa en A549 selle met X-strale te behandel. Die MCF-7-sellyn het die grootste potensiaal vir terapeutiese voordele getoon met 'n meer as twee keer hoër radiosensitiwiteit, relatief tot die normale MCF-12A-selle. Die A549-sellyn het die laagste potensiaal vir terapeutiese voordele getoon in vergelyking met die L132-sellyn. Die inhibering van PI3K en mTOR met NVP-BEZ235 het 'n beduidende terapeutiese voordeel ingehou vir die long- en servikale kankersellyne, geringe terapeutiese voordele in die MCF-7-sellyn, en geen voordeel vir die MDA-MB-231-sellyn nie. Bcl-2-inhibering met ABT-263 het óf geen effek op die MDA-MB-231 en A549-sellyne gehad nie, óf dit het potensiële terapeutiese voordele vir MCF-7- en HeLa-sellyne ingehou. Voorbehandeling van bors- (MDA-MB-231 en MCF-7) en long(A549)-kankerselle met 'n mengsel van 'n EGFR (AG-1478), PI3K/mTOR (NVP-BEZ235), of Bcl-2 (ABT-263) inhibeerders het 'n verhoogde uitwerking op

radiosensitiwiteit en sellulêre metaboliese aktiwiteit gehad. Dieselfde behandeling het radiobeskerming en verlaagde metaboliese aktiwiteit van die servikale kankersellyn, HeLa, gebied.

Hierdie bevindings dui daarop dat gelyktydige inhibering van EGFR, PI3K, mTOR en Bcl-2 tydens radioterapie die behandelingsrespons van bors- en longkanker by pasiënte kan verbeter. Toekomstige studies wat hierdie bevindings vir laer inhibitorkonsentrasie bevestig, kan meer relevant in die kliniese omgewing wees, aangesien sistemiese toksisiteit 'n groot bron van kommer is. 'n Studie wat selle blootstel aan gefraksioneerde radioterapie, ná voorbehandeling van die inhibitor, kan moontlik die terapeutiese potensiaal van die inhibitors wat in hierdie studie gebruik is, openbaar. Evaluering van die effek van inhibitorvoorbehandeling en radiofrekwensieveld, wat getoon het dat dit radiomodulatoriese effekte op kanker en normale sellyne kan hê, kan insig bied in die ontwikkeling van 'n nuwe terapeutiese strategie.

Delineations

This study used inhibitors of EGFR, PI3K, mTOR and Bcl-2 to radiosensitise human cell lines (MCF-7, MDA-MB-231, MCF-12A, HeLa, A549, and L132). The expression levels of the selected targets in each cell line were not determined prior to inhibition, as these have been reported in several studies (Subik et al., 2010; Lida et al., 2011; Sundarraj et al., 2014; Hamunyela et al., 2015; Zhang et al., 2015).

The research variables determined in this study are intrinsic cellular radiosensitivity, the potential therapeutic effect of X-rays, cytotoxicity of specific inhibitors of EGFR, PI3K, mTOR and Bcl-2, the potential therapeutic effect of inhibitors, inhibitor interaction, radiomodulatory effects of inhibitors given either singly or in combination, and treatment effect on cellular metabolic activity.

The clonogenic survival, of the cell lines used in this study, was determined after X-ray irradiation to enable comparison of intrinsic cellular radiosensitivity and the potential therapeutic benefit of X-rays. Cytotoxicity of inhibitors was determined, using the colony assay to extract the equivalent concentration for 50% cell kill (EC_{50}) for each cell line. From this cytoxicity data, the combination indices were determined, and used to decipher the models by which inhibitors interacted with each other when combined in a cocktail. The EC_{50}-values had also been used to determine the potential therapeutic benefit of inhibitor treatment and guide subsequent radiomodulatory experiments in which radiation modifying factors which were derived to determine how a particular inhibitor or inhibitor cocktail impacted on cellular radiosensitivty. The effect of a particular inhibitor or inhibitor cocktail in combination

with X-ray irradiation had on cell metabolic activity had also been evaluated. The change in radiosensitivity due to inhibitor and X-ray treatment had been compared to the change in metabolic activity to determine if there may be a relation between these variables.

Limitations:

- This work only used six cell lines: two breast cancer cell lines (MDA-MB-231, MCF-7), one apparently normal breast cell line (MCF-12A), one cervical carcinoma cell line (HeLa), one lung cancer cell line (A549) and one apparently normal lung cell line (L-132).
- In section 3.6, the peculiarities in survival curves would produce unreliable α/β ratios, as a result of inhibitor pre-treatment. The mean inactivation dose ($\overline{D}$) of each survival curve had been used to derive the modification in radiosensitivity. To maintain uniformity the a/β ratios had also not be used in the parameters to determine the intrinsic radiosensitivity in section 3.1.
- The study investigated the effect of pre-treating 6 cell lines with an equivalent dose that would kill 50% of the cell population (EC_{50}) in combination with X-ray irradiation. Evaluating lower or higher concentrations of inhibitor may lead to varying modulatory results.

ACKNOWLEDGEMENTS

I would like to express my sincere appreciation and thanks to the following:

My parents, for all that they do and sacrifice so that I am able to pursue my dreams.

My supervisors, Professor John Akudugu and Dr Antonio Serafin, for their help, guidance, support and shared wisdom over the past 6 years. I have truly learnt a lot from them and would have not been able to complete my degree without them.

My colleagues for their friendship, assistance, motivation, and for creating a great working environment.

The Department of Medical Imaging and Clinical Oncology of the Faculty of Medicine and Health Science of the University of Stellenbosch.

I would also like to gratefully acknowledge the Department of Radiobiology of the Faculty of Medicine and Health Sciences at the University of Stellenbosch and NRF for their financial assistance.

DEDICATIONS

For their love and support I would like to dedicate this thesis to the following people:

My father Muhsien Hamit, My mother Shanaaz Gool-Hamit

My late grandfather Ameer Gool, My grandmother Aziza Gool

My grandfather Karriem Hamit, My late grandmother Fatima Hamit

My siblings:

Mogammad Ghusam Hamit

Mogammad Basheer Hamit

The Late Uncle Fuad Kagee, Aunty Khadija Kagee

Taariq Kagee

Mishkah Kagee

TABLE OF CONTENTS

LIST OF FIGURES

LIST OF TABLES

ABBREVIATIONS

Akt	Serine-threonine protein kinase
AREG	Amphiregulin
ATP	Adenosine triphosphate
α	Linear coefficient of cell inactivation
β	Quadratic coefficient of cell inactivation
Bak	Bcl-2 antagonist killer
Bax	Bcl-2-like protein 4
Bcl-2	B-cell lymphoma 2
Bcl-2-w	B-cell leukemia/lymphoma-w
Bcl-X_L	Bcl-2 lymphoma-extra large
BH3	B-cell homology 3
BTC	Betacellulin
cat	Catalogue
CI	Combination indices
cm^2	Centimetre squared
^{60}Co	Cobalt-60
°C	Degree Celsius
D_{50}	Equivalent dose of radiation to kill 50% of cell population
DMSO	Dimethyl Sulfoxide
DNA	Deoxyribose Nuclei Acid
EC_{50}	Equivalent concentration for 50% cell kill
EGF	Epidermal growth factor

EGFR	Epidermal growth factor receptor
EPGN	Epigen
ER	Oestrogen receptor
EREG	Epiregulin
FBS	Foetal bovine serum
Gy	Gray
HB-EGF	EGF-like growth
HER	Human epidermal growth factor receptor
HER-1/ erbB1	Human epidermal growth factor receptor 1
HER-2 /erbB2/Neu	Human epidermal growth factor receptor 2
HER-3/ erbB3	Human epidermal growth factor receptor 3
HER-4/ erbB4	Human epidermal growth factor receptor 4
(HIF)-1α	Hypoxia inducible factor alpha
HPV	Human papillomavirus
IC_{50}	Inhibitory concentration at 50%
IGF	Insulin growth factor
IGFR	Insulin growth factor receptor
IgG	Immunoglobulin G
Inc.	Incorporated
LET	Linear energy transfer
µl	Microliter
µg	Microgram
MF	Modifying factor

mg	Milligram
ml	Millilitre
mM	Millimolar
min	Minute
nm	Nanometer
nM	Nanomolar
mTOR	Mammalian target for rapamycin
mTORC1	mTOR complex 1
mTORC2	mTOR complex 2
mSIN1	Mammalian orthologue of Sin1
MTT	3-(4,5-Dimethylthiazol-2-yl)-2,5-Diphenyltetrazolium Bromide
NSCLC	Non-small cell lung cancer
OD	Optical density
PBS	Phosphate buffered saline
PIK3CA	Phosphatidylinositol-4,5-bisphosphate 3-kinase catalytic subunit alpha
PDK1	Phosphoinositide-dependent kinase 1
PI3K	Phosphoinositide 3-kinase
PIP_2	Phosphatidylinositol-4,5-biphosphate
PIP_3	Phosphatidylinositol-3,4,5-triphosphate
PKC	Protein kinase C
PR	Progesterone receptor
PTEN	Phosphatase and tensin homolog
RHEB	Ras homolog enriched in brain
REF	Radiation enhancement factor

RNA	Ribonucleic acid
RPM	Revolutions per minute
RPMI	Roswell Park Memorial Institute
RS	Relative sensitivity
S6K	S6 kinase
SCLC	Small cell lung cancer
SEM	Standard error of the mean
SF	Survival fraction
SF_2	Surviving fraction at 2 Gy
SF_6	Surviving fraction at 6 Gy
SGK	Serum glucose kinase
SREBP	Sterol regulatory element-binding protein
TGF-α	Transforming growth factor-α
TKIs	Tyrosine kinase inhibitors

CHAPTER 1

1.1. INTRODUCTION

Cancer remains a growing health burden worldwide. In 2018, an estimated 9.6 million cancer-related deaths and 18.1 million new cases had been predicted to occur (Bray et al., 2018). As the world's population continues to age and adopt unhealthy lifestyles, the incidence of cancer and cancer-related deaths are predicted to continue to climb (Jemal et al., 2011; Bray et al., 2018). Even though economically developed countries are experiencing lower incidence and mortality rates, the economically developing world, such as sub-Saharan Africa, has seen an increase in the incidence of cancer and cancer-related deaths (Jemal et al., 2011; Bray et al., 2018). Thus, cancer poses a significant health burden globally, especially in the developing regions.

There are various types of cancers, each developing and sustaining itself through unique biological processes. These processes bolster the complex nature of this disease and contribute to therapeutic challenges, and clinical outcomes can therefore range from very poor to excellent (Higgins et al., 2011; Misra et al., 2012). Although there are many therapeutic options available to treat cancer, most of these therapies have shortcomings as a consequence of high normal tissue toxicity and tumour resistance. New innovative treatment strategies are thus warranted, to address these clinical challenges.

Radiotherapy has been used for decades as the primary therapy for many types of cancers. More than 50% of all cancer patients receive radiotherapy throughout the

duration of their illness (Baskar et al., 2012). Exposing cancer cells to ionising radiation has proved effective in gaining control of tumour size as it invokes damage to cellular DNA and induces cell death (Pearce et al., 2001; Liang et al., 2003; Buchholz, 2009; Duru et al., 2012).

Radioresistant tumours constitute a significant clinical obstacle as they limit the effectiveness of radiotherapy (Duru et al., 2012; Li et al., 2012). Despite its benefits, radiotherapy is also damaging to normal tissue and, thus, many patients suffer from short-term and long-term side effects (Buchholz, 2009). A large number of patients would therefore benefit from any improvement in the efficacy of radiation therapy (Begg et al., 2011).

The discovery of biological markers essential for the regulation of cancer cell survival, has led to the development of target-based therapies that are highly specific, less invasive and less toxic than conventional treatment (Normanno et al., 2009). Unfortunately, treatment resistance, especially when single agents are used, is also a challenge for the efficacy of this treatment modality.

There is evidence to suggest that cellular exposure to ionising radiation may activate potential therapeutic components of the cell survival signalling pathways that may be implicated in resistance to targeted therapy (Contessa et al., 2002; Escriva et al., 2008; Chandarlapaty et al., 2012). It is also suggested that inhibiting these components may significantly radiosensitise cancer cells (Reisterer et al., 2004; No et al., 2009).

Taking the abovementioned into account, it can thus be reasoned that a viable therapeutic strategy for cancer management would be to combine targeted therapies with radiotherapy. The objective of this study was to develop potential therapeutic strategies, using radiotherapy in combination with agents that target specific cell signalling pathways which regulate certain hallmarks of cancer.

1.2. PROBLEM STATEMENT

Advancements in cancer treatment have led to improved patient response. However, optimal patient benefit remains mostly unattainable as various clinical challenges still exist (Misra et al., 2012). Inherent and acquired resistance to treatment, which increases the risk of tumour recurrence, are just two of these challenges (Higgins and Baselga, 2011; Hurvitz et al., 2013). The heterogeneous expression of target antigens is another clinical obstacle in targeted therapy, as this may result in the inability to effectively target malignant cells with toxic levels of a single agent. This phenomenon has been demonstrated for radiopharmaceuticals, chemotherapeutic drugs and radioimmunotherapeutics (Kvinnsland et al., 2001; Akudugu et al., 2011; Akudugu and Howell, 2012a). Treatment of most cancers with a single agent has, therefore, had limited success and novel treatment strategies are crucial in addressing these therapeutic challenges.

1.3. LITERATURE REVIEW

1.3.1. Cancer

Originating in the body, cancer is a somatic disease which is characterised by irregular cell proliferation and apoptosis (programmed cell death). Most cancers are thought to develop as a consequence of a series of DNA repair abnormalities which ultimately establishes a growth advantage for the clones of cancer cells in which these repair processes have occurred (Bamford et al., 2004). These cells possess the ability to be self-sufficient in growth signalling and insensitive to anti-growth signalling. Tumour cells generate their own growth signals so that they may be independent of growth stimulation from their normal tissue microenvironment. The dysregulation of growth signals and their respective receptors enable cancer cells to be hyper-responsive to growth stimuli that would normally not trigger their development. It allows these cells to remain independent from external growth factors. These characteristics assist in the ability of cancers to evade apoptosis and replicate continuously (Hanahan and Weinberg, 2000, 2011).

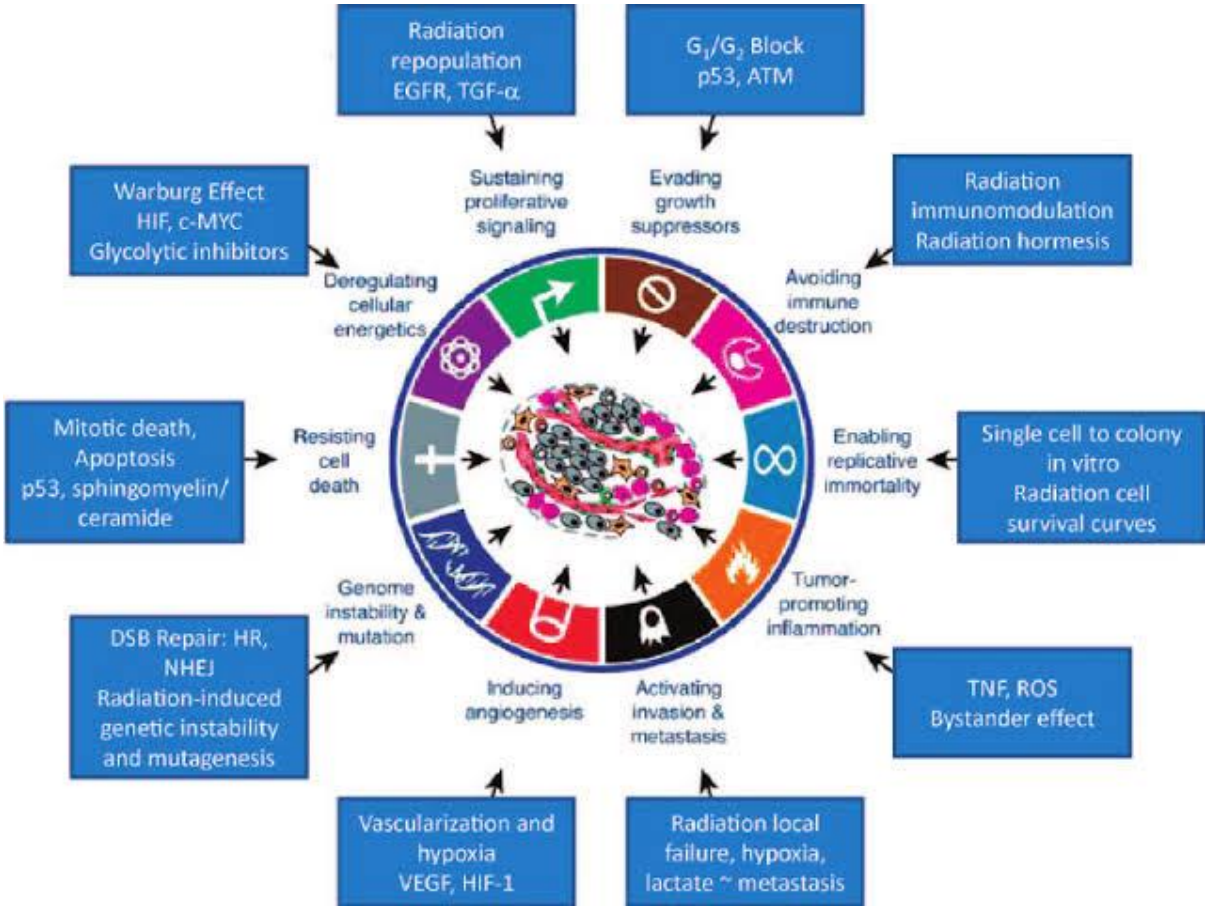

Figure 1.1: Hallmarks of cancer and the cellular responses invoked by exposing cancer cells to ionising radiation (Boss et al., 2014).

Many cancers may also sustain themselves through the initiation and development of new blood vessels (angiogenesis), which provide nutrients and oxygen. These cells may alter their energy metabolism to a state favouring the development of new cancer cells. Cancer cells are able to spread (metastasise) from their original location to other parts of the body or infiltrate the surrounding tissue (Hanahan and Weinberg, 2000, 2011). Figure 1.1 elucidates the self-sustaining characteristics of cancer and the cellular responses to ionising radiation. An example of this phenomenon would be the lethal DNA damage and p53 gene activation, caused by exposing these cells to ionising radiation, which may lead to programmed cell death.

This response to ionising radiation may be in conflict with the resisting cell death, evading growth factors and replicative immortality hallmarks of cancer (Boss et al., 2014).

Generally, there are more than 200 different types of cancers with characteristics dependent on their tissue of origin (Madani et al., 2011). Lung, breast and cervical cancer have the highest incidence and mortality rates globally (Bray et al., 2018). Thus, further evaluation of new therapeutic approaches for these cancers is warranted.

1.3.1.1. Breast Cancer

Breast cancer is the most commonly diagnosed cancer and the leading cause of cancer-related death among women worldwide (Bray et al., 2018). It accounts for one in every four cancer cases among females (Bray et al., 2018). This heterogeneous disease originates from the mammary gland epithelium and is categorised into various subtypes, with unique molecular profiles, which impact histopathological presentation and clinical responses (Perou et al., 2000; Park et al., 2012; Kondov et al., 2018). These subtypes are defined by the levels of expression of the oestrogen receptor (ER), progesterone receptor (PR), and the human epidermal growth factor receptor-2 (HER-2) on the membrane of the malignant cells, and the level of the Ki67 antigen expression (Kondov et al., 2018). There are five frequently used categories which sub-divide breast cancer, namely: luminal A, luminal B, HER-2 enriched, basal-like (triple negative), and normal breast cell-like.

Luminal breast cancers are the most frequently diagnosed subtypes (Kondov, et al. 2018). The luminal A subtype is commonly diagnosed in older patients. It is defined by positive ER and PR expression, a lower HER-2 expression, and a lower proliferative index (Ki67 < 14% expression). This subtype constitutes 50-60% of all breast cancers. Luminal A breast cancer is associated with good tumour differentiation, better treatment response and a lower risk of local recurrence or relapse. Thus, patients diagnosed with this subtype of malignant breast cancer have a better prognosis (van Diest et al., 2004; Carey et al., 2007; Vallejos et al., 2010; Yesral et al., 2014; Hashmi et al., 2018).

Luminal B breast cancer is commonly diagnosed in younger patients and constitutes 15-20% of all breast cancers. This subtype is characterised by positive ER and PR expression, a positive or negative HER-2 expression and a higher proliferative index (van Diest et al., 2004; Carey et al., 2007; Vallejos et al., 2010; Hashmi et al., 2018; Kondov et al., 2018). When compared to the luminal A subtype, luminal B breast cancer is more aggressive and is associated with poor tumour differentiation and poor patient prognosis (van Diest et al., 2004; Carey et al., 2007; Vallejos et al., 2010; Yesral et al., 2014; Hashmi et al., 2018).

The HER-2 enriched subtype is an aggressive non-luminal malignancy defined by HER-2 overexpression, a high proliferative index, negative ER and PR expression and a p53 mutation (Bacus et al., 1990; Goldhirsch et al., 2011; Kondov et al., 2018). This subtype also correlates with poor tumour differentiation, a poor clinical outcome and a low patient survival rate (Bacus et al., 1990; Goldhirsch et al., 2011; Kondov et al., 2018).

Devoid of ER, PR and HER-2 expression, the basal-like breast cancer subtype is an extremely aggressive carcinoma with the highest proliferative index, the worst patient prognosis and clinical outcome, and a higher risk of recurrence (Cheang et al., 2008; Leidy et al., 2014; Masood et al., 2016; Kondov et al., 2018).

The normal breast cell-like cancer subtype constitutes 5-10% of breast cancers. This subtype is poorly characterised and is said to be defined by its lack of ER, PR and HER-2 expression. The existence of this subtype has been questioned as some researchers believe that its discovery was due to a technical artefact from contamination with normal tissue during microarrays (Weigelt et al., 2010; Yersal and Baructa, 2014).

1.3.1.2. Cervical Cancer

Cervical cancer is ranked fourth of the cancers with the highest incidence and mortality rates globally, and is a rapidly growing burden in middle-low income countries, due to under-resourced health systems (Allemani et al., 2017; Ginsburg et al., 2017; Bray et al., 2018). Persistent infection by the human papillomavirus (HPV), immunosuppression and smoking are factors attributed to the development of cervical cancer (Allemani et al., 2017; Ginsburg et al., 2017). HPV oncogenic subtypes, HPV 16 and HPV 18, have been detected in most of the cervical cancer cases, and are thought to be the major contributing factors in its development (Colombo et al., 2012). There are three histological classifications of cervical cancer,

namely, squamous carcinoma, adenocarcinoma (glandular) and an undifferentiated carcinoma (Colombo et al., 2012).

1.3.1.3. Lung Cancer

The incidence of lung cancer is high and it is among the leading causes of cancer-related mortalities worldwide (Bray et al., 2018). There are two major histopathological types of lung cancer, namely, non-small cell lung cancer (NSCLC) and small cell lung cancer (SCLC). NSCLC constitutes 85-90% of lung cancer cases, of which ~40% are adenocarcinomas, ~25-30% are squamous cell carcinomas and ~10-15% are large cell carcinomas (Ginsberg et al., 2007; Novaes et al., 2008; Youlden et al., 2008; Lemjabbar-Alaoui et al., 2015). Lung cancer is a heterogeneous, highly invasive, extremely aggressive and rapidly metastasising carcinoma, and patients often present to the clinic at an advanced stage (Lemjabbar-Alaoui et al., 2015). These factors largely have a negative impact on patient prognosis and treatment outcome.

1.3.2. Cancer Therapy

Surgery, chemotherapy and radiotherapy have been used as the mainstay of cancer therapy for decades. Although the response to the various treatment modalities has been high, many patients still relapse years later, creating various therapeutic challenges (Karrison et al., 1999; Weckermann et al., 2001; Pfitzenmaier, et al. 2006; Aguirre-Ghiso, 2007). Radiotherapy is the focus of the investigation reported herein.

1.3.2.1. Radiotherapy

A typical form of radiation is energy (or photon) that travels and is emitted as it moves through its travel path. It forms part of a spectrum called the electromagnetic spectrum which categorises different forms of radiation in terms of energy, wavelength, or frequency (Kumar and Dangi, 2016). Clinical grade radiation possesses the highest energy, a short wavelength and the highest frequency on the electromagnetic spectrum. It is said to be ionising, since it charges (or ionises) the molecules it transfers the energy to, and possesses biologically hazardous properties (Kumar and Dangi, 2016). Figure 1.1 is an illustration of how ionising radiation interacts with atoms or molecules.

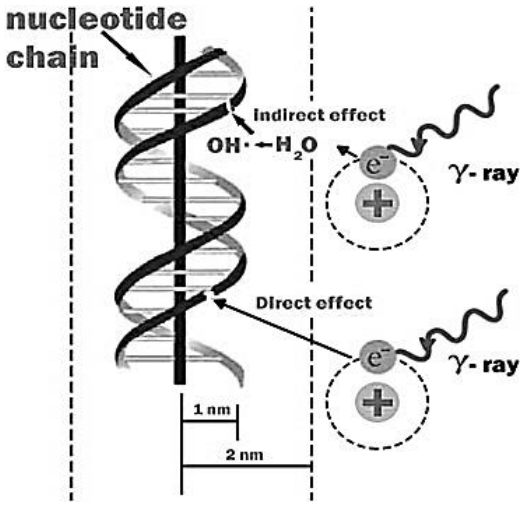

Figure 1.2: Ionising radiation (γ-rays) interacting with an electron, has direct or indirect effects on DNA (Desouky et al., 2015).

Ionising radiation, such as X-rays and gamma rays (γ-rays), deposits energy sparsely through its path, and is characterised as low linear energy transfer (LET)

radiation. However, high LET radiation, such as neutrons and α-particles, deposit energy in an abundant, more dense manner (Desouky et al., 2015). Radiation has a direct or indirect effect on its target. In Figure 1.1, ionising radiation ejects an electron and directly causes damage to the nucleotide chain (direct effect), or it causes radiolysis of a water molecule and the resultant reactive oxygen species causes a nucleotide chain break (indirect effect) (Desouky et al., 2015).

Direct cell injury is predominantly caused by high LET radiation and includes deoxyribonucleic acid (DNA), ribonucleic acid (RNA), lipid, and protein damage. Indirect damage is mostly caused by low LET radiation which, through its interaction with water, generates reactive oxygen species, especially superoxide and hydroxide radicals, which have an effect on DNA, RNA, lipids, and proteins, as well as, the intracellular signalling pathways (Rhee 1999; Rhee et al., 2003; Bubici et al., 2006; Hall and Giaccia, 2006; Naumov and von Sonntag, 2008).

DNA is the most critical target of radiation as it is vital to many cellular processes (Hutchison, 1966). Single- and double-strand breaks, along with nucleotide mutations occur during cellular exposure to ionising radiation. Double-strand breaks are the most lethal form of radiation damage, and may lead to mutagenesis or cell death, if not adequately repaired (Jonathan et al., 1999; Pollycove et al., 2003). Radiotherapy achieves therapeutic effect by inducing DNA damage and eventual cell death (Baskar et al., 2012). Evidence suggests that cancer cells produce more DNA breaks and repair damage at a slower rate than normal cells (Parshad et al., 1993; Shahidi et al., 2007; Mohseni-Meybodi et al., 2009; Shahidi et al., 2010). These

aspects, along with radiotherapy being non-invasive and cost-effective, make an attractive and effective treatment modality for cancer.

Radiotherapy is a highly effective cancer management tool and is used for curative or palliative care (Prise, 2006; Guadagnolo et al., 2013; Liauw et al., 2013). Ionising radiation is clinically applied in multiple fractions and is used throughout the course of treatment for a large majority of cancer patients (Bentzen, 2006; Durante and Loeffler, 2010; Baskar et al., 2012; Moding et al., 2013). Patients who have had incomplete tumour resections or patients who have recurrent tumours are mostly treated with radiotherapy, while for patients with inoperable tumours, radiotherapy may be the only option (Durante and Loeffler, 2010).

The response of tumours to radiation may be characterised according to the factors which influence the ability of ionising radiation to damage DNA, as well as, those that affect the DNA repair capacity of the tumour cell population (Brown and Brenner, 2013). Repair of sublethal cellular damage, repopulation of cells after ionising radiation exposure, redistribution of cells within the cell cycle, reoxygenation of the surviving cells and intrinsic radiosensitivity, are the factors used to determine the net effect of ionising radiation on tumours (Brown et al., 2014). For fractionated doses of ionising radiation, redistribution and reoxygenation assist cell kill, as radioresistant cells are redistributed into more radiosensitive states over time and oxygen acts as a radiosensitiser. However, DNA repair and repopulation may elicit an increase in cell survival, as these factors allow for the recovery of cells, as well as, the proliferation of surviving cells after each fraction of radiotherapy (Brown et al., 2014).

Although radiotherapy is a mainstay treatment for cancer, radioresistance remains one of the major therapeutic obstacles hindering its effectiveness. Hypoxia is a common characteristic of tumours. In this tumour environment, devoid of oxygen, damaged DNA is not readily complexed with oxygen molecules (i.e. the damage is not “fixed” by oxygen). Unfixed damage is readily repaired and more cells survive, thus enhancing tumour radioresistance (Wang et al., 2019). Cancer cells may also use a plethora of mechanisms to recover from the damaging effects of ionising radiation. Manipulating the tumour metabolism to provide sufficient energy and vital metabolites for DNA damage repair, regulating autophagy (self-eating) to protect damaged organelles, and cell cycle arrest to repair DNA damage, are a few examples of these phenomena (Tang et al., 2018). Radioresistance may lead to a poor prognosis, ultimately resulting in tumour recurrence and metastasis (Rycaj and Tang, 2014).

Tumour control probability (TCP) and normal tissue complication probability (NTCP) are models used in the clinic to describe the relationship between the dose of ionising radiation and probability of tumour control or normal tissue complication (Chargari et al., 2015). The equilibrium between these models has been suggested to provide an indication of the therapeutic index of a treatment modality (Beasely et al., 2005). The development of treatment strategies which improve the therapeutic index of radiotherapy by increasing TCP and decreasing NTCP are thus required to enable clinicians to design effective treatment regimens.

Exposure to ionising radiation activates the signal transduction pathways which confer treatment resistance through intrinsic or acquired biological processes

(Toulany and Rodemann, 2013). These signalling pathways may provide cancer cells with the means to evade cell death, through manipulating proliferation. An example is the survival pathway consisting of proteins such as the epidermal growth factor receptor (EGFR), phosphatidylinositol 3-kinase (PI3K) and the mammalian target of rapamycin (mTOR).

1.3.2.2. Targeted Therapy

The increasing understanding of the oncogenic process has driven the development of molecular target agents for cancer therapy. These drugs specifically target molecules that play critical roles in tumour growth, progression or cell survival.

Targeted therapy has many other options, such as, signal transduction inhibitors, gene expression modulators, apoptosis inducers, angiogenesis inhibitors, and immunotherapies. Although there are many options available, most targeted therapies are hindered by the development of treatment resistant cancer cells (Burris et al., 2013). Resistance to targeted therapy may be acquired through the loss of target expression which may occur as a result of continuous exposure to therapy and the activation of additional pathways that promote cell survival (Higgins and Baselga, 2011). The heterogenic distribution of target expression may contribute to target specific treatment resistance. The target antigen may be expressed at varying levels the single-cell level in a particular cell population. This may lead to the inability to effectively target all cells with a toxic level of a therapeutic agent. This phenomenon has been demonstrated for radiopharmaceuticals, chemotherapeutic drugs, and radioimmunotherapeutics (Kvinnsland et al., 2001; Akudugu et al., 2011; Akudugu

and Howell, 2012a, b). Variations in target morphology may also limit the effectiveness of targeted therapy. This has led to the search for more effective targets and treatment strategies.

Trastuzumab and lapatinib are two examples of clinically available targeted therapies that have become standard treatment for HER-2 positive breast cancer. Trastuzumab is a monoclonal antibody which targets the extracellular domain of the HER-2 receptor, and lapatinib is a tyrosine kinase inhibitor that targets the intracellular domain of HER-2 and epidermal growth factor receptor (EGFR) (Hurvitz et al., 2013). A change in antigen shape may make it difficult for this antigen-specific agent to bind to the relevant target and exert its toxic effect, as seen in breast cancer cells expressing truncated HER-2 (p95HER-2). Truncated HER-2 lacks the epitope for trastuzumab, which is found in the full length version of this receptor (Zagozdzon et al., 2011). Figure 1.2 shows how EGFR is involved in numerous vital cellular processes.

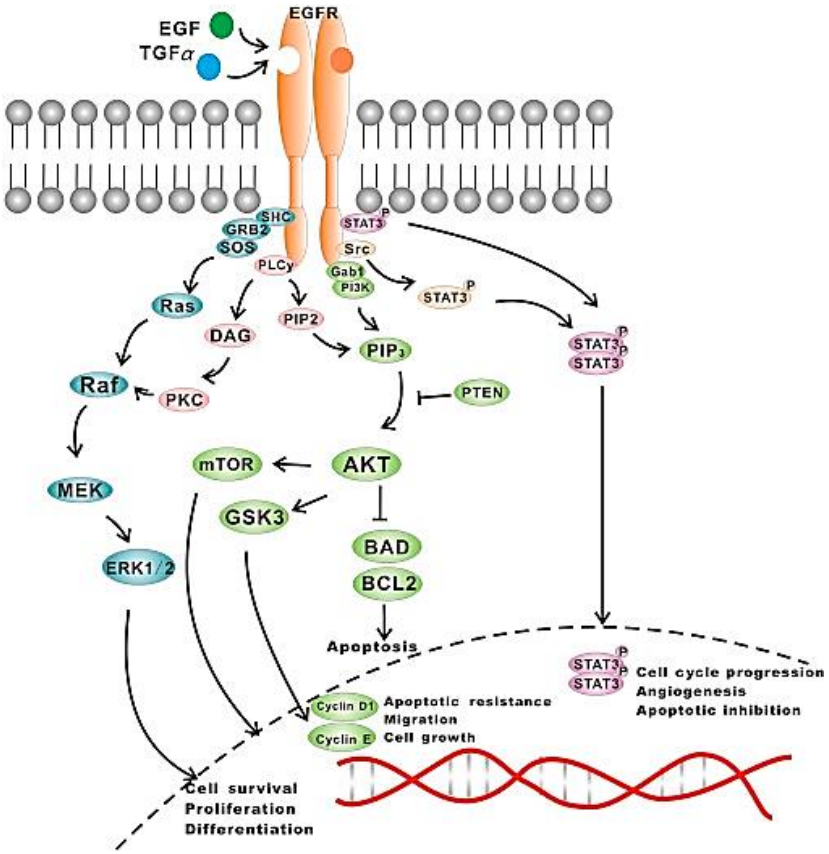

Figure 1.3: EGFR signalling pathway. Ligand binding activates the EGFR dimer, which transduces its activating signal to downstream pathways, thus regulating vital cellular protocols (Huang and Fu, 2015).

The EGFR is a membrane bound tyrosine kinase receptor which plays a major role in regulating downstream proteins, PI3K and mTOR. These proteins ultimately regulate signal transducers and transcription activators, impacting genes associated with cell survival and proliferation (Rodemann and Blaese, 2007; Rodemann et al., 2007). These pathways are said to regulate most of the self-sustaining hallmarks of cancer (Huang et al., 2000; Nyati et al., 2006). The PI3K-AKT-mTOR signalling pathway, a higher activated pathway in human tumours, is regarded as one the most challenging survival signalling pathways in cancer treatment resistance (Engelman, 2009; Castellano et al., 2011). Targeting these proteins with the appropriate inhibitors may be an effective strategy to manipulate cancer treatment resistance.

1.3.2.2.1. EGFR

Also known as HER1/ErbB1, EGFR is part of a four-member transmembrane tyrosine kinase family which also includes HER2 (ErbB2/Neu), HER3 (ErbB3), HER4 (ErbB4) (Higashiyama et al., 2008; Pines et al., 2010). The expression of EGFR in normal cells is estimated to be from 40 000-100 000 receptors per cell (Carpenter and Cohen, 1979). Activation of EGFR initiates signal transduction to a variety of downstream pathways which regulate cell proliferation, differentiation, survival, cell cycle progression, apoptosis inhibition, angiogenesis, invasion/metastasis, and other tumour promoting activities (Oda et al., 2005; Normanno et al., 2006; Black and Dinney, 2008; Uberall et al., 2008; Eccles, 2011; Mangelberger et al., 2012).

The structure of this receptor consists of an extracellular ligand binding domain, a dimerisation arm, an intracellular domain associated with tyrosine kinase activity and a C-terminal tail, which are involved in signal transduction (Higashiyama et al., 2008; Roskoski, 2014). The formation of homogeneous or heterogeneous dimers with itself and other members of its family is vital for the activation of EGFR (Lemmon et al., 2010). Ligand binding is crucial to EGFR activation and dimerisation. A number of ligands activate EGFR, namely, epidermal growth factor (EGF), transforming growth factor-α (TGF-α), amphiregulin (AREG), epiregulin (EREG), betacellulin (BTC), heparin-binding EGF-like growth factor (HB-EGF), and epigen (EPI) (Singh et al., 2016). EGF, TGF-α, HB-EGF and BTC are suggested to have a high-affinity for EGFR, whereas AREG, EREG and EPGN are thought to have a lower affinity (Singh, et al. 2016).

Ligand affinity has been shown to be affected by pH. It has been reported that EGF and TGF-α may bind to EGFR with similar affinities at a relatively neutral pH of 7.4, whereas, a slightly acidic pH (pH 6) leads to the dissociation of TGF-α from EGFR (French et al., 1995).

The ligands of juxtacrine, paracrine, and endocrine origins depend on the biological event that triggered their activation of EGFR. EGF production is typically locally controlled, as opposed to being delivered, as in the case of hormones, which allows different organs to elicit their own EGF-mediated response (Singh and Harris, 2005; Conte and Sigismund, 2016). Once EGF and related ligands have been released into the extracellular environment they begin to search for their cognate receptors, thereby, activating survival protocols (Massague and Pandiella, 1993; Sahin, et al. 2004; Li et al., 2012; Chen et al., 2017). Even though these ligands may activate EGFR in a similar manner, individual ligands cause distinct downstream biological responses (Graus-Porta et al., 1997; Singh and Harris, 2005).

EGFR ligand activation may occur through ligand binding, receptor dimerisation, receptor phosphorylation and the recruitment of signalling proteins or adaptors (Deurs, 2009). Ligand binding may also induce EGFR internalisation and transport to endosomes (Deurs, 2009). Active EGFR internalisation by endocytosis results in EGFR signal attenuation, and has been studied by many groups (Levkowitz et al., 1999; Goh et al., 2010; Sousa et al., 2012; Wang et al., 2015; Conte and Sigismund, 2016).

Generally, ligand activated EGFR leads to receptor dimerisation, transphosphorylation of the C-terminal tail and, finally, the propagation of the signal through signalling pathways to induce the expression of new genes. Ligand independent activation of EGFR occurs in EGFR mutations and truncated EGFR, which leads to the upregulation of oncogenesis.

The role of EGFR in oncogenesis has made it an essential therapeutic target. Two major classes of EGFR-targeted therapies have been developed. The first class includes monoclonal antibodies which target the EGFR extracellular domain, designed to block ligand binding or to mediate the downregulation of the receptor (Martinelli et al., 2009). Cetuximab (Erbitux) and panitimumab (Vectibix) are examples of US FDA approved monoclonal antibodies. The second class includes tyrosine kinase inhibitors (TKIs). TKIs are ATP mimetics that bind to the receptor's kinase pocket, which excludes ATP and prevents signal transduction (Paul and Mukhopadhyay, 2004). Approved TKIs include Erlotinib (Tarceva), Gerfitinib (Iressa), and Lapatinib (Tykerb).

Anti-EGFR therapy has been shown to improve survival in EGFR-positive cancer patients (Harandi et al., 2009). However, therapeutic challenges limit the effectiveness of EGFR inhibitors. The response to anti-EGFR therapy can be modified by factors, such as, the type of somatic EGFR mutations, EGFR gene amplification, increased autocrine EGFR ligands, and mutations in EGFR signalling pathway proteins (Modjtahedi and Essapen, 2009; Bertotti et al., 2015). Another challenge facing the use of EGFR inhibitors is that the duration of the response is often limited, and many tumours invariably develop resistance (Bertotti et al., 2015).

1.3.2.2.2. PI3K

The stimulation of EGFR through EGF binding leads to PI3K activation (Bjorge et al., 1990). The PI3K family is classified into three sub-groups. Each group is separated, characterised by its structure, regulation and function (Thorpe et al., 2015). Class I of PI3K is a downstream effector of EGFR, and is further sub-classified into IA (PI3Kα, β, δ), which is activated by receptor tyrosine kinases, and IB (PI3Kγ) which is triggered by G-protein-coupled receptors (Fruman and Cantley, 2002). Furthermore, PI3K consists of a regulatory subunit p85 that mediates binding to the receptor and a catalytic p110 domain, which phosphorylates the 3-OH group of the membrane lipid phosphatidylinositol-4,5-biphosphate (PIP_2), when PI3K is transported to the cell membrane, to generate phosphatidylinositol-3,4,5-triphosphate (PIP_3) (Whitman et al., 1988; Auger et al., 1989; Carpenter, et al. 1990; Zhao and Vogt, 2008). PIP_3 recruits phosphoinositide-dependent kinase 1 (PDK1) and serine/threonine kinase Akt at threonine 308 (Cantley, 2002; Alessi et al., 1997). Phosphorylated Akt propagates this signal by activating Ras homolog enriched in brain (RHEB), which enables the activation of mammalian target of rapamycin (mTOR) (Manning and Cantley, 2003).

In cancer, the PI3K signalling pathway located upstream of the mTOR complexes often consists of various mutations, such as the mutation and amplification of Akt and PIK3CA, and amplification of EGFR and insulin growth factor receptor (IGFR) (Guertin and Sabatini, 2007; Guertin et al., 2009; Liu et al., 2009). PI3K and Ras are parallel pathways, and amplification of growth factor receptors that are upstream of

either signal can also result in abnormal signal transduction on both mTOR complexes (Mayer and Arteaga, 2016).

1.3.2.2.3. mTOR

Mammalian/mechanistic target of rapamycin (mTOR) is a serine/threonine kinase which carries out its function through mTOR complex 1 (mTORC1) and mTOR complex 2 (mTORC2) which detect and consolidate cellular and environmental signals (Laplante and Sabatini, 2012; Saxton and Sabatini, 2017). These complexes regulate various stimuli, such as, nutrients, growth factors, energy, hormones and hypoxia. These complexes may also affect glucose metabolism through various mechanisms (Wullschleger et al., 2006; Laplante and Sabatini, 2012; Paquette et al., 2018).

The PI3K/Akt pathway plays a predominant role in the activation of mTORC1 (Zhang et al., 2007). mTORC1 phosphorylates downstream effectors, such as, eukaryotic translation initiation factor 4E binding protein 1 (4EBP1), S6 kinase (S6K), and sterol regulatory element-binding protein (SREBP), to encourage protein translation, synthesis of nucleotides and lipids, the recruitment of lysosomes and the suppression of autophagy (Ben-Sahra and Manning, 2017). mTORC1 may respond to fluctuations in cellular factors, such as, DNA damage, intracellular adenosine triphosphate (ATP), glucose, amino acids and oxygen. The p53 target genes are used by several pathways to suppress mTORC1 in response to DNA damage (Feng et al., 2005). They also promote the synthesis of proteins, lipids and nucleotides in aberrant cells, and tissue and organism growth in cancer (Azpiazu et al., 1996;

Peterson et al., 1999; Yokogami et al., 2000; Hudson et al., 2002; Huffman et al., 2002; Saxton and Sabatini, 2017). mTOR activation also leads to an increase in cell size and proliferation (Fingar et al., 2002; Dowling et al., 2010). mTORC2 is localised at the plasma membrane where it binds to the substrates, Akt, serum glucose kinase (SGK), and protein kinase C (PKC), through the mammalian orthologue of Sin1 (mSIN1) (Liu et al., 2015). This mTOR complex increases the rebuilding of the cytoskeleton and cell migration, inhibits apoptosis, and affects cell metabolism (Nobes and Hall, 1999). It also regulates cytoskeleton reorganisation and cell movement involved in tumour development (Jacinto et al., 2004; Sarbassov et al., 2004; Gan et al., 2012; Thomanetz et al., 2013).

mTOR signalling is enhanced in various types of cancers. This enhanced signal occurs in almost 30% of cancers and is one of the most frequently affected signalling pathways in cancer (Fruman and Rommel, 2014). Thirty-three mTOR mutations have been reported to contribute to the hyperactivation of mTOR signalling in cancer (Grabiner et al., 2014). mTOR activation in cancer depends on three mechanisms: mutations in the mTOR gene lead to a hyper-activated mTOR signalling pathway; mutations in mTORC1 and mTORC2 result in mTOR activation; an aberrant mTOR pathway may also be a consequence of mutations in upstream genes, loss-of-function mutations in tumour suppressor genes and gain-of-function mutations in oncogenes (Conciatori et al., 2018). This activation regulates the cell proliferation and metabolism involved in tumour initiation and progression. Its activation also leads to increased ribosome synthesis, which provides the equipment to maintain enhanced cell growth (Laplante and Sabatini, 2012).

In cancer, the metabolism is manipulated to maintain the demands of rapid cell growth. The mTOR complex has been depicted as a nutrient sensor in the metabolism of cancer, especially of glucose and amino acids, nucleotides, fatty acids, growth factors and other stresses. Nutrient sensing activates mTORC1 and the metabolic changes in cancer cells and, in turn, sustains mTORC1 activation (Saxton and Sabatini, 2017; Harachi et al., 2018; Paquette et al., 2018; Mossmann et al., 2018).

Glucose metabolism is used to provide energy for vital survival processes. mTORC1 can enhance the translation of two key transcription factors, namely, hypoxia inducible factor (HIF)-1α and Myc, which drive expression of a variety of glycolytic enzymes to regulate glycolysis (Majumder et al., 2004; Gordan et al., 2007; Duvel et al., 2010). Glucose metabolism may also be affected by mTORC2, through the activation of Akt (Elstrom et al., 2004). mTORC1 activates the critical transcription factor sterol regulatory element-binding protein 1 (SRE-BP1), driving gene transcription in lipid synthesis via Akt activation and phosphorylation of Lipin1 and S6K1 (Porstmann et al., 2008; Peterson et al., 2011). Synthesis of purine and pyrimidine, significant for cancer DNA replication, can be promoted by mTORC1, via S6K1 phosphorylation (Ben-Sahra et al., 2013, 2016).

mTOR is also involved in the regulation of autophagy, a process that degrades and recycles cytosolic components in response to a shortage of nutrients and energy. Autophagy is an inhibition process against tumorigenesis, and blockage of autophagy contributes to cancer initiation (White, 2015). mTOR involvement in these crucial cellular processes makes it a prime therapeutic target.

A study by Hamunyela and colleagues investigated whether treating low HER-2 expressing human breast cancer cells with a cocktail of specific inhibitors of HER-2, PI3K and mTOR, namely, TAK-165 and NVP-BEZ235, would sensitise these cells to ionising radiation, and demonstrated a 2-fold radiosensitisation (Hamunyela et al., 2015). In another study by Maleka and colleagues, the effect of pre-treating human prostate carcinoma and normal prostate cells with a cocktail of inhibitors targeting EGFR (AG-1478), and PI3K and mTOR (NVP-BEZ235) was investigated. It was found that while prostate cancer cells were radiosensitised, their normal counterparts were protected against the lethal effects of radiation when only PI3K and mTOR were inhibited with NVP-BEZ235 (Maleka et al., 2015). This could contribute to the development of a promising treatment strategy for prostate cancer, as NVP-BEZ235 pre-treatment radiosensitised prostate cancer cells and protected normal prostate cells against ionising radiation exposure.

1.3.2.2.4. BCL-2

Apoptosis is a form of programmed cell death initiated by various physiological and pathological stimuli. Apoptosis is morphologically characterised by cell shrinkage followed by the formation of cell fragments cleared by phagocytosis (Hengartner, 2000; Meng et al., 2006; Taylor et al., 2008). This cell death process involves the conversion of various signals into caspase-mediated intracellular protease activity (Earnshaw et al., 1999; Hengartner, 2000; Meng, et al., 2006). Figure 1.4 describes the intrinsic and extrinsic apoptotic pathways (Indran et al., 2011).

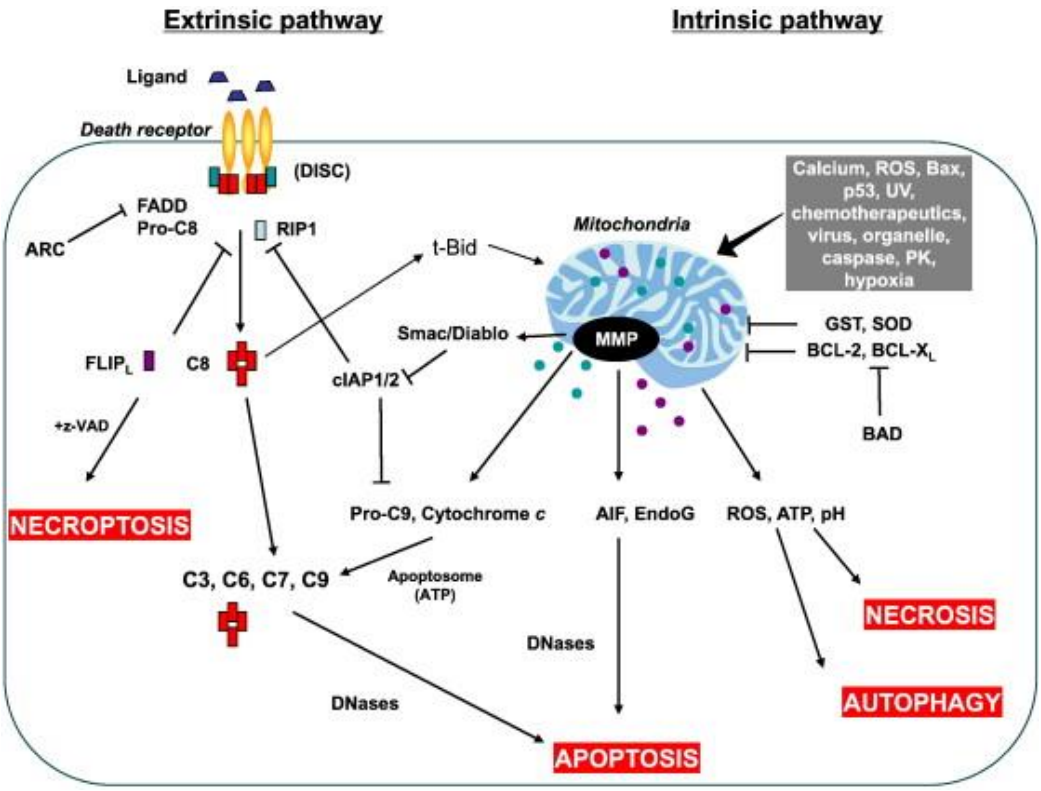

Figure 1.4: Description of intrinsic and extrinsic apoptotic pathways (Indran et al., 2011).

The leakage of cytochrome C into the cytoplasm is synonymous with the activation of the mitochondrial apoptotic pathway (Liu, et al. 1996; van Delft and Huang, 2006; Wang and Youle, 2009). This facilitates the recruitment of caspase 9 which activates the caspase cascade (Hengartner, 2000; Jiang and Wang, 2004; Taylor, et al. 2008).

Cytochrome C release from the mitochondria into the cytoplasm is regulated by the Bcl-2 protein family. This family consists of: (i) pro-apoptotic proteins, Bcl-2-like protein 4 (Bax) and Bcl-2 antagonist killer 1 (Bak), which regulate the permeabilisation of the mitochondrial outer membrane; (ii) anti-apoptotic family members, Bcl-2, B-cell lymphoma-extra large (Bcl-X_L), myeloid cell leukaemia-1 (Mcl-1), B-cell leukaemia/lymphoma-w (Bcl-w) and Bcl-2 A1, which mediate the impermeabilisation of the mitochondrial outer membrane; and (iii) pro-apoptotic B-

cell homology 3 (BH3)-only proteins, which promote apoptosis by binding to and oligomerising Bax and Bak or indirectly by neutralising anti-apoptotic family members (Strasser et al., 2011; Czabotar et al., 2014; Moldoveanu et al., 2014; Renault and Chipuk, 2014).

The overexpression of anti-apoptotic proteins, Bcl-2 and Bcl-X_L, has been reported to occur in a variety of tumours (Krajewski et al., 1997; Olopade et al., 1997; Scheinder et al., 1997; Pena et al., 1999; Trask et al., 2002). Resistance to radiotherapy and chemotherapy and poor treatment response have also been associated with enhanced levels of Bcl-2 and Bcl-X_L (Minn et al., 1995; Reed et al., 1996; Simonian et al., 1997; Gallo et al., 1999; Ong et al., 2001).

The survival proteins mentioned above play an essential role in cancer cell propagation and response to radiotherapy. Targeting these proteins with specific targeted therapy may assist in manipulating cancer cell radiosensitivity, and using these treatment modalities in combination may improve treatment outcomes.

1.3.2.3. Combination Therapy

In combination therapy, one molecule may improve the action of another by increasing its penetration or preventing its destruction (Reece et al., 2007). A two-fold rationale has been suggested for the use of concomitant therapy. Firstly, when multiple drugs with different targets are applied, the process of cancer cells adapting to therapy can be delayed. Secondly, multiple drugs targeting the same cellular

pathway could function synergistically for higher therapeutic efficacy and higher target selectivity (Lee and Nan, 2012).

The combination of inhibitors and radiotherapy may compensate for the activation of survival signals after ionising radiation exposure elucidated in Section 1.3.2.1. Therefore, this study aimed to investigate whether a cocktail of targeted therapies can be used to target proteins pertinent to cancer hallmarks, to increase the radiosensitivity of cancer cells so that radiotherapy may be used to eliminate these cells.

1.3.3. Cell Metabolism

Cell metabolism is a term used to summarise the network of biochemical processes used by the cell to fulfil its various biological functions (DeBerardinis and Thompson, 2012; Metallo and Vander Heiden, 2013; Fernandez-de-Cossio-Diaz and Vazquez, 2018). Metabolism may be categorised into anabolic and catabolic processes (Metallo and Vander Heiden, 2013). Anabolic metabolism constitutes the building of macromolecules such as lipids and proteins. Catabolic metabolism constitutes the breaking down of molecules, such as the carbohydrate and glucose, to produce energy (Gomes and Blenis, 2015).

An important hallmark of cancer cells, is the reprogramming of these processes to adapt to changes in their microenvironment and support their high metabolic activity requirements (Wellen and Thompson, 2010; Hanahan and Weinberg, 2011; Anastasiou, 2017; Muir et al., 2017).

Cell metabolism has also been suggested to play a role in DNA damage through the production of reactive oxygen species (Turgeon et al., 2018). This process has also been implicated in assisting DNA repair, as it produces metabolites which play an essential role in DNA structure and stability (Turgeon et al., 2018).

The aberration of the survival PI3K-Akt-mTOR pathway has been suggested to assist cancer cells in manipulating metabolic activity to support the dysregulated development of these cells, previously elucidated in Section 1.3.2.2.3.

Thus, monitoring the metabolic activity after treatment could provide insights into the cellular metabolic response to treatment and the cells' ability to repair damage.

1.4. HYPOTHESIS AND OBJECTIVES

It is clear that improving the efficacy of radiotherapy and minimising its related normal tissue toxicity would be beneficial for a large percentage of cancer patients. Identification and manipulation of components of pathways which regulate the self-sustaining hallmarks of cancer cells could overcome treatment resistance. The studies reported here sought to formulate combined treatment modalities that would target more than one of these components to effectively inhibit them and enhance the radiosensitivity of a selection of cancer cell lines. It is, therefore, hypothesised that inhibiting the activity of EGFR, PI3K, mTOR, and Bcl-2 can significantly sensitise cancer cells to ionising radiation and that this sensitising effect could correlate with a change in metabolic activity.

To test this hypothesis, the specific study objectives are as follows:

1. To determine the intrinsic radiosensitivity of a panel of breast, lung, and cervical cancer cell lines.
2. To evaluate the effect of an EGFR, mTOR, PI3K, and BcL-2 inhibitors on the survival of the panel of cell lines in Objective 1.
3. To evaluate potential interaction between inhibitors in the panel of cell lines in Objective 1.
4. To investigate the effects of a combination of inhibitors and X-rays on the panel of cell lines in Objective 1.

5. To determine the effect of inhibitors and X-ray therapy on metabolic activity of the panel of cell lines in Objective 1.

CHAPTER 2

2. MATERIALS AND METHODS

2.1. Study Location and Ethical Consideration

All experiments were performed in the Division of Radiobiology, Faculty of Medicine and Health Sciences, Stellenbosch University, Tygerberg. The study was approved by the Health Research Ethics Committee (HREC) of the Faculty of Medicine and Health Sciences, Stellenbosch University, South Africa (HREC Reference #: X19/02/003; Appendix A).

2.2. Cell Lines

2.2.1. MCF-7

MCF-7 is a human mammary adenocarcinoma-derived cell line established from a metastatic lesion. MCF-7 is classified as a luminal A breast cancer subtype (Subik et al., 2010). It has an epithelial-like morphology, is adherent and grows as a monolayer in Roswell Park Memorial Institute medium (RPMI-1640) (Sigma-Aldrich, USA, cat # R8758), supplemented with 10% heat-inactivated foetal bovine serum (FBS) (HyClone, UK, cat # SV30160.03), penicillin (100 U/ml) and streptomycin (100 µg/ml) (Lonza, Belgium, cat # DE17-602E). A frozen vial of cells was obtained from Professor S. Prince (University of Cape Town, South Africa). MCF-7 was used between passages 7-17 for all experiments.

2.2.2. MDA-MB-231

MDA-MB-231 is a human mammary adenocarcinoma-derived cell line established from a metastatic lesion. MDA-MB-231 is classified as a basal-like breast cancer subtype (Subik et al., 2010). It has an epithelial-like morphology, is adherent and grows as a monolayer in RPMI-1640 medium (Sigma-Aldrich, USA, cat # R8758), supplemented with 10% heat-inactivated foetal bovine serum (HyClone, UK, cat # SV30160.03), penicillin (100 U/ml) and streptomycin (100 µg/ml) (Lonza, Belgium cat # DE17-602E). The cells were obtained from Professor S. Prince (University of Cape Town, South Africa). MDA-MB-231 was used between passages 59-69 for all experiments.

2.2.3. MCF-12A

MCF-12A is a non-tumour-forming breast cell line derived from the excised breast tissue of a postmenopausal nulliparous female who had been diagnosed with a fibrocystic breast disease and had undergone a reduction mammoplasty (Sweeney et al., 2018; Paine et al., 1992), and was used to represent normal tissue for breast and cervical cancer. It has an epithelial-like morphology, is adherent and grows as a monolayer in Dulbecco's modified Eagle's medium / Nutrient Formulation F-12 HAM (Lonza, Belgium, cat # BE12-719F). This pre-constituted liquid growth medium was supplemented with 15 mM HEPES, 0.365 g/L L-glutamine, 1.2 g/L sodium bicarbonate, 20 ng/ml human epidermal growth factor (Sigma-Aldrich, Germany), 0.01 mg/ml bovine insulin (Sigma-Aldrich, Germany), 500 ng/ml hydrocortisone (Sigma-Aldrich, Germany), 10% heat-inactivated foetal bovine serum (HyClone, UK,

cat # SV30160.03), penicillin (100 U/ml) and streptomycin (100 µg/ml) (Lonza, Belgium, cat # DE17-602E). The cells were obtained from Professor AM Engelbrecht (Stellenbosch University, South Africa). MCF-12A was used between passages 30-40 for all experiments.

2.2.4. HeLa

HeLa is a cervical cancer cell line derived from an adenocarcinoma of the cervix (Korch and Varella-Garcia, 2018; Lucey et al., 2009). It has an epithelial-like morphology, is adherent and grows as a monolayer in McCoy's 5A medium (Sigma-Aldrich, USA, cat # M9309), supplemented with 10% heat-inactivated foetal bovine serum (HyClone, UK, cat # SV30160.03), penicillin (100 U/ml) and streptomycin (100 µg/ml) (Lonza, Belgium cat # DE17-602E). The cells were a gift from Professor E. van Helden (Stellenbosch University, South Africa). HeLa was used between passages 8-18 for all experiments.

2.2.5. A549

A549 is a human adenocarcinoma cell line derived from human lung cancer tissue (Yamagata et al., 2018). It has an epithelial-like morphology, is adherent and grows as a monolayer in RPMI-1640 medium (Sigma-Aldrich, USA, cat # R8758), supplemented with 10% heat-inactivated foetal bovine serum (HyClone, UK, cat # SV30160.03), penicillin (100 U/ml) and streptomycin (100 µg/ml) (Lonza, Belgium cat # DE17-602E). The cells were purchased from Cellonex (Johannesburg, South

Africa, cat # CA54-C). A549 was used between passages 101-110 for all experiments.

2.2.6. L132

L132 is a human pulmonary epithelial cell line (Jin et al., 2019), and was used to mimic normal tissue for lung cancer. It has an epithelial-like morphology, is adherent and grows as a monolayer in RPMI-1640 medium (Sigma-Aldrich, USA, cat # R8758), supplemented with 10% heat-inactivated foetal bovine serum (HyClone, UK, cat # SV30160.03), penicillin (100 U/ml) and streptomycin (100 µg/ml) (Lonza, Belgium cat # DE17-602E). These cells were retrieved from the liquid nitrogen storage of the Division of Radiobiology (Department of Medical Imaging and Clinical Oncology, Stellenbosch University). L132 was used between passages 22-32 for all experiments.

2.3. Cell Culture Maintenance

All cell cultures were kept at 37ºC in a humidified atmosphere of 95% air and 5% CO_2 in SHEL LAB incubators (Sheldon Manufacturing Inc., USA), and procedures were carried out in vertical laminar flow cabinets using aseptic techniques. Cells were routinely grown in 75 cm^2 flasks and passaged at a cell culture confluency of 80 to 90%. For cryopreservation, cells were trypsinised, pelleted by centrifugation (4000 RPM for 5 minutes), resuspended in a mixture of 0.9 ml foetal bovine serum and 0.1 ml of dimethyl sulfoxide (DMSO) (Sigma-Aldrich, USA, cat # 41640) stored at -80°C overnight, and then transferred to liquid nitrogen for use at a later stage.

2.4. Irradiation of Cell Cultures

Cell culture irradiation was performed using a Precision MultiRad 160 X-irradiator (Precision X-Ray Inc., Branford, CT, USA) at the Division of Radiobiology (Faculty of Medicine and Health Sciences, Stellenbosch University). Samples were irradiated at a source-to-sample distance of 65 cm, measured to the base of the experimental flasks, at a dose rate of 1.0 Gy/min. For this, build-up also consisted of 5-10 ml of medium in the 25 cm^2 culture flasks. In all cases, cell cultures were irradiated at room temperature (22ºC).

2.5. Clonogenic Cell Survival Assay

To determine the relative radiosensitivities of the breast cancer cell lines used in this study, clonogenic cell survival assays were performed. Near-confluent stock cultures were washed with sterile phosphate buffered saline (PBS) (Lonza, Belgium, cat # 17-512F) trypsinised, and the cells counted using a haemocytometer. Cells were then seeded in triplicate per experiment in 25 cm^2 tissue culture flasks at numbers ranging from 200 - 10 000 per flask, depending on radiation absorbed dose, and left to settle for 3-5 hours before being exposed to ionising radiation. Cells were irradiated to graded doses ranging from 0-10 Gy. After an appropriate incubation period (usually 7-14 days), the colonies were fixed by decanting the medium in the flask, and replacing it with 10 ml of fixative, and a mixture of glacial acetic acid, methanol and water in a ratio 10:10:8 v:v:v, for 10 minutes. The fixative was then decanted and replaced with 10 ml of Amido Black stain, consisting of 10 ml of 0.01% Amido Black in 1 litre of fixative. The colonies were left to stain for 10 minutes. The

stain was then decanted, and the flasks left to dry. The colonies were counted using a dissection microscope. The means (± SD) of the surviving fractions (*SF*) for three experiments were plotted against the irradiation dose, and cell survival curves obtained by fitting the data to the linear-quadratic survival equation:

$$SF = \exp[-\alpha D - \beta D^2] \qquad (2.1),$$

where α and β are the linear and quadratic cell inactivation constants, respectively, and D is the dose in Gy (Cornforth and Loucas, 2019; Fertil et al., 1984). Radiosensitivity of cell lines was expressed in terms of the surviving fraction at 2 Gy (SF_2), the surviving fraction at 6 Gy (SF_6), absorbed dose for 50% cell killing (D_{50}), and the mean inactivation dose ($\overline{D}$). $\overline{D}$ is the area under the cell survival curve and depicts radiosensitivity over low-high doses.

2.6. Target Inhibitors

Three inhibitors, AG-1478, NVP-BEZ235 and ABT-263, which targeted vital cell survival proteins, namely EGFR, PI3K, mTOR and Bcl-2, were used in this study.

2.6.1. AG-1478

AG-1478 is an epidermal growth factor receptor (EGFR) kinase inhibitor with an IC_{50} of 3 nM in non-small cell lung cancer cells (Shi et al., 2018; Puri and Salgia, 2008; Levitzki and Gazit, 1995). AG-1478 has a molecular weight of 352.22 and a chemical

formula of $C_{16}H_{14}ClN_3O_2HCl$ (Tocris Bioscience, UK, cat # 1276) and depicted structurally in Figure 2.1.

For this study, a stock solution of 9.5 mM of AG-1478 was reconstituted in dimethyl sulfoxide (DMSO) and stored at -20ºC until needed.

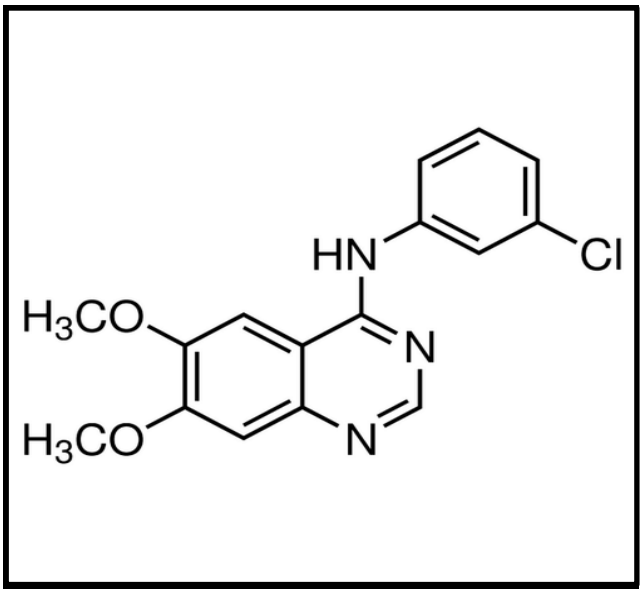

Figure 2.1: Chemical structure of AG-1478.

2.6.2. NVP-BEZ235

NVP-BEZ235 is a dual phosphoinositide-3-kinase (PI3K) and mammalian target of rapamycin (mTOR) inhibitor with an inhibitory concentration for 50% inhibition of p110δ activity and an IC_{50} of 7 nM (Maira et al., 2008). Biochemically, NVP-BEZ235 reversibly inhibits class 1 PI3K catalytic activity by competing for its ATP-binding sites. It also inhibits mTOR catalytic activity but does not target other protein kinases (Maira et al., 2008). NVP-BEZ235 has a molecular weight of 469.55 and chemical

formula $C_{30}H_{23}N_5O$ (Santa Cruz Biotechnology, Texas, USA, cat # 364429), and is soluble in DMSO. Figure 2.2 is an illustration of the chemical structure of NVP-BEZ235.

For this study, a stock solution of 106 mM NVP-BEZ235 was reconstituted in dimethyl sulfoxide and stored at -20ºC until needed.

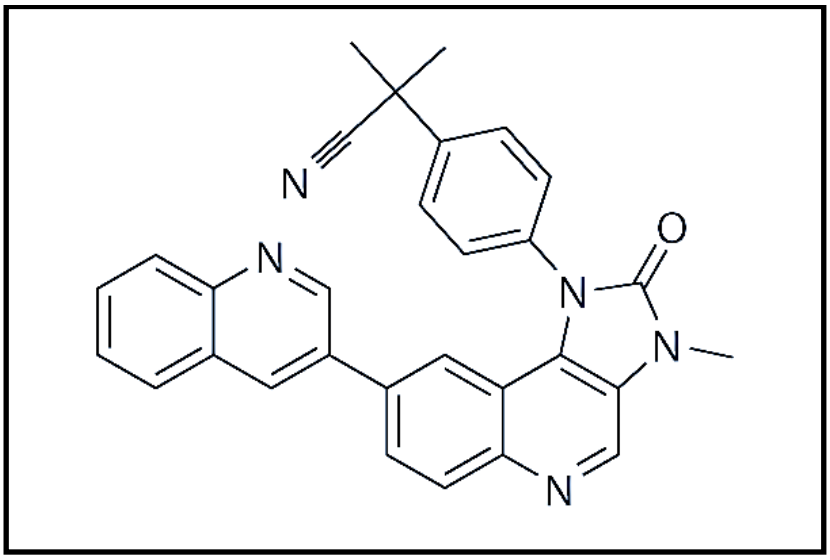

Figure 2.2: Chemical structure of NVP-BEZ235.

2.6.3. ABT-263

ABT-263 ($C_{47}H_{55}ClF_3N_5O_6S_3$; MW = 974.61; a gift from the Chemotherapeutic Agents Repository of the Drug Synthesis and Chemistry Branch, National Cancer Institute, USA)(Abcam, UK, cat # ab218114), depicted structurally in figure 2.3, is a Bad-like BH3 mimic for Bcl-2, Bcl-xl, and Bcl-w, with an IC_{50} of < 1nM (Tse et al., 2008). ABT-263 disrupts Bcl-2/Bcl-xL interactions with pro-death proteins, leading to induced apoptosis within 2 hours after treatment. More so, in human cancer cells,

ABT-263 induces Bax translocation, Cytochrome C release, and subsequent apoptosis (Bajwa et al., 2012).

For this study, the stock solution consisted of 0.955 mM of ABT-263, in DMSO, and was stored at -20ºC until needed.

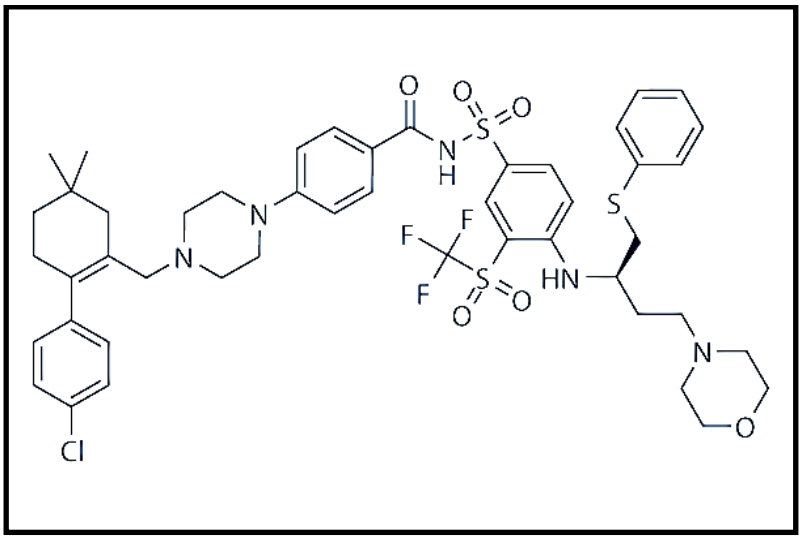

Figure 2.3: Chemical structure of ABT-263.

2.7. Target Inhibitor Toxicity Measurements

Single-cell suspensions were seeded (200-4000 cells per flask) into 25 cm^2 tissue culture flasks and incubated for 3-4 hours to allow the cells to attach. To assess the influence of inhibitor concentration on cytotoxicity, cells were exposed to AG-1478 (0.06-50 µM), NVP-BEZ235 (0.6-34 nM) and ABT-263 (0.3-10000 nM), then incubated for 7-14 days for colony formation. After this incubation period, the colonies were fixed, stained, washed in tap water, air-dried, and counted. To

determine the equivalent concentration of each inhibitor for 50% cell kill (EC_{50}), the surviving fractions (SF) were plotted as a function of log(inhibitor concentration) and were fitted to a 4-parameter logistic equation of the form:

$$SF = B + \frac{T-B}{\{1-10^{[(logEC_{50}-D)HS}\}} \quad (2.2),$$

where *B* and *T* are the minimum and maximum of the sigmoidal curve, respectively, *D* is the log(inhibitor concentration), and *HS* is the steepest slope of the curve. Three independent experiments were performed for each cell line and dose point.

2.8. Evaluation of Therapeutic Potential

To assess whether the various treatment protocols (X-rays or inhibitors) used in this study had a potential therapeutic benefit, a relative sensitivity (*RS*) was determined. For this, the D_{50} and EC_{50} of the normal cell lines (L132 for lung; MCF-12A for breast and cervix) were compared with those for the respective tumour cell lines (A549 for lung; MDA-MB-231, MCF-7, HeLa for breast and cervix), according to Maleka et al., (2019), as follows:

$$RS = \frac{D_{50}(normal)}{D_{50}(tumour)} \ or \ \frac{EC_{50}(normal)}{EC_{50}(tumour)} \quad (2.3).$$

The criteria for potential therapeutic benefit, no potential benefit, and no potential benefit with possible undesirable effects of each agent are $RS>1.0$, $RS=1.0$ and $RS<1.0$, respectively.

2.9. Effect of Inhibitors on Radiation Response

Radiosensitisation induced by inhibitors, AG-1478, NVP-BEZ235 and ABT-263, added 30 minutes prior to irradiation was assessed by clonogenic assay in each cell line. Cells were seeded in 5 or 10 ml of cell line specific medium at numbers ranging from 200-8000 per 25 cm^2 flask. The flasks were incubated at 37ºC for 4-5 hours to allow the cells to settle before administration of a corresponding EC_{50} dose of inhibitor, as determined in Section 2.7, followed by exposure to a dose of X-rays ranging from 2-8 Gy. The flasks were then re-incubated until colony formation had occurred. Exposure to the inhibitor was for the duration of the experiment. After an incubation period of 7-14 days, colonies were fixed, stained, and counted. The corresponding surviving fractions were calculated. Unirradiated cell cultures, with and without inhibitors, served as controls. Three independent experiments were performed for each cell line and dose point.

The modulatory effect of inhibitors on radiosensitivity was expressed as a survival modifying factor ($MF_{survival}$), given as the ratio of the mean inactivation dose ($\bar{D}$) in the absence and presence of inhibitor:

$$MF_{survival} = \frac{\bar{D}(X-rays)}{\bar{D}(inhibitor+X-rays)} \qquad (2.4).$$

The criteria for inhibition, no effect, and enhancement of radiosensitivity by inhibitors are $MF<1.0$, $MF=1.0$, and $MF>1.0$, respectively.

2.10. Inhibitor Interaction

To test for potential interaction between inhibitors, the toxicity data obtained in Section 2.7 were fitted to the function:

$$log(f_a/f_u) = m \times log(D) - m \times log(D_m) \qquad (2.5),$$

where f_a and f_u are the affected and unaffected fractions of cells, respectively, to generate median-effect plots for each inhibitor. D is the concentration of inhibitor, D_m is the median-effect concentration of inhibitor, and the coefficient m is an indicator of the shape of the inhibitor concentration-effect relationship (Chou, 2006; Hamunyela et al., 2017). The shape parameter m = 1, >1, and <1 for hyperbolic, sigmoidal, and flat-sigmoidal inhibitor concentration-effect curves, respectively.

The mode of interaction between any two inhibitors was assessed by determining combination indices (CI) for each inhibitor cocktail from the fitted parameters of equation (2.3) according to the equation:

$$CI = \frac{D_1}{\left\{D_{m1} \times \left(\frac{f_{a1}}{1-f_{a1}}\right)^{\frac{1}{m_1}}\right\}} + \frac{D_2}{\left\{D_{m2} \times \left(\frac{f_{a2}}{1-f_{a2}}\right)^{\frac{1}{m_2}}\right\}} \qquad (2.6),$$

where D_1 is the concentration of Inhibitor 1 and D_2 is the concentration of Inhibitor 2. m_1 and m_2 are the respective shape parameters. f_{a1} and f_{a2} are given as: (1 – SF, as defined in equation (2.2)). D_{m1} and D_{m2} are the corresponding median-effect concentrations. Synergism, additivity, and antagonism are indicated by CI < 1, CI =

1, and *CI* > 1, respectively. Furthermore, the criteria for very strong synergism, strong synergism, and synergism are *CI* < 0.1, 0.1 ≤ CI ≤ 0.3, 0.3 < CI ≤ 0.7, respectively (Chou, 2006).

2.11. MTT Assay

The 3-(4, 5-dimethylthiazol-2-yl)-2, 5-diphenyltetrazolium bromide (MTT) assay was used to determine the effect of the various treatment protocols used in this study on the metabolic activity of the MCF-7, MDA-MB-231, MCF-12A, HeLa, L132 and A549 cell lines.

For this, cells were seeded in quadruplicate in 96-well plates (Corning, USA), that had been treated for cell culture, at 100 000 cells per well and incubated at 37ºC for 4-5 hours. After incubation, the cells were either given a 2-Gy dose of X-rays (a clinically relevant single fraction), or treated with an EC_{50} concentration of inhibitor, or a combination of inhibitors, or a combination of an EC_{50} concentration of inhibitor and irradiation. After treatment, the cells were incubated for 0.5, 2, 24, and 52 hours. These time points were chosen in order to assess early, intermediate, and late changes in cellular metabolism. After incubation, 100 µl of MTT (Sigma, USA, cat # M2128) (dissolved in PBS to a concentration of 50 mg/ml) was added to each well in a darkened laminar flow cabinet, whereupon the plates were wrapped in foil and re-incubated at 37ºC for 4 hours. One hundred microlitres of DMSO was added to each well, and the absorbances (optical densities, OD; blank subtracted) read at 570 nm on a microplate spectrophotometer (Labtech International, Sussex, UK; Model #: LT-4000) ten minutes later as a measure of metabolic activity.

The mean absorbances in samples treated with X-rays only were compared to those obtained for the growth medium controls (OD_{2Gy}/OD_{medium}) to give radiation induced relative metabolic activities. Similarly, the ratios of mean absorbances in samples treated with combinations of X-rays and inhibitors to those obtained for the inhibitor controls ($OD_{2Gy+inhibitor}/OD_{inhibitor}$) were determined as combination treatment induced relative metabolic activity. The ratios of the former to the latter (or modifying factors) were then derived to represent the mode by which the inhibitors modified metabolic activity in irradiated cells. The criteria for a reduction, no effect, and an enhancement in metabolic activity in irradiated cells by inhibitors are $MF>1$, $MF=1$, and $MF<1$, respectively.

2.12. Data Analysis

Statistical analysis and data fitting were performed by means of GraphPad Prism (GraphPad Software, San Diego, USA). The unpaired two-sided Student's *t*-test was used to compare two data sets. A $P < 0.05$ indicates a statistically significant difference between the data sets. Data were presented as the mean ± SEM of three independent experiments. Where necessary, errors were determined using appropriate error propagation formulae. For associations, linear regression analyses were used.

CHAPTER 3

3. RESULTS

3.1. Intrinsic Radiosensitivity

Figure 3.1 shows the resultant cell survival curves for three human breast cell lines (MDA-MB-231, MCF-7 and MCF-12A), following X-ray exposure. To evaluate the intrinsic radiosensitivity of these cell lines, the surviving fraction at 2 and 6 Gy (SF_2 and SF_6), the dose at which 50% of the cell population is killed (D_{50}), and the area under the curve ($\bar{D}$) were extrapolated from these survival curves and summarised in Table 3.1.

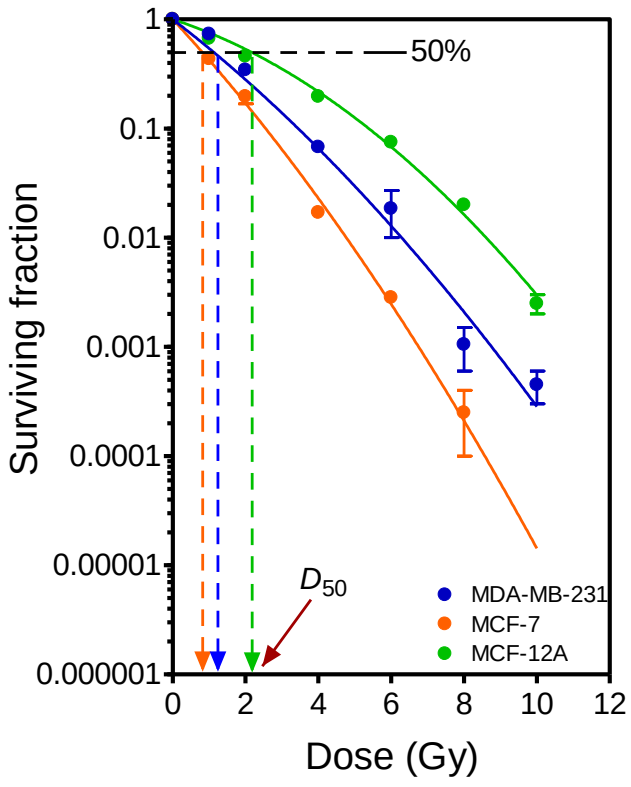

Figure 3.1: Clonogenic cell survival curves for 3 human breast cell lines after X-ray irradiation. Symbols represent the mean surviving fraction ± SEM from three independent experiments. Survival curves were obtained by fitting experimental data to the linear-quadratic model. The dose at which 50% of cells survive (D_{50}) is the dose at which each survival curve intersects the horizontal dashed line.

Based on all parameters, the rank order of increasing radiosensitivity in the breast cell lines was found to be MCF-12A<MDA-MB-231<MCF-7.

Table 3.1: Summary of radiobiological parameters for the 6 human cell lines. SF_2 and SF_6 denote the surviving fraction at 2 and 6 Gy, respectively. $\overline{D}$ denotes the mean inactivation dose (area under the cell survival curve). D_{50} the radiation absorbed dose for 50% cell killing. Data are presented as the mean ± SEM from 3 independent experiments.

Cell Lines	SF_2	SF_6	D_{50} (Gy)	$\overline{D}$ (Gy)
MDA-MB-231	0.28±0.02	0.010±0.003	1.14±0.07	1.93±0.03
MCF-7	0.17±0.03	0.003±0.000*	0.82±0.11	1.33±0.13
MCF-12A	0.52±0.04	0.067±0.001	2.11±0.09	2.56±0.11
HeLa	0.33±0.07	0.040±0.000*	1.24±0.03	1.95±0.03
A549	0.54±0.05	0.068±0.01	2.20±0.23	2.87±0.05
L132	0.67±0.06	0.066±0.03	2.79±0.26	3.11±0.03

*errors less than 0.001.

The survival curves for the two human lung cell lines (L132 and A549) and a cervical carcinoma cell line (HeLa) are shown in Figure 3.2. The cervical cancer cell line was more radiosensitive at doses less 8 Gy, but shows higher radioresistance at doses

greater than 8 Gy. Overall, the parameters ranked these cell lines in order of increasing radiosensitivity as HeLa<A549<L132 (Table 3.1).

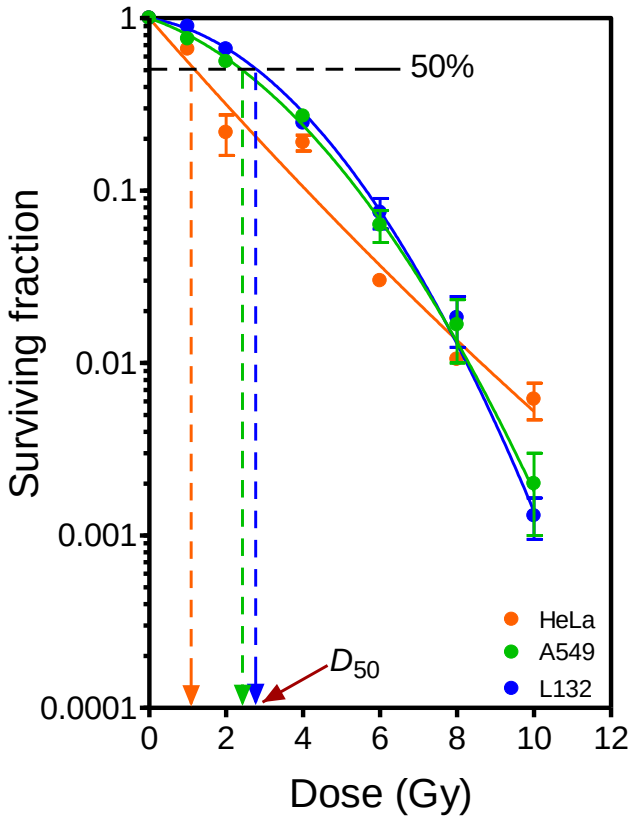

Figure 3.2: Clonogenic cell survival curves for 2 lung cell lines and a cervical cancer cell line after X-ray irradiation. Symbols represent the mean surviving fraction ± SEM from three independent experiments. Survival curves were obtained by fitting experimental data to the linear-quadratic model. The dose at which 50% of cells survive (D_{50}) is the dose at which each survival curve intersects the horizontal dashed line.

Given the inconsistency in radiosensitivity ranking when a single radiobiological parameter is used, it is necessary to consider using multiple parameters to obtain a more representative reflection of relative cellular radiosensitivity. For this, a rank order was constructed based on SF_2, SF_6, D_{50}, and $\bar{D}$, as presented in Table 3.2. Using the frequency of occurrence of each cell line under each rank, the cell lines

may be arranged in order of increasing radiosensitivity as: L132 → A549 → MCF-12A → HeLa → MDA-MB-231 → MCF-7.

Table 3.2: Arrangement of the studied panel of cell lines from most radioresistant to most radiosensitive, according to the extrapolated parameters.

Parameters	**Increasing Radiosensitivity** →					
SF_2	L132	A549	MCF-12A	HeLa	MDA-MB-231	MCF-7
SF_6	A549	L132	MCF-12A	HeLa	MDA-MB-231	MCF-7
D_{50}	L132	A549	MCF-12A	HeLa	MDA-MB-231	MCF-7
$\overline{D}$	L132	A549	MCF-12A	HeLa	MDA-MB-231	MCF-7

3.2. Therapeutic Potential of X-rays

To determine whether treatment of the cancer cell lines with X-rays has a potential therapeutic benefit, the relative sensitivities (*RS*), as described in Section 2.8, were determined on the basis of the D_{50}-values. The data presented in Table 3.3 summarise the relative radiosensitivities of the tumour cells. The *RS*-values in Table 3.3 suggest that potential therapeutic benefit may be derived from treating MDA-MB-

231, MCF-7, HeLa and A549 cells with X-rays. MCF-7 showed the highest potential of therapeutic benefit with a greater than 2-fold relative sensitivity. The lung cancer cell line, A549, showed the lowest potential for therapeutic benefit.

Table 3.3: Summary of D_{50}-values for 3 human breast cell lines (normal: MCF-12A; cancer: MCF-7, MDA-MB-231), 2 human lung cell lines (normal: L132; cancer: A549), and a cervical cancer cell line (HeLa). Their relative radiosensitivities (*RS*), determined by clonogenic cell survival, after exposure to X-rays (Equation 2.3). *RS*-values were derived by comparing the D_{50}-values of the normal cell lines (MCF-12A and L132) to those of the tumour cell lines (MCF-7 and MDA-MB-231) and (A549 and HeLa), respectively.

Cell Line	D_{50} **(Gy)**	***RS****
MCF-12A	2.11±0.09	−
MDA-MB-231	1.14±0.07	1.85 ± 0.13
MCF-7	0.82±0.11	2.57 ± 0.37
L132	2.79±0.26	-
A549	2.20±0.23	1.27 ± 0.18
HeLa	1.24±0.03	1.70 ± 0.08

*Errors were calculated using error propagation formulae for ratios.

3.3. Inhibitor Cytotoxicity

3.3.1. Cytotoxicity of AG-1478, NVP-BEZ235 and ABT-263 in Breast Cell Lines

Treating the human breast cell lines with inhibitors induced a concentration-dependent cell kill (Figure 3.3-3.5). From these sigmoidal graphs and summary of data in Table 3.4, NVP-BEZ235 emerged as more potent than ABT-263 and AG-1478 in all cell lines. The least toxic of this inhibitor panel was observed to be AG-1478.

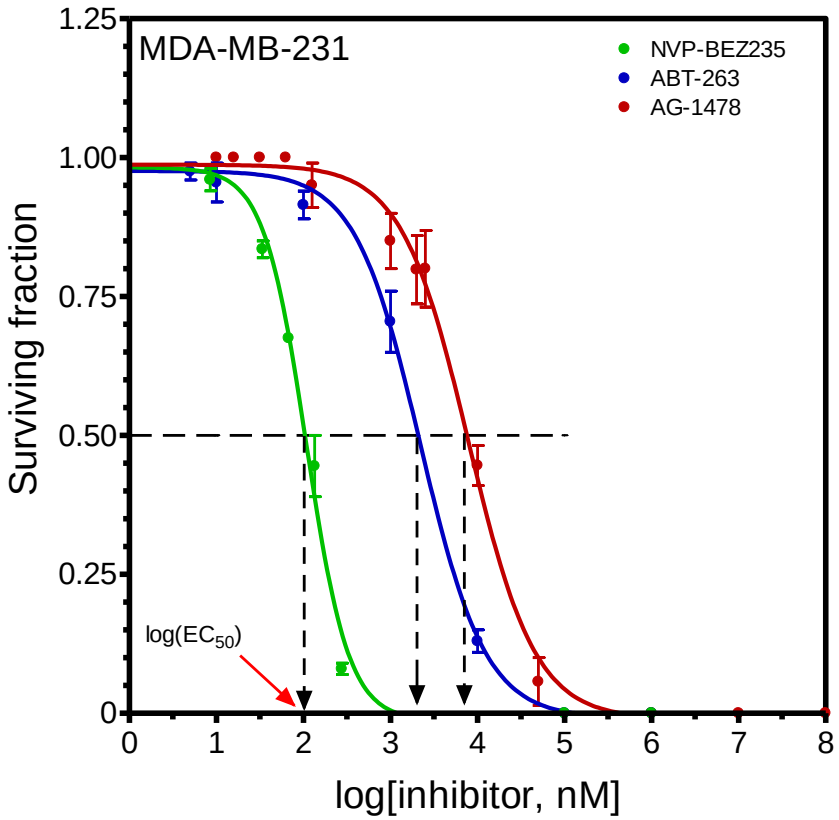

Figure 3.3: Cytotoxicity curves for an EGFR inhibitor (AG-1478), a PI3K and mTOR inhibitor (NVP-BEZ235), and a Bcl-2 inhibitor (ABT-263) for the triple negative human breast cancer cell line, MDA-MB-231. Curves were obtained by plotting the cell survival as a function of log(inhibitor concentration). Cell survival was determined by the colony assay, and data were fitted to a 4-parameter logistic equation. Data points are means ± SEM of 3 independent experiments. The log of the concentration at which 50% of cells survive (EC_{50}) is that at which each survival curve intersects the horizontal dashed line (as indicated by the red arrow).

The equivalent concentrations of NVP-BEZ235, ABT-263 and AG-1478 for 50% cell survival for the MDA-MB-231 cell line were found to be 108.2 ± 6.90, 2212 ± 246, and 7895 ± 826 nM, respectively. The corresponding EC_{50}-values for the MCF-7 cell line emerged as 16.90 ± 0.69, 1217 ± 227, and 3466 ± 259 nM. Treatment of the apparently normal human breast cell line MCF-12A with NVP-BEZ235, ABT-263, and AG-1478 yielded EC_{50}-values of 26.19 ± 3.35, 1157 ± 86 and 8185 ± 474 nM, respectively.

Table 3.4: Summary of cytotoxicity data for 3 human breast cell lines (MDA-MB-231, MCF-7 and MCF-12A) treated with EGFR inhibitor (AG-1478), PI3K and mTOR inhibitor (NVP-BEZ235), and Bcl-2 inhibitor (ABT-263). EC_{50} denotes the equivalent concentration for 50% cell survival. *T* and *B* are the maximum and minimum of the concentration-response curve, respectively (Figures 3.3-3.5). *HS* is the steepest slope of the curve.

Cell line	Treatment	EC_{50} (nM)	*T*	*B*	*HS*
MDA-MB-231	AG-1478	7895±826	0.99±0.02	-0.01±0.02	-1.13±0.11
	NVP-BEZ235	108.2±6.9	0.98±0.02	-0.01±0.02	-1.78±0.18
	ABT-263	2212±246	0.98±0.01	-0.01±0.02	-1.16±0.11
MCF-7	AG-1478	3466±259	0.98±0.02	-0.02±0.02	-1.59±0.18
	NVP-BEZ235	16.90±0.69	1.01±0.01	0.01±0.01	-2.25±0.02
	ABT-263	1217±227	1.01±0.03	-0.02±0.03	-0.80±0.11
MCF-12A	AG-1478	8185±474	0.99±0.01	-0.01±0.01	-1.93±0.14
	NVP-BEZ235	26.19±3.35	1.01±0.03	-0.01±0.03	-1.32±0.17
	ABT-263	1157±86	0.99±0.00	0.00±0.01	-3.61±1.77

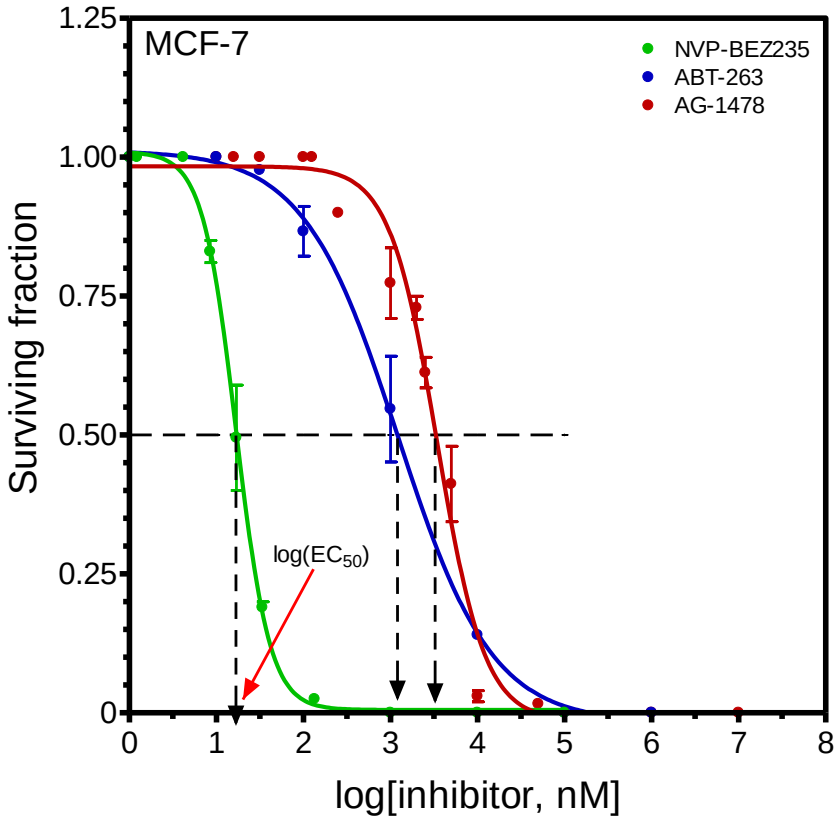

Figure 3.4: Cytotoxicity curves for an EGFR inhibitor (AG-1478), a PI3K and mTOR inhibitor (NVP-BEZ235), and a Bcl-2 inhibitor (ABT-263) for the luminal A subtype human breast cancer cell line, MCF-7. Curves were obtained by plotting the cell survival as a function of log(inhibitor concentration). Cell survival was determined by the colony assay, and data were fitted to a 4-parameter logistic equation. Data points are means ± SEM of 3 independent experiments. The log of the concentration at which 50% of cells survive (EC_{50}) is that at which each survival curve intersects the horizontal dashed line (as indicated by red red arrow).

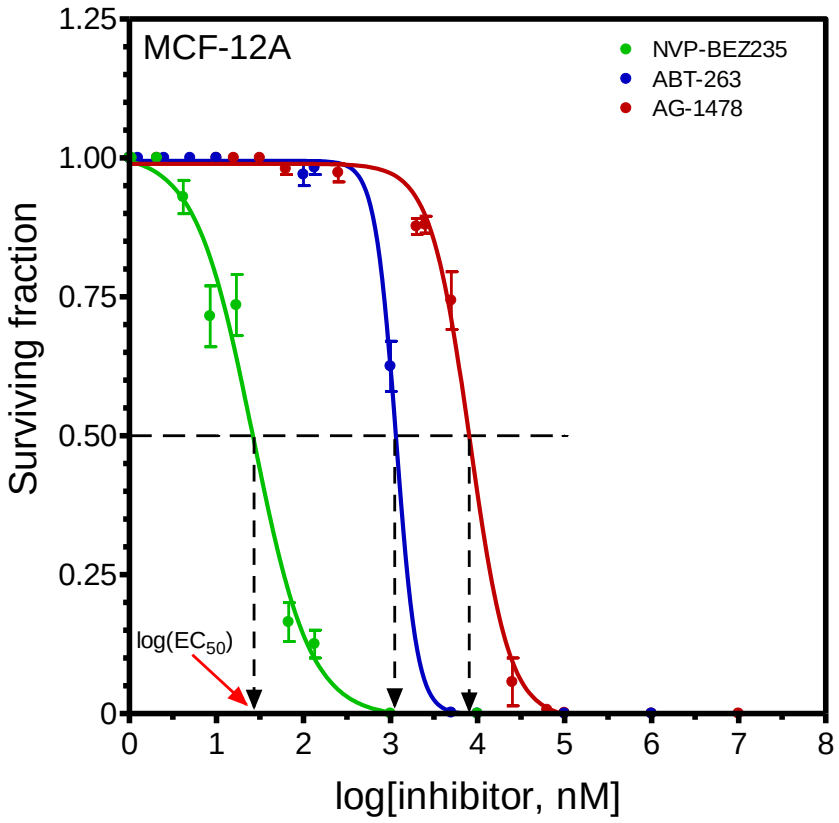

Figure 3.5: Cytotoxicity curves for an EGFR inhibitor (AG-1478), a PI3K and mTOR inhibitor (NVP-BEZ235), and a Bcl-2 inhibitor (ABT-263) for an apparent normal human breast cell line, MCF-12A. Curves were obtained by plotting the cell survival as a function of log(inhibitor concentration). Cell survival was determined by the colony assay, and data were fitted to a 4-parameter logistic equation. Data points are means ± SEM of 3 independent experiments. The log of the concentration at which 50% of cells survive (EC_{50}) is that at which each survival curve intersects the horizontal dashed line (as indicated by the red arrow).

3.3.2. Cytotoxicity of AG-1478, NVP-BEZ235 and ABT-263 in Lung and Cervix Cell Lines

Inhibition of EGFR, PI3K/mTOR, and Bcl-2 with AG-1478, NVP-BEZ235, and ABT-263, respectively, also yielded a concentration-dependent cell kill in the A549, L132 and HeLa cell lines (Figures 3.6-3.8). These figures and summarised data in Table

3.5 also indicate that NVP-BEZ235 is the most toxic inhibitor in these cell lines and that AG-1478 had the least cytotoxic effect.

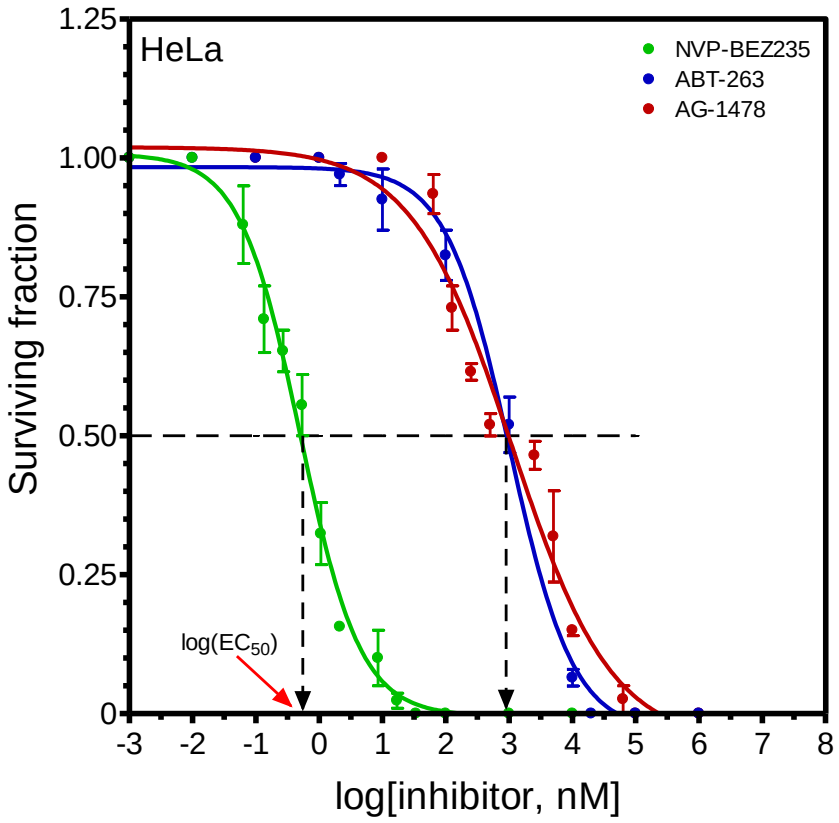

Figure 3.6: Cytotoxicity curves for an EGFR inhibitor (AG-1478), a PI3K and mTOR inhibitor (NVP-BEZ235), and a Bcl-2 inhibitor (ABT-263) for the human cervical carcinoma cell line, HeLa. Curves were obtained by plotting the cell survival as a function of log(inhibitor concentration). Cell survival was determined by the colony assay, and data were fitted to a 4-parameter logistic equation. Data points are means ± SEM of 3 independent experiments. The log of the concentration at which 50% of cells survive (EC_{50}) is that at which each survival curve intersects the horizontal dashed line (as indicated by the red arrow).

Table 3.5: Summary of cytotoxicity data for 2 human lung cell lines (A549 and L132) and a cervix carcinoma cell line (HeLa) treated with EGFR inhibitor (AG-1478), PI3K and mTOR inhibitor (NVP-BEZ235), and Bcl-2 inhibitor (ABT-263). EC_{50} denotes the equivalent concentration for 50% cell survival. *T* and *B* are the maximum and minimum of the concentration-response curve, respectively (Figures 3.6-3.8). *HS* is the steepest slope of the curve.

Cell line	Treatment	EC_{50} (nM)	*T*	*B*	*HS*
HeLa	AG-1478	1096±287	1.02±0.02	-0.05±0.05	-0.55±0.07
	NVP-BEZ235	0.50±0.06	1.01±0.03	0.00±0.01	-0.91±0.08
	ABT-263	1027±146	0.98±0.01	-0.03±0.02	-0.87±0.09
A549	AG-1478	5458±485	0.99±0.02	-0.02±0.02	-1.63±0.21
	NVP-BEZ235	15.23±1.16	0.99±0.01	-0.02±0.02	-1.13±0.08
	ABT-263	2161±189	0.99±0.01	0.00±0.01	-1.89±0.19
L132	AG-1478	8934±332	0.99±0.01	0.01±0.02	-4.19±0.73
	NVP-BEZ235	114±6.36	0.99±0.01	0.01±0.02	-2.43±0.30
	ABT-263	1599±178	0.99±0.01	0.00±0.02	-1.26±0.17

The EC_{50}-values for HeLa emerged as 1096 ± 287, 0.50 ± 0.06, and 1027 ± 146 nM for AG-1478, NVP-BEZ235, and ABT-263 treatment, respectively. The corresponding EC_{50}-values for the human lung carcinoma cell line, A549, were found to be 5485 ± 485, 15.23 ± 1.16, and 2161 ± 189 nM. For the normal lung cell line, L132, the EC_{50}-values were 8934 ± 332, 114 ± 6.36, and 1599 ± 178 nM, after treatment with AG-1478, NVP-BEZ235, and ABT-263, respectively.

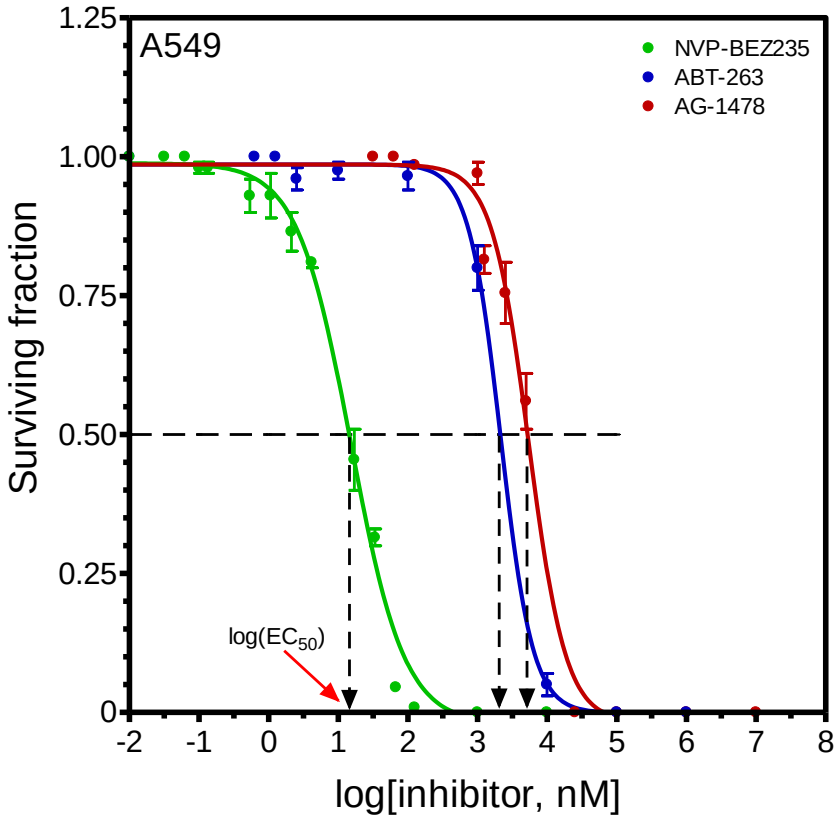

Figure 3.7: Cytotoxicity curves for an EGFR inhibitor (AG-1478), a PI3K and mTOR inhibitor (NVP-BEZ235), and a Bcl-2 inhibitor (ABT-263) for the human lung cancer cell line, A549. Curves were obtained by plotting the cell survival as a function of log(inhibitor concentration). Cell survival was determined by the colony assay, and data were fitted to a 4-parameter logistic equation. Data points are means ± SEM of 3 independent experiments. The log of the concentration at which 50% of cells survive (EC_{50}) is that at which each survival curve intersects the horizontal dashed line (as indicated by the red arrow).

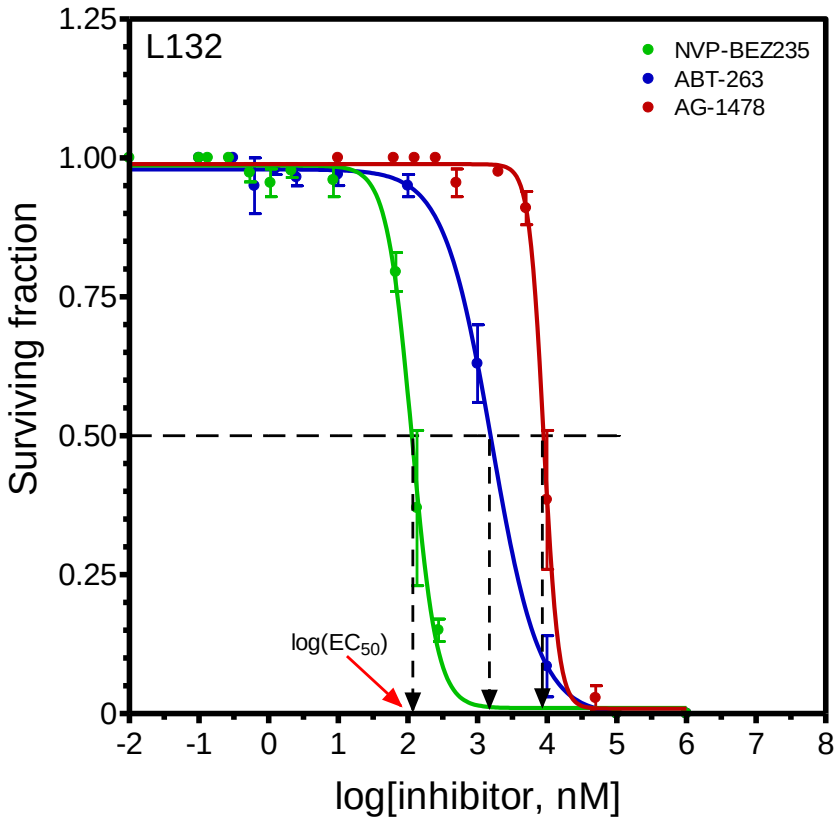

Figure 3.8: Cytotoxicity curves for an EGFR inhibitor (AG-1478), a PI3K and mTOR inhibitor (NVP-BEZ235), and a Bcl-2 inhibitor (ABT-263) for an apparent normal human lung cell line, L132. Curves were obtained by plotting the cell survival as a function of log(inhibitor concentration). Cell survival was determined by the colony assay, and data were fitted to a 4-parameter logistic equation. Data points are means ± SEM of 3 independent experiments. The log of the concentration at which 50% of cells survive (EC_{50}) is that at which each survival curve intersects the horizontal dashed line (as indicated by the red arrow).

3.4. Therapeutic Potential of Inhibitors

To evaluate the existence of a potential therapeutic benefit when the cell lines are treated with the specified inhibitors, relative sensitivities (*RS*), as described in Section 2.8, were determined on the basis of the EC_{50}-values. The data presented in Table 3.6 summarise the relative sensitivities of the tumour cells.

Table 3.6: Summary of EC_{50}-values for 3 human breast cell lines (normal: MCF-12A; cancer: MCF-7, MDA-MB-231), 2 human lung cell lines (normal: L132; cancer: A549), and a cervical cancer cell line (HeLa). Their relative radiosensitivities (*RS*), determined by clonogenic cell survival, after exposure to X-rays (Equation 2.3). *RS*-values were derived by comparing the EC_{50}-values of the normal cell lines (MCF-12A and L132) to those of the tumour cell lines (MCF-7 and MDA-MB-231) and (A549 and HeLa), respectively.

Cell line	Treatment	EC_{50} (nM)	*RS**
MCF-12A	AG-1478	8185 ± 474	-
	NVP-BEZ235	26.19 ± 3.35	-
	ABT-263	1157 ± 86	-
MDA-MB-231	AG-1478	7895 ± 826	1.04 ± 0.12
	NVP-BEZ235	108 ± 7	0.24 ± 0.04
	ABT-263	2212 ± 246	0.52 ± 0.07
MCF-7	AG-1478	3466 ± 259	2.36 ± 0.22
	NVP-BEZ235	16.90 ± 0.69	1.62 ± 0.22
	ABT-263	1217 ± 227	0.95 ± 0.19
L132	AG-1478	8934 ± 332	-
	NVP-BEZ235	114 ± 6	-
	ABT-263	1599 ± 178	-
A549	AG-1478	5458 ± 485	1.67 ± 0.16
	NVP-BEZ235	15.23 ± 1.16	7.48 ± 0.71
	ABT-263	2161 ± 189	0.74 ± 0.11
HeLa	AG-1478	1096 ± 287	7.47 ± 2.00
	NVP-BEZ235	0.50 ± 0.06	52.38 ± 9.19
	ABT-263	1027 ± 146	1.13 ± 0.18

*Errors were calculated using error propagation formulae for ratios.

EGFR inhibition (using AG-1478), yielded relative sensitivities of equal to or greater than 1.0, indicating that such treatment results in a therapeutic benefit or no effect.

Inhibition of PI3K and mTOR with NVP-BEZ235 results in a huge therapeutic benefit for the lung and cervical cancer cell lines, a slight benefit in the MCF-7 cell line, and no benefit (with potential harmful effects) for the MDA-MB-231 cell line.

Bcl-2 inhibition with ABT-263 has either no effect (MDA-MB-231 and A549) or results in potential harmful effects (MCF-7 and HeLa).

3.5. Mode of Inhibitor Action in Cells and Inhibitor Interaction

To determine the nature of cellular response to treatment with the EGFR, PI3K/mTOR, and Bcl-2 inhibitors in the cell lines, the cell survival data presented in Figures 3.3-3.8 were log transformed as described in Section 2.10, to obtain median-effect plots for the inhibitors.

3.5.1. Inhibitor Interaction in the MDA-MB-231, MCF-7, and MCF-12A Cell Lines

Figure 3.9 represents the median-effect plots for the MDA-MB-231 cell line. The Bcl-2, EGFR, and PI3K/mTOR inhibitors seem to have different modes of interaction with these cells, as the slopes of the curves emerged as 0.73, 1.08, and 1.36, indicating flat-sigmoidal, hyperbolic, and sigmoidal concentration-effects, respectively (Table

3.7). The corresponding median-effect concentrations (D_m) were ~145, 5332, and 1543 nM.

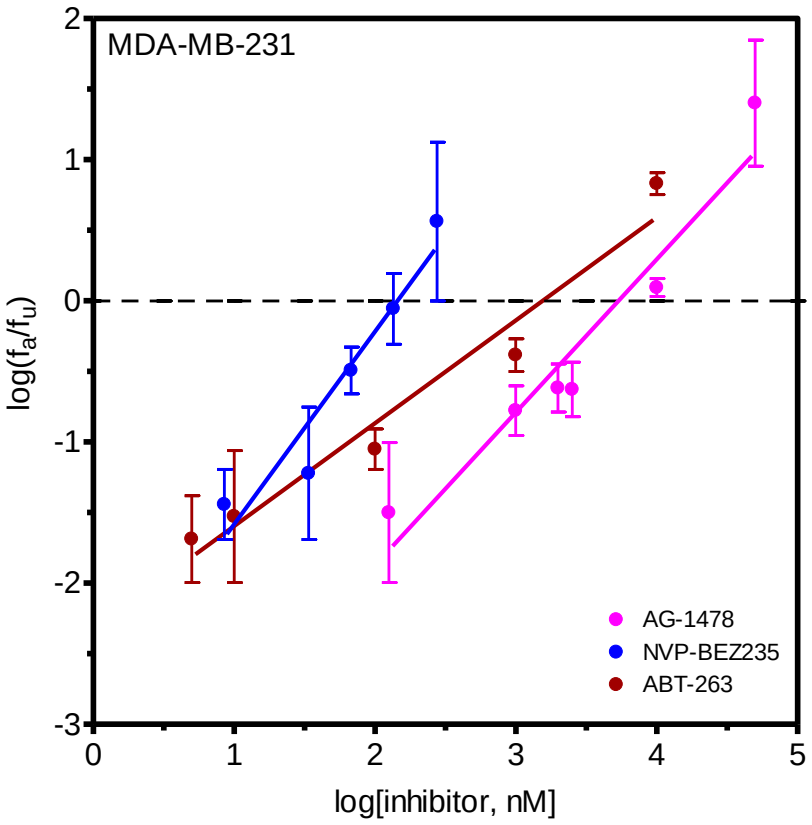

Figure 3.9: Median-effect plots (Section 2.10) for the triple negative human breast cancer cell line (MDA-MB-231), treated with AG-1478, NVP-BEZ235, and ABT-263, from toxicity data presented in Figure 3.3. Horizontal dashed line is the median-effect axis.

The median-effect plots for the MCF-7 cell line are presented in Figure 3.10. While inhibition of Bcl-2 in these cells with ABT-263 yielded a shallow median-effect curve with a slope of 0.95 (flat-sigmoidal), inhibition of EGFR and PI3K/mTOR resulted in steeper curves with slopes of 1.67 and 1.33, respectively (Table 3.6). Therefore, cytotoxicity of AG-1478 and NVP-BEZ235 in these cells follow a sigmoidal pattern.

The D_m-values for NVP-BEZ235, ABT-263, and AG-1478 were ~18, 1300, and 2916 nM, respectively.

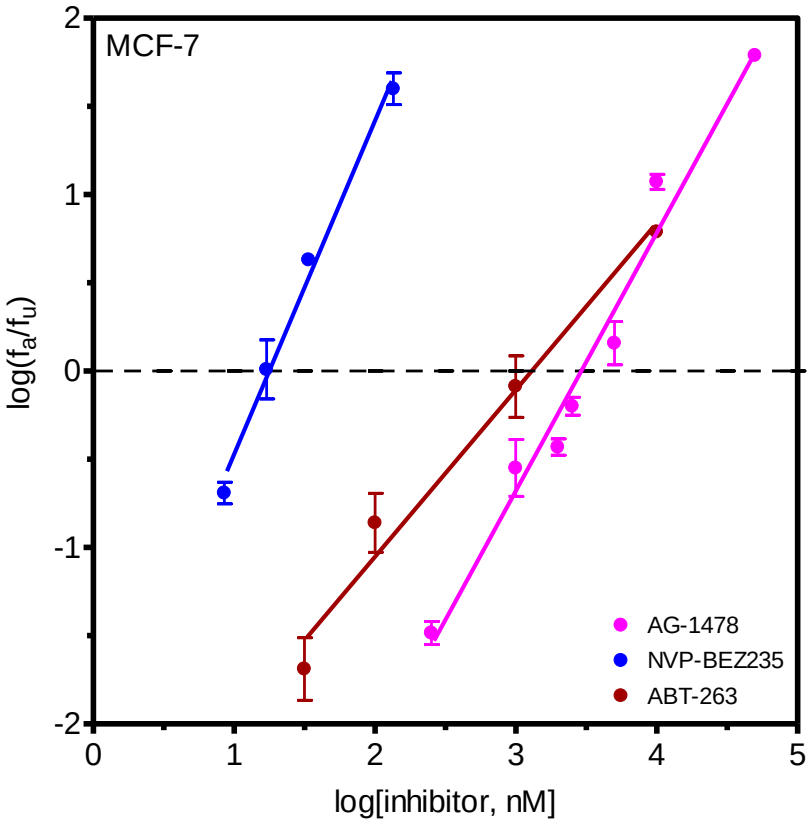

Figure 3.10: Median-effect plots (Section 2.10) for the luminal A human breast cancer cell line (MCF-7), treated with AG-1478, NVP-BEZ235, and ABT-263, from toxicity data presented in Figure 3.4. Horizontal dashed line is the median-effect axis.

Figure 3.11 represents the median-effect plots for the apparently normal breast cell line (MCF-12A). In these cells, inhibition of PI3K/mTOR, Bcl-2, and EGFR follows a sigmoidal pattern, with the slopes of the median-effect curves emerging as 1.33,

2.69, and 1.67, respectively (Table 3.6). The median-effect concentrations of respective inhibitors were found to be ~26, 606, and 4268 nM.

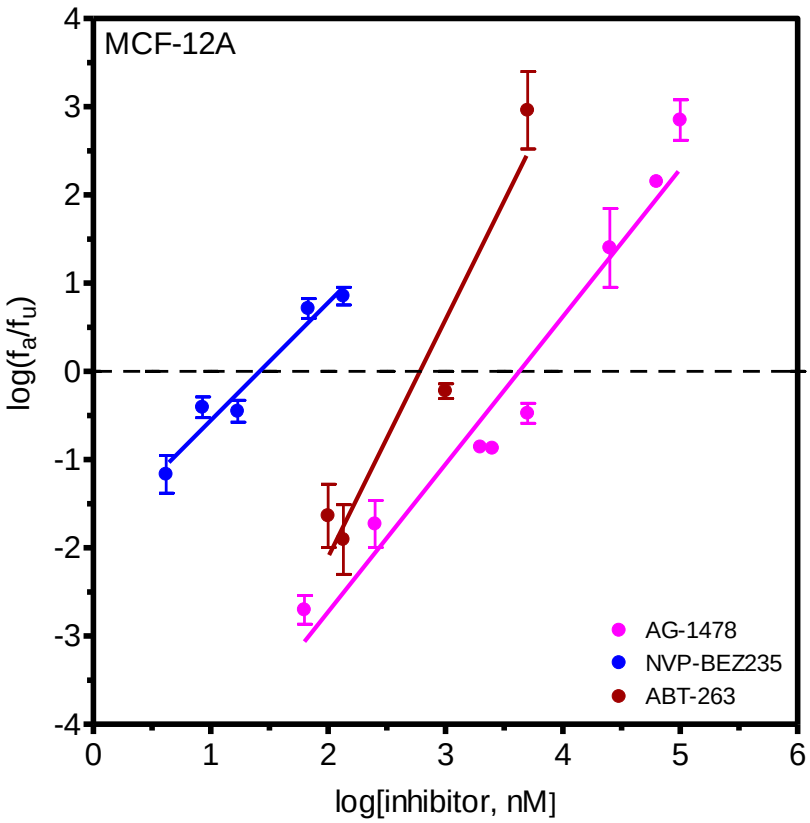

Figure 3.11: Median-effect plots (Section 2.10) for the apparently normal human breast cell line (MCF-12A), treated with AG-1478, NVP-BEZ235, and ABT-263, from toxicity data presented in Figure 3.5. Horizontal dashed line is the median-effect axis.

Table 3.7: Summary of parameters of median-effect plots for EGFR inhibitor (AG-1478), PI3K and mTOR inhibitor (NVP-BEZ235), and Bcl-2 inhibitor (ABT-263) in 3 human breast cell lines (MDA-MB-231, MCF-7 and MCF-12A).

Cell line	Treatment	*m*	D_m (nM)	Shape of concentration-effect curve
MDA-MB-231	AG-1478	1.08 ± 0.15	5332 ± 6	hyperbolic
	NVP-BEZ235	1.36 ± 0.29	144.93 ± 3.01	sigmoidal
	ABT-263	0.73 ± 0.09	1543 ± 4	flat-sigmoidal
MCF-7	AG-1478	1.46 ± 0.09	2916 ± 3	sigmoidal
	NVP-BEZ235	1.89 ± 0.12	17.79 ± 0.35	sigmoidal
	ABT-263	0.95 ± 0.08	1300 ± 3	flat-sigmoidal
MCF-12A	AG-1478	1.67 ± 0.11	4268 ± 3	sigmoidal
	NVP-BEZ235	1.33 ± 0.14	26.11 ± 0.70	sigmoidal
	ABT-263	2.69 ± 0.38	606 ± 4	sigmoidal

The potential mode of interaction between the panel of inhibitors in the breast cell lines, used in this study, was interrogated using combination indices (*CI*) obtained from the fitted parameters of the median-effect plots (Figures 3.9-3.11), as defined under Section 2.10. For each cocktail treatment of MDA-MB-231, *CI*-values were significantly less than 0.1 (Table 3.8), indicating very strong synergism between inhibitors when combined at EC_{50} concentrations. Inhibitor cocktail treatment of MCF-7 cells produced combination indices ranging from 0.0585 to 0.1351, indicating that inhibitor-inhibitor interaction varied from synergism to strong synergism. Similarly, mild to strong synergism emerged between inhibitors in the apparently

normal breast cell line (MCF-12A), with combination indices ranging between 0.1553 and 0.4683.

Table 3.8: Summary of combination indices for EGFR inhibitor (AG-1478), PI3K and mTOR inhibitor (NVP-BEZ235), and Bcl-2 inhibitor (ABT-263), when used concurrently at their respective EC_{50} concentrations in 3 human breast cell lines (MDA-MB-231, MCF-7 and MCF-12A).

Cell line	Agent 1	Agent 2		
		AG-1478	NVP-BEZ235	ABT-263
MDA-MB-231	AG-1478	-	0.0465	0.0237
	NVP-BEZ235	0.0465	-	0.0281
	ABT-263	0.0237	0.0281	-
MCF-7	AG-1478	-	0.1351	0.0585
	NVP-BEZ235	0.1351	-	0.0914
	ABT-263	0.0585	0.0914	-
MCF-12A	AG-1478	-	0.1553	0.4683
	NVP-BEZ235	0.1553	-	0.3788
	ABT-263	0.4683	0.3788	-

3.5.2. Inhibitor Interaction in the HeLa, A549, and L132 Cell Lines

Figure 3.12 represents the median-effect plots for the HeLa cell line. While the inhibition of EGFR and Bcl-2 in these cells followed a flat sigmoidal pattern with slopes of 0.86 and 0.74, respectively, inhibiting PI3K/mTOR yielded a hyperbolic response with a slope of 1.00 (Table 3.9). The median-effect concentrations (D_m)

following treatment of these cells with AG-1478, NVP-BEZ235, and ABT-263 were ~856, 0.49, and 538 nM, respectively.

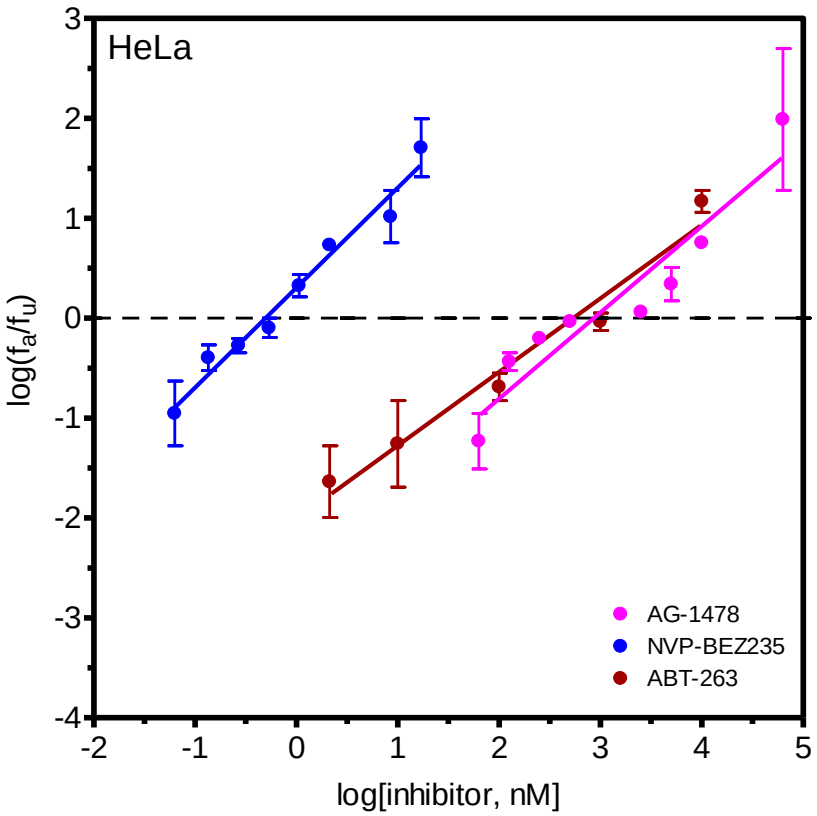

Figure 3.12: Median-effect plots (Section 2.10) for the human cervical carcinoma cell line (HeLa), treated with AG-1478, NVP-BEZ235, and ABT-263, from toxicity data presented in Figure 3.6. Horizontal dashed line is the median-effect axis.

The median-effect plots for the lung cancer cell line (A549) are shown in Figure 3.13. Inhibition of EGFR in these cells with AG-1478 yielded a sigmoidal median-effect plot with a slope of 1.64, while the inhibition of PI3K/mTOR and Bcl-2 produced shallower (flat-sigmoidal) median-effect plots with slopes of ~0.84 and 0.91, respectively (Table 3.9). The corresponding median-effect concentrations (D_m) were ~ 6251, 17.15, and 816 nM.

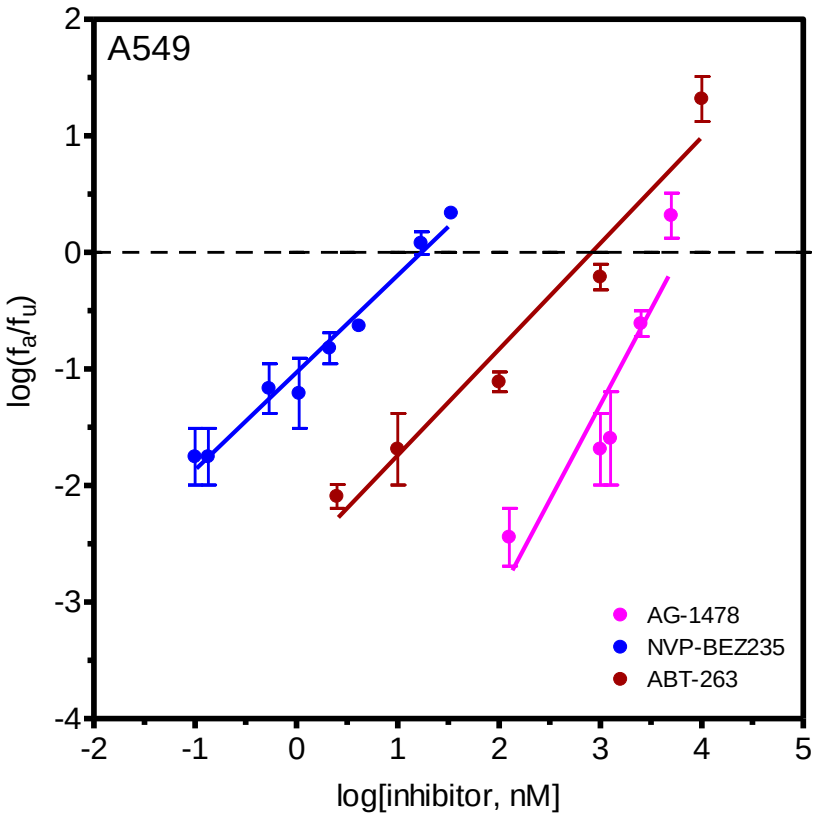

Figure 3.13: Median-effect plots (Section 2.10) for the human lung cancer cell line (A549), treated with AG-1478, NVP-BEZ235, and ABT-263, from toxicity data presented in Figure 3.7. Horizontal dashed line is the median-effect axis.

Figure 3.14 depicts the median-effect plots of apparently normal lung cell line, L132. The response of these cells to EGFR, PI3K/mTOR and Bcl-2 inhibition followed similar patterns as seen in the A549 cell line, with the slopes of the median-effect plots emerging as 1.70, 0.87, and 0.70, respectively (Table 3.9). The median-effect concentrations for the respective inhibitors were found to be 8396, 79.97, and 798 nM.

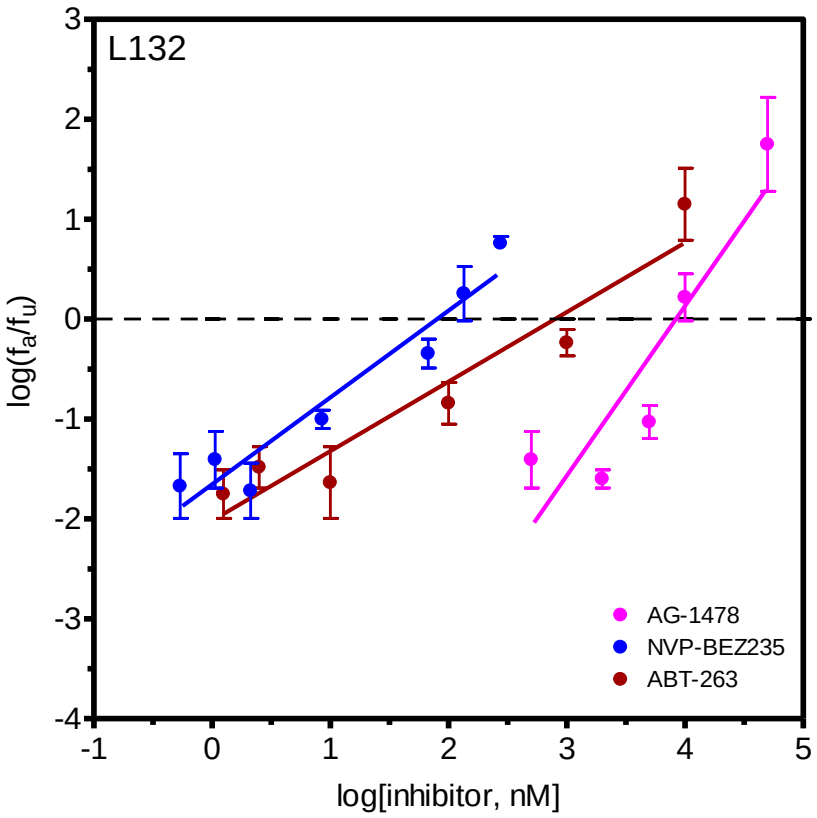

Figure 3.14: Median-effect plots (Section 2.10) for the apparently normal human lung cell line (L132), treated with AG-1478, NVP-BEZ235, and ABT-263, from toxicity data presented in Figure 3.8. Horizontal dashed line is the median-effect axis.

Table 3.9: Summary of parameters of median-effect plots for EGFR inhibitor (AG-1478), PI3K and mTOR inhibitor (NVP-BEZ235), and Bcl-2 inhibitor (ABT-263) in 2 human lung cell lines (A549 and L132) and a cervix carcinoma cell line (HeLa).

Cell line	Treatment	*m*	D_m (nM)	Shape of concentration-effect curve
HeLa	AG-1478	0.86 ± 0.11	856 ± 4	flat-sigmoidal
	NVP-BEZ235	1.00 ± 0.08	0.49 ± 0.05	hyperbolic
	ABT-263	0.74 ± 0.08	538 ± 3	flat-sigmoidal
A549	AG-1478	1.64 ± 0.30	6251 ± 8	sigmoidal
	NVP-BEZ235	0.84 ± 0.07	17.15 ± 0.35	flat-sigmoidal
	ABT-263	0.91 ± 0.08	816 ± 2	flat-sigmoidal
L132	AG-1478	1.70 ± 0.31	8396 ± 9	sigmoidal
	NVP-BEZ235	0.87 ± 0.10	79.97 ± 1.16	flat-sigmoidal
	ABT-263	0.70 ± 0.09	798 ± 3	flat-sigmoidal

The mode of interaction between the panel of inhibitors in the cervical and lung cell lines was also assessed using combination indices, when the inhibitors were combined at EC_{50} concentrations. While a cocktail of AG-1478 and ABT-263 showed very strong synergism in HeLa cells (CI = 0.01), a strong antagonism ($CI \approx 4.1$) emerged for a cocktail of AG-1478 and NVP-BEZ235 (Table 3.10). For the A549 cell line, all cocktail treatments showed very strong inhibitor-inhibitor interactions, with combination indices ranging from ~0.02 to 0.07. Similarly, a very strong synergism emerged between inhibitors in the apparently normal lung cell line, L132 ($0.0101 \leq CI \leq 0.0785$).

Table 3.10: Summary of combination indices for EGFR inhibitor (AG-1478), PI3K and mTOR inhibitor (NVP-BEZ235), and Bcl-2 inhibitor (ABT-263), when used concurrently at their respective EC_{50} concentrations in 2 human lung cell lines (A549 and L132) and a cervix carcinoma cell line (HeLa).

Cell line	Agent 1	Agent 2		
		AG-1478	NVP-BEZ235	ABT-263
HeLa	AG-1478	-	4.0835	0.0100
	NVP-BEZ235	4.0835	-	4.0812
	ABT-263	0.0100	4.0812	-
A549	AG-1478	-	0.0581	0.0700
	NVP-BEZ235	0.0581	-	0.0221
	ABT-263	0.0700	0.0221	-
L132	AG-1478	-	0.0785	0.0741
	NVP-BEZ235	0.0785	-	0.0101
	ABT-263	0.0741	0.0101	-

3.6. Radiomodulation by Inhibitors

To evaluate the radiomodulatory effects of the EGFR, PI3K/mTOR, and Bcl-2 inhibitors in the cell lines employed in this study, cell survival data were fitted to the linear-quadratic model, as described in Section 2.5. Mean activation doses ($\bar{D}$) were obtained and used to derive modifying factors, defined in Equation 2.4. The mean inactivation dose was selected for this assessment, as some of the cell survival curves (especially those from inhibitor treatment) tended to turn upward at higher X-ray doses, indicating some radioprotection. With such a peculiarity in survival curves,

cell survival at a single low or high dose (e.g. SF_2 or SF_6) would not be a reliable representation of the overall radiosensitivity of a particular cell line.

3.6.1. Radiomodulation in the MCF-12A, MDA-MB-231, and MCF-7 Cell Lines

Figure 3.15, represents the survival data of the apparently normal breast cell line (MCF-12A) after inhibitor and X-ray treatment.

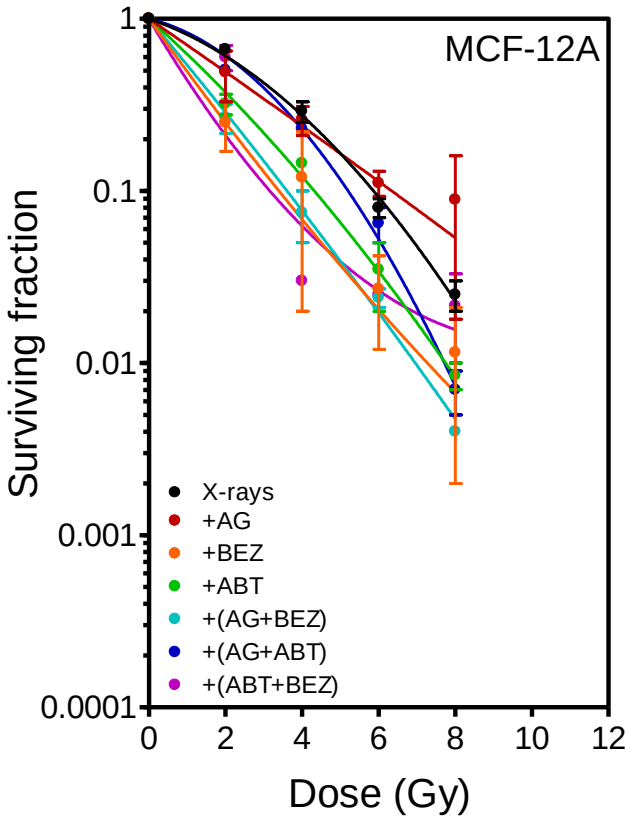

Figure 3.15: Cell survival curves for the apparently normal human breast cell line (MCF-12A) after X-ray irradiation. Cells were irradiated without or in the presence of AG-1478 (AG), NVP-BEZ235 (BEZ), and ABT-263 (ABT), administered either singly or in combination. Symbols represent the mean surviving fraction ± SEM from three independent experiments.

A decrease in cell survival was observed when the inhibitor-pre-treated cells were compared to cells treated with X-rays alone. However, these cells appeared to

survive better at doses greater than 4 Gy, when pre-treated with AG-1478. The mean inactivation dose ($\bar{D}$) for the MCF-12A cell line, in this set of experiments, was found to be 3.10 ± 0.09 Gy. The modifying factors, based on mean inactivation dose, are summarised in Table 3.11. For this cell line, a significant enhancement in radiosensitivity emerged when PI3K/mTOR and Bcl-2 were inhibited ($0.0080 \leq P \leq 0.0192$). A small, but insignificant, radiosensitisation was seen when the cells were pre-treated with AG-1478. Except for the combination of AG-1478 and NVP-BEZ235, the radiosensitisation induced by the other inhibitor cocktails in these cells did not reach statistical significance.

The survival data for the MDA-MB-231 cells are presented in Figure 3.16. Pre-treatment of these cells with the EGFR inhibitor had no effect on radiosensitivity. A general decrease in cell survival was observed when the cells were pre-treated with the other inhibitors or inhibitor cocktails. However, at doses greater than 4 Gy, pre-treatment of the MDA-MB-231 cells with NVP-BEZ235 or a combination of NVP-BEZ235 and AG-1478 resulted in an increase in cell survival compared to that when cells were treated with X-rays alone. This seems to suggest that pre-treating the triple negative breast cancer cells with NVP-BEZ235 or an AG-1478/NVP-BEZ235 cocktail may protect them from the toxic effects of large fractions of radiation, such as those used in hyperfractionated regimes. The $\bar{D}$ for X-ray treatment alone in this cell line, on which inhibitor radiomodulation was based, emerged as 1.77 ± 0.05 Gy.

Table 3.11: Modifying factors (*MF*), relative to X-ray treatment alone, derived from and $\bar{D}$ values, as described in Section 2.9 for 3 human breast cell lines (normal: MCF-12A; cancer: MCF-7, MDA-MB-231) irradiated in the presence of AG-1478 (AG), NVP-BEZ235 (BEZ), and ABT-263 (ABT). Errors in modifying factors were calculated using error propagation formulae for ratios.

Cell line	Treatment	$\bar{D}$ (Gy)	*P-value*	*MF*
MCF-12A	X-rays + AG	2.81 ± 0.31	0.4738	1.10 ± 0.13
	X-rays + BEZ	1.81 ± 0.08	0.0080*	1.71 ± 0.09
	X-rays + ABT	2.01 ± 0.13	0.0192*	1.54 ± 0.11
MDA-MB-231	X-rays + AG	1.92 ± 0.12	0.3342	0.92 ± 0.06
	X-rays + BEZ	1.61 ± 0.50	0.7086	1.10 ± 0.34
	X-rays + ABT	1.53 ± 0.25	0.3950	1.16 ± 0.19
MCF-7	X-rays + AG	1.51 ± 0.06	0.8935	1.01 ± 0.05
	X-rays + BEZ	1.27 ± 0.10	0.0879	1.20 ± 0.10
	X-rays + ABT	1.39 ± 0.03	0.1666	1.09 ± 0.04
MCF-12A	X-rays + AG + BEZ	1.73 ± 0.14	0.0134*	1.79 ± 0.15
	X-rays + BEZ + ABT	2.33 ± 0.19	0.0662	1.33 ± 0.12
	X-rays + ABT + AG	2.61 ± 0.14	0.0937	1.19 ± 0.07
MDA-MB-231	X-rays + AG + BEZ	1.23 ± 0.01	0.0038*	1.44 ± 0.04
	X-rays + BEZ + ABT	1.32 ± 0.06	0.0107*	1.34 ± 0.07
	X-rays + ABT + AG	1.45 ± 0.13	0.0686	1.22 ± 0.12
MCF-7	X-rays + AG + BEZ	1.33 ± 0.05	0.0987	1.14 ± 0.06
	X-rays + BEZ + ABT	1.12 ± 0.03	0.0109*	1.36 ± 0.06
	X-rays + ABT + AG	1.28 ± 0.01	0.0403*	1.19 ± 0.04

*Statistically significant difference between X-ray treatment alone and irradiation in the presence of inhibitor.

Put together, single inhibitor treatment either had no effect or resulted in insignificant radiosensitisation in this cell line (Table 3.11). Inhibitor cocktail pre-treatments yielded significant radiosensitisation in the MDA-MB-231 cells, except for AG-1478 and ABT-263 combination.

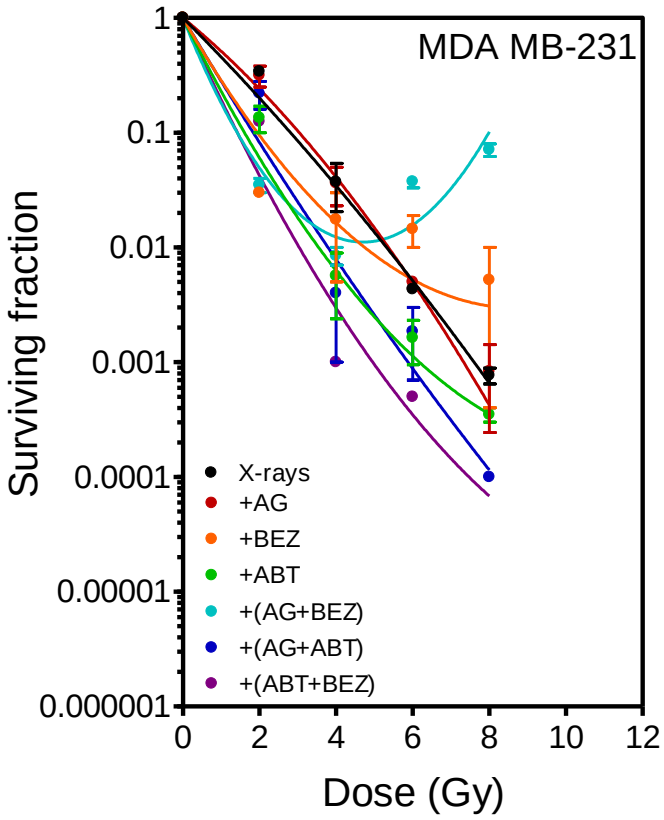

Figure 3.16: Cell survival curves for the triple negative human breast cancer cell line (MDA-MB-231) after X-ray irradiation. Cells were irradiated without or in the presence of AG-1478 (AG), NVP-BEZ235 (BEZ), and ABT-263 (ABT), administered either singly or in combination. Symbols represent the mean surviving fraction ± SEM from three independent experiments.

Treating MCF-7 cells with AG-1478, NVP-BEZ235, and ABT-263, or a cocktail of these inhibitors prior to irradiation appeared to decrease cell survival, when compared to MCF-7 cells treated with X-rays alone (Figure 3.17). Treatment of these cells with X-rays alone, yield a $\bar{D}$-value of 1.52 ± 0.05 Gy. However, an upward trend

in cell survival at higher radiation doses was also observed when cells were treated with NVP-BEZ235, an ABT-263/AG-1478 cocktail, or an ABT-263/NVP-BEZ235 cocktail. In this cell line, significant enhancement in radiosensitivity was observed only in ABT-263/NVP-BEZ235 and ABT-263/AG-1478 cocktail pre-treated cell cultures (Table 3.11).

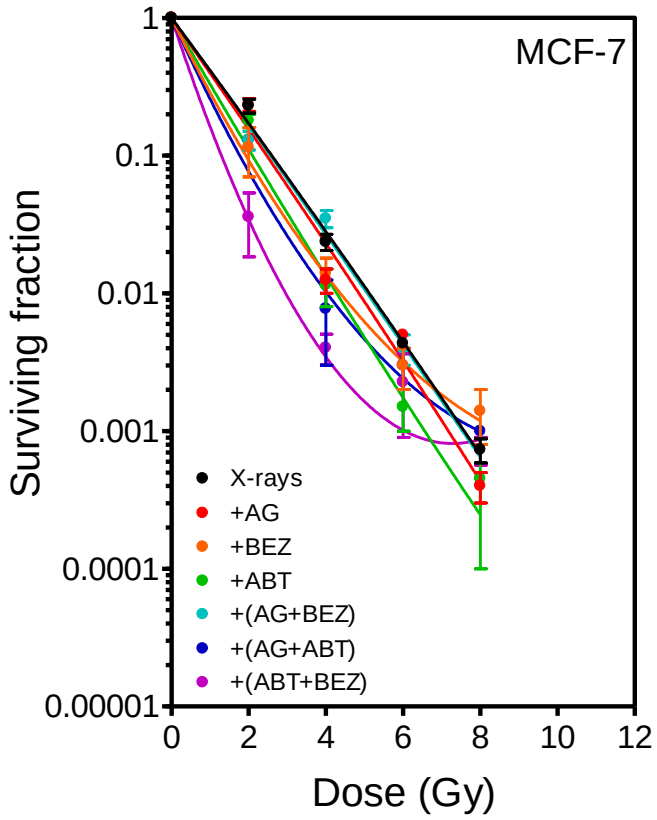

Figure 3.17: Cell survival curves for the luminal A human breast cancer cell line (MCF-7) after X-ray irradiation. Cells were irradiated without or in the presence of AG-1478 (AG), NVP-BEZ235 (BEZ), and ABT-263 (ABT), administered either singly or in combination. Symbols represent the mean surviving fraction ± SEM from three independent experiments.

3.6.2. Radiomodulation in the HeLa, A549, and L132 Cell Lines

Figure 3.18 represents the cell survival curves for apparently normal L132 cells after single inhibitor or cocktail treatment prior to irradiation. The mean inactivation dose

for these cells was 3.01 ± 0.18 Gy. Except for the AG-1478 pre-treatment which appeared to enhance cell survival relative to X-ray treatment alone, all other inhibitor permutations resulted in increased radiosensitivity. Again, an upward trend in cell survival was apparent when cells were pre-treated with NVP-BEZ235, an AG-1478/NVP-BEZ235 cocktail, or an ABT-263/NVP-BEZ235 cocktail (Figure 3.18). Taken together, ~3-fold enhancement in radiosensitivity occurred when the L132 cells were pre-treated with NVP-BEZ235, an AG-1478/NVP-BEZ235 cocktail, or an ABT-263/NVP-BEZ235 cocktail (Table 3.12).

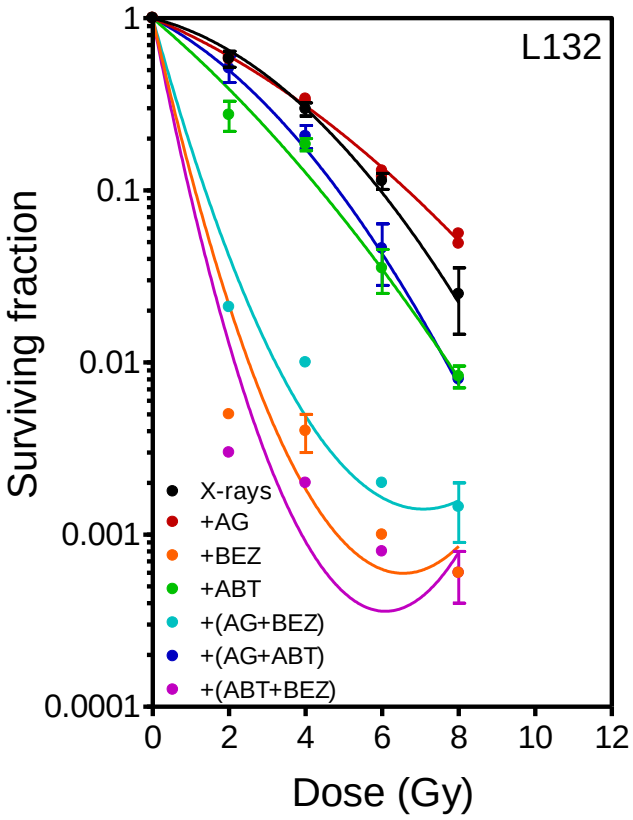

Figure 3.18: Cell survival curves for the apparently normal human lung cancer cell line (L132) after X-ray irradiation. Cells were irradiated without or in the presence of AG-1478 (AG), NVP-BEZ235 (BEZ), and ABT-263 (ABT), administered either singly or in combination. Symbols represent the mean surviving fraction ± SEM from three independent experiments.

Table 3.12: Modifying factors (*MF*), relative to X-ray treatment alone, derived from $\bar{D}$ values, as described in Section 2.9 for 2 human lung cell lines (A549 and L132) and a cervix carcinoma cell line (HeLa) irradiated in the presence of AG-1478 (AG), NVP-BEZ235 (BEZ), and ABT-263 (ABT). Errors in modifying factors were calculated using error propagation formulae for ratios.

Cell line	Treatment	$\bar{D}$ (Gy)	*P-value*	*MF*
	X-rays + AG	3.15 ± 0.04	0.5968	0.96 ± 0.06
L132	X-rays + BEZ	1.02 ± 0.01	0.0034*	2.95 ± 0.18
	X-rays + ABT	2.37 ± 0.36	0.1868	1.27 ± 0.21
	X-rays + AG	2.63 ± 0.47	0.5822	0.85 ± 0.16
HeLa	X-rays + BEZ	2.04 ± 0.16	0.4421	1.10 ± 0.10
	X-rays + ABT	3.84 ± 0.24	0.0244*	0.59 ± 0.04
	X-rays + AG	2.82 ± 0.05	0.4772	1.04 ± 0.05
A549	X-rays + BEZ	2.02 ± 0.17	0.0125*	1.45 ± 0.14
	X-rays + ABT	2.85 ± 0.21	0.7613	1.03 ± 0.09
	X-rays + AG + BEZ	1.07 ± 0.01	0.0037*	2.81 ± 0.17
L132	X-rays + BEZ + ABT	1.01 ± 0.01	0.0034*	2.98 ± 0.18
	X-rays + ABT + AG	2.54 ± 0.13	0.1010	1.19 ± 0.09
	X-rays + AG + BEZ	3.11 ± 0.68	0.4034	0.72 ± 0.16
HeLa	X-rays + BEZ + ABT	2.74 ± 0.08	0.0226*	0.82 ± 0.04
	X-rays + ABT + AG	3.12 ± 0.03	0.0121*	0.72 ± 0.03
	X-rays + AG + BEZ	2.10 ± 0.34	0.0820	1.39 ± 0.23
A549	X-rays + BEZ + ABT	1.47 ± 0.03	0.0026*	1.99 ± 0.09
	X-rays + ABT + AG	2.70 ± 0.14	0.3195	1.08 ± 0.07

*Statistically significant difference between X-ray treatment alone and irradiation in the presence of inhibitor.

It is apparent that inhibiting EGFR, PI3K/mTOR and ABT-263 (via single inhibitor or cocktail treatment) resulted in an increase in cell survival in the cervical cancer cell line (HeLa) after X-ray exposure, when compared with X-ray treatment alone ($\overline{D}$ = 2.25 ± 0.09 Gy for X-rays alone; Figure 3.19). However, use of NVP-BEZ235 alone either had no effect (at doses up to 4 Gy) or resulted in a mild radiosensitisation at higher X-ray doses. In general, pre-treatment of HeLa cells with these inhibitors, either singly or in combination, mostly tended to enhance radioresistance, with modifying factors ranging between 0.59 and 1.10 (Table 3.12).

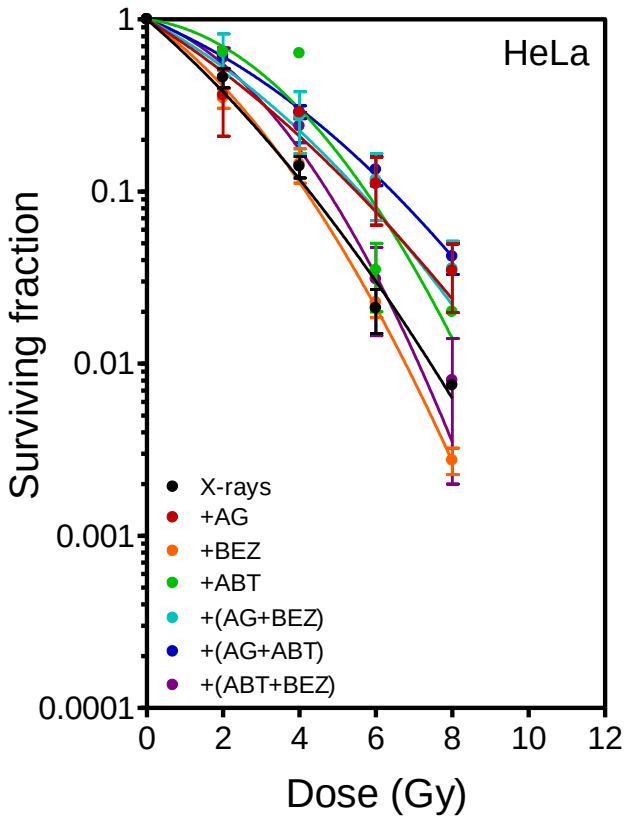

Figure 3.19: Cell survival curves for the human cervical cancer cell line (HeLa) after X-ray irradiation. Cells were irradiated without or in the presence of AG-1478 (AG), NVP-BEZ235 (BEZ), and ABT-263 (ABT), administered either singly or in combination. Symbols represent the mean surviving fraction ± SEM from three independent experiments.

The effect of targeting EGFR, PI3K/mTOR and Bcl-2 on A549 cell survival after X-ray exposure is illustrated in Figure 3.20. The $\bar{D}$-value for X-ray treatment alone was found to be 2.92 ± 0.12 Gy. While pre-treatment of these cells with AG-1478 or ABT-263 yielded no measurable change in radiosensitivity, NVP-BEZ235 pre-treatment resulted in a significant radiosensitisation (P = 0.0125; Table 3.12). An AG-1478/ABT-263 cocktail pre-treatment also had no effect on radiosensitivity. However, pre-treatment with the other inhibitor cocktails yielded an enhanced radiosensitisation.

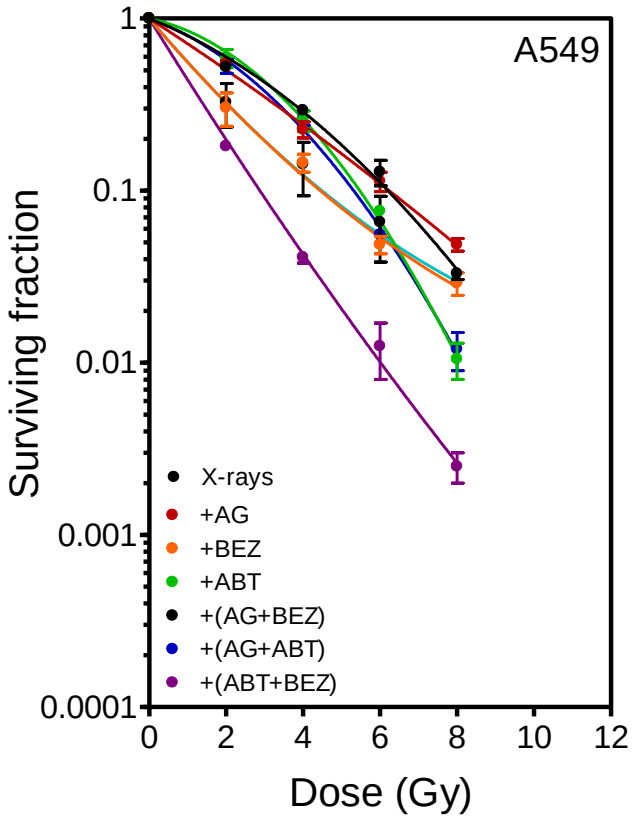

Figure 3.20: Cell survival curves for the human lung cancer cell line (A549) after X-ray irradiation. Cells were irradiated without or in the presence of AG-1478 (AG), NVP-BEZ235 (BEZ), and ABT-263 (ABT), administered either singly or in combination. Symbols represent the mean surviving fraction ± SEM from three independent experiments.

3.7. Treatment-Induced Changes in Metabolic Activity

In this study, the MTT assay was used to evaluate the radiation-induced metabolic activity of breast, lung, and cervical cell lines at 0.5, 2, 24 and 52 hours (for early, intermediate, and late changes in metabolic activity) after single or inhibitor cocktail and 2 Gy of X-ray treatment.

As described under Section 2.10, the treatment-induced modifying factors are summarised in Tables 3.13A-3.13B for the 0.5-hour time point. At this time point, all treatment configurations resulted in increased metabolic activity (*MF* < 1.0) in the breast cell lines (Table 3.13A). The data in Table 3.13B demonstrate that only the HeLa cell line showed decreased metabolic activity for all treatments.

Table 3.13A: Modifying factors (*MF*), relative to X-ray treatment alone (2 Gy), derived from the relative metabolic activities, as described in Section 2.11 for 3 human breast cell lines (normal: MCF-12A; cancer: MCF-7, MDA-MB-231), 0.5 hours after treatment. Errors were calculated using error propagation formulae for ratios.

Cell line	Treatment	*MF*
MCF-12A	2 Gy + AG-1478	0.68 ± 0.02
	2 Gy + NVP-BEZ235	0.76 ± 0.03
	2 Gy + ABT-263	0.74 ± 0.04
MDA-MB-231	2 Gy + AG-1478	0.66 ± 0.04
	2 Gy + NVP-BEZ235	0.57 ± 0.06
	2 Gy + ABT-263	0.32 ± 0.03
MCF-7	2 Gy + AG-1478	0.79 ± 0.11
	2 Gy + NVP-BEZ235	0.58 ± 0.05
	2 Gy + ABT-263	0.54 ± 0.06
MCF-12A	2 Gy + AG-1478 + NVP-BEZ235	0.77 ± 0.04
	2 Gy + NVP-BEZ235 + ABT-263	0.72 ± 0.05
	2 Gy + ABT-263 + AG-1478	0.46 ± 0.07
MDA-MB-231	2 Gy + AG-1478 + NVP-BEZ235	0.49 ± 0.02
	2 Gy + NVP-BEZ235 + ABT-263	0.31 ± 0.01
	2 Gy + ABT-263 + AG-1478	0.30 ± 0.02
MCF-7	2 Gy + AG-1478 + NVP-BEZ235	0.47 ± 0.05
	2 Gy + NVP-BEZ235 + ABT-263	0.51 ± 0.06
	2 Gy + ABT-263 + AG-1478	0.58 ± 0.08

Table 3.13B: Modifying factors (*MF*), relative to X-ray treatment alone (2 Gy), derived from the relative metabolic activities, as described in Section 2.11 for 2 human lung cell lines (normal: L132; cancer: A549), and a cervical cancer cell line (HeLa), 0.5 hours after treatment. Errors were calculated using error propagation formulae for ratios.

Cell line	Treatment	*MF*
L132	2 Gy + AG-1478	0.66 ± 0.02
	2 Gy + NVP-BEZ235	0.58 ± 0.09
	2 Gy + ABT-263	0.68 ± 0.06
HeLa	2 Gy + AG-1478	1.85 ± 0.15
	2 Gy + NVP-BEZ235	1.36 ± 0.17
	2 Gy + ABT-263	1.22 ± 0.14
A549	2 Gy + AG-1478	0.73 ± 0.05
	2 Gy + NVP-BEZ235	0.80 ± 0.07
	2 Gy + ABT-263	0.81 ± 0.06
L132	2 Gy + AG-1478 + NVP-BEZ235	0.85 ± 0.04
	2 Gy + NVP-BEZ235 + ABT-263	0.81 ± 0.05
	2 Gy + ABT-263 + AG-1478	0.68 ± 0.04
HeLa	2 Gy + AG-1478 + NVP-BEZ235	1.09 ± 0.16
	2 Gy + NVP-BEZ235 + ABT-263	1.04 ± 0.12
	2 Gy + ABT-263 + AG-1478	1.50 ± 0.17
A549	2 Gy + AG-1478 + NVP-BEZ235	0.82 ± 0.07
	2 Gy + NVP-BEZ235 + ABT-263	0.88 ± 0.09
	2 Gy + ABT-263 + AG-1478	0.61 ± 0.05

At 2 hours, single inhibitor treatment of the MCF-12A cell line had no effect on radiation-induced metabolic activity (Table 3.14A). Treatment of the MDA-MB-231 and MCF-7 cell lines with the inhibitors tended to decreased and increased metabolic activity, respectively. While combined treatment of the MCF-12A cells with ABT-263 and AG-1478 had no effect, concomitant treatment with NVP-BEZ235 and ABT-263 or AG-1478 resulted in a decrease (*MF* > 1.0). Combined treatment of the MDA-MB-231 and MCF-7 cell lines tended to decrease metabolic activity.

For the L132 cell line, single inhibitor treatment showed a decrease in metabolic activity (Table 3.14B). Combination treatment of these cells with NVP-BEZ235 and ABT-263 also resulted in a decrease, while ABT-263 and AG-1478 treatment led to an increase (*MF* < 1.0) in activity. Concomitant treatment with AG-1478 and NVP-BEZ235 had no effect. Except for irradiation with NVP-BEZ235, which resulted in a reduction in metabolic activity (*MF* > 1.0) in the HeLa cell line, all other treatments showed an increase. While irradiation with AG-1478 had no effect on metabolic activity of A549 cells, the other inhibitors showed a decrease. Whereas combined treatment with NVP-BEZ235 and ABT-263 resulted in decreased activity in these cells, other combinations tended to show an increase.

Table 3.14A: Modifying factors (*MF*), relative to X-ray treatment alone (2 Gy), derived from the relative metabolic activities, as described in Section 2.11 for 3 human breast cell lines (normal: MCF-12A; cancer: MCF-7, MDA-MB-231), 2 hours after treatment. Errors were calculated using error propagation formulae for ratios.

Cell line	Treatment	*MF*
MCF-12A	2 Gy + AG-1478	0.90 ± 0.10
	2 Gy + NVP-BEZ235	1.10 ± 0.13
	2 Gy + ABT-263	0.90 ± 0.13
MDA-MB-231	2 Gy + AG-1478	1.15 ± 0.14
	2 Gy + NVP-BEZ235	1.25 ± 0.19
	2 Gy + ABT-263	1.17 ± 0.13
MCF-7	2 Gy + AG-1478	0.84 ± 0.13
	2 Gy + NVP-BEZ235	0.88 ± 0.16
	2 Gy + ABT-263	0.90 ± 0.15
MCF-12A	2 Gy + AG-1478 + NVP-BEZ235	1.50 ± 0.26
	2 Gy + NVP-BEZ235 + ABT-263	1.71 ± 0.21
	2 Gy + ABT-263 + AG-1478	0.96 ± 0.21
MDA-MB-231	2 Gy + AG-1478 + NVP-BEZ235	1.18 ± 0.16
	2 Gy + NVP-BEZ235 + ABT-263	1.23 ± 0.14
	2 Gy + ABT-263 + AG-1478	1.57 ± 0.20
MCF-7	2 Gy + AG-1478 + NVP-BEZ235	1.08 ± 0.20
	2 Gy + NVP-BEZ235 + ABT-263	1.26 ± 0.20
	2 Gy + ABT-263 + AG-1478	1.03 ± 0.21

Table 3.14B: Modifying factors (*MF*), relative to X-ray treatment alone (2 Gy), derived from the relative metabolic activities, as described in Section 2.11 for 2 human lung cell lines (normal: L132; cancer: A549), and a cervical cancer cell line (HeLa), 2 hours after treatment. Errors were calculated using error propagation formulae for ratios.

Cell line	Treatment	*MF*
L132	2 Gy + AG-1478	1.48 ± 0.10
	2 Gy + NVP-BEZ235	1.23 ± 0.09
	2 Gy + ABT-263	1.52 ± 0.12
HeLa	2 Gy + AG-1478	0.70 ± 0.11
	2 Gy + NVP-BEZ235	1.35 ± 0.13
	2 Gy + ABT-263	0.77 ± 0.09
A549	2 Gy + AG-1478	0.94 ± 0.13
	2 Gy + NVP-BEZ235	1.30 ± 0.19
	2 Gy + ABT-263	1.17 ± 0.16
L132	2 Gy + AG-1478+ NVP-BEZ235	0.93 ± 0.13
	2 Gy + NVP-BEZ235 + ABT-263	1.62 ± 0.11
	2 Gy + ABT-263 + AG-1478	0.80 ± 0.08
HeLa	2 Gy + AG-1478+ NVP-BEZ235	0.82 ± 0.07
	2 Gy + NVP-BEZ235 + ABT-263	0.76 ± 0.08
	2 Gy + ABT-263 + AG-1478	0.78 ± 0.10
A549	2 Gy + AG-1478+ NVP-BEZ235	0.84 ± 0.13
	2 Gy + NVP-BEZ235 + ABT-263	1.30 ± 0.21
	2 Gy + ABT-263 + AG-1478	0.93 ± 0.21

At 24 hours, single and combined inhibitor treatment of the MCF-12A cell line shows decreased metabolic activity, *MF* >1.0 (Table 3.15A). For both treatments, the MCF-

7 cell line showed increased activity. Except for single treatment with ABT-263, which showed increased activity in the MDA-MB-231 cell line, all other treatments had no effect. On average, all combination treatments resulted in decreased, no effect, and increased radiation-induced metabolic activity for the MCF-12A, MDA-MB-231, and MCF-7 cell lines, respectively.

In the L132 cell line, single inhibitor treatment resulted in a reduction in metabolic activity, except for ABT-263 which showed an increase (Table 3.15B). Combination treatment with AG-1478/NVP-BEZ235, NVP-BEZ235/ABT-263, and ABT-263/AG-1478 led to decreased, no effect, and increased activity in these cells, respectively. Radiation-induced metabolic activity increased across the board, 2 hours after all treatments in the HeLa cell line. Except for treatment with AG-1478 which showed no effect, the other inhibitors showed a decrease in metabolic activity in the A549 cell line. All combination treatments, however, showed an increase in metabolic activity.

Table 3.15A: Modifying factors (*MF*), relative to X-ray treatment alone (2 Gy), derived from the relative metabolic activities, as described in Section 2.11 for 3 human breast cell lines (normal: MCF-12A; cancer: MCF-7, MDA-MB-231), 24 hours after treatment. Errors were calculated using error propagation formulae for ratios.

Cell line	Treatment	*MF*
MCF-12A	2 Gy + AG-1478	1.09 ± 0.09
	2 Gy + NVP-BEZ235	1.15 ± 0.20
	2 Gy + ABT-263	1.43 ± 0.10
MDA-MB-231	2 Gy + AG-1478	1.00 ± 0.10
	2 Gy + NVP-BEZ235	0.99 ± 0.21
	2 Gy + ABT-263	0.51 ± 0.10
MCF-7	2 Gy + AG-1478	0.67 ± 0.14
	2 Gy + NVP-BEZ235	0.83 ± 0.11
	2 Gy + ABT-263	0.62 ± 0.10
MCF-12A	2 Gy + AG-1478 + NVP-BEZ235	1.55 ± 0.18
	2 Gy + NVP-BEZ235 + ABT-263	1.37 ± 0.17
	2 Gy + ABT-263 + AG-1478	1.17 ± 0.08
MDA-MB-231	2 Gy + AG-1478 + NVP-BEZ235	1.10 ± 0.18
	2 Gy + NVP-BEZ235 + ABT-263	1.01 ± 0.15
	2 Gy + ABT-263 + AG-1478	1.13 ± 0.20
MCF-7	2 Gy + AG-1478 + NVP-BEZ235	0.69 ± 0.11
	2 Gy + NVP-BEZ235 + ABT-263	0.90 ± 0.17
	2 Gy + ABT-263 + AG-1478	0.41 ± 0.06

Table 3.15B: Modifying factors (*MF*), relative to X-ray treatment alone (2 Gy), derived from the relative metabolic activities, as described in Section 2.11 for 2 human lung cell lines (normal: L132; cancer: A549), and a cervical cancer cell line (HeLa), 24 hours after treatment. Errors were calculated using error propagation formulae for ratios.

Cell line	Treatment	*MF*
L132	2 Gy + AG-1478	1.30 ± 0.12
	2 Gy + NVP-BEZ235	1.63 ± 0.21
	2 Gy + ABT-263	0.80 ± 0.10
HeLa	2 Gy + AG-1478	1.29 ± 0.07
	2 Gy + NVP-BEZ235	1.88 ± 0.34
	2 Gy + ABT-263	2.54 ± 0.27
A549	2 Gy + AG-1478	1.00 ± 0.08
	2 Gy + NVP-BEZ235	1.38 ± 0.10
	2 Gy + ABT-263	1.40 ± 0.13
L132	2 Gy + AG-1478 + NVP-BEZ235	1.59 ± 0.14
	2 Gy + NVP-BEZ235 + ABT-263	0.96 ± 0.16
	2 Gy + ABT-263 + AG-1478	0.58 ± 0.06
HeLa	2 Gy + AG-1478 + NVP-BEZ235	2.13 ± 0.26
	2 Gy + NVP-BEZ235 + ABT-263	2.14 ± 0.14
	2 Gy + ABT-263 + AG-1478	2.11 ± 0.16
A549	2 Gy + AG-1478 + NVP-BEZ235	0.84 ± 0.13
	2 Gy + NVP-BEZ235 + ABT-263	0.77 ± 0.09
	2 Gy + ABT-263 + AG-1478	0.74 ± 0.22

At 52 hours, all treatments tended to decrease (*MF* > 1.0) metabolic activity in the MCF-12A cell line (Table 3.16A). Treatment with AG-1478 increased activity in the

MDA-MB-231 cell line, whereas the other inhibitors showed a decrease. NVP-BEZ235 and ABT-263 combination treatment of these cells resulted in increased metabolic activity, while the other inhibitor combinations showed a decrease. Except for AG-1478 treatment in MCF-7 cells, which showed a decrease, all other treatments resulted in an increase in metabolic activity.

On average, metabolic activity in the L132 cell line for all treatments tended to decrease (Table 3.16B). For the cervical cell line (HeLa), all treatments showed an increase in metabolic activity ($MF < 1.0$). In general, all treatments resulted in increased metabolic activity in the A549 cell line.

Table 3.16A: Modifying factors (*MF*), relative to X-ray treatment alone (2 Gy), derived from the relative metabolic activities, as described in Section 2.11 for 3 human breast cell lines (normal: MCF-12A; cancer: MCF-7, MDA-MB-231), 52 hours after treatment. Errors were calculated using error propagation formulae for ratios.

Cell line	Treatment	*MF*
MCF-12A	2 Gy + AG-1478	1.94 ± 0.36
	2 Gy + NVP-BEZ235	1.32 ± 0.25
	2 Gy + ABT-263	1.55 ± 0.31
MDA-MB-231	2 Gy + AG-1478	0.84 ± 0.01
	2 Gy + NVP-BEZ235	1.05 ± 0.08
	2 Gy + ABT-263	1.33 ± 0.73
MCF-7	2 Gy + AG-1478	1.24 ± 0.24
	2 Gy + NVP-BEZ235	0.59 ± 0.15
	2 Gy + ABT-263	0.88 ± 0.13
MCF-12A	2 Gy + AG-1478 + NVP-BEZ235	1.06 ± 0.23
	2 Gy + NVP-BEZ235 + ABT-263	1.33 ± 0.26
	2 Gy + ABT-263 + AG-1478	1.04 ± 0.23
MDA-MB-231	2 Gy + AG-1478 + NVP-BEZ235	1.26 ± 0.23
	2 Gy + NVP-BEZ235 + ABT-263	0.90 ± 0.13
	2 Gy + ABT-263 + AG-1478	2.51 ± 0.29
MCF-7	2 Gy + AG-1478 + NVP-BEZ235	0.60 ± 0.10
	2 Gy + NVP-BEZ235 + ABT-263	0.60 ± 0.08
	2 Gy + ABT-263 + AG-1478	0.29 ± 0.05

Table 3.16B: Modifying factors (*MF*), relative to X-ray treatment alone (2 Gy), derived from the relative metabolic activities, as described in Section 2.11 for 2 human lung cell lines (normal: L132; cancer: A549), and a cervical cancer cell line (HeLa), 52 hours after treatment. Errors were calculated using error propagation formulae for ratios.

Cell line	Treatment	*MF*
L132	2 Gy + AG-1478	1.12 ± 0.11
	2 Gy + NVP-BEZ235	1.12 ± 0.11
	2 Gy + ABT-263	1.07 ± 0.11
HeLa	2 Gy + AG-1478	0.64 ± 0.08
	2 Gy + NVP-BEZ235	0.51 ± 0.09
	2 Gy + ABT-263	0.38 ± 0.05
A549	2 Gy + AG-1478	0.95 ± 0.06
	2 Gy + NVP-BEZ235	0.96 ± 0.08
	2 Gy + ABT-263	0.86 ± 0.06
L132	2 Gy + AG-1478 + NVP-BEZ235	1.59 ± 0.24
	2 Gy + NVP-BEZ235 + ABT-263	1.01 ± 0.09
	2 Gy + ABT-263 + AG-1478	1.61 ± 0.20
HeLa	2 Gy + AG-1478 + NVP-BEZ235	0.68 ± 0.08
	2 Gy + NVP-BEZ235 + ABT-263	0.68 ± 0.08
	2 Gy + ABT-263 + AG-1478	0.28 ± 0.03
A549	2 Gy + AG-1478 + NVP-BEZ235	0.90 ± 0.07
	2 Gy + NVP-BEZ235 + ABT-263	0.91 ± 0.09
	2 Gy + ABT-263 + AG-1478	0.88 ± 0.20

3.8. Relationship between Changes in Radiosensitivity and Metabolic Activity

To determine whether there is a link between inhibitor-mediated radiosensitivity modulation and treatment-induced changes in metabolic activity, the modifying factors (*MF*) derived from cell survival and metabolic activity, as described in Sections 2.9 and 2.11, were plotted as depicted in Figure 3.21. The metabolic activity data for the 0.5-hour window was chosen, as it was the most consistent time point across inhibitors, singly and in combination.

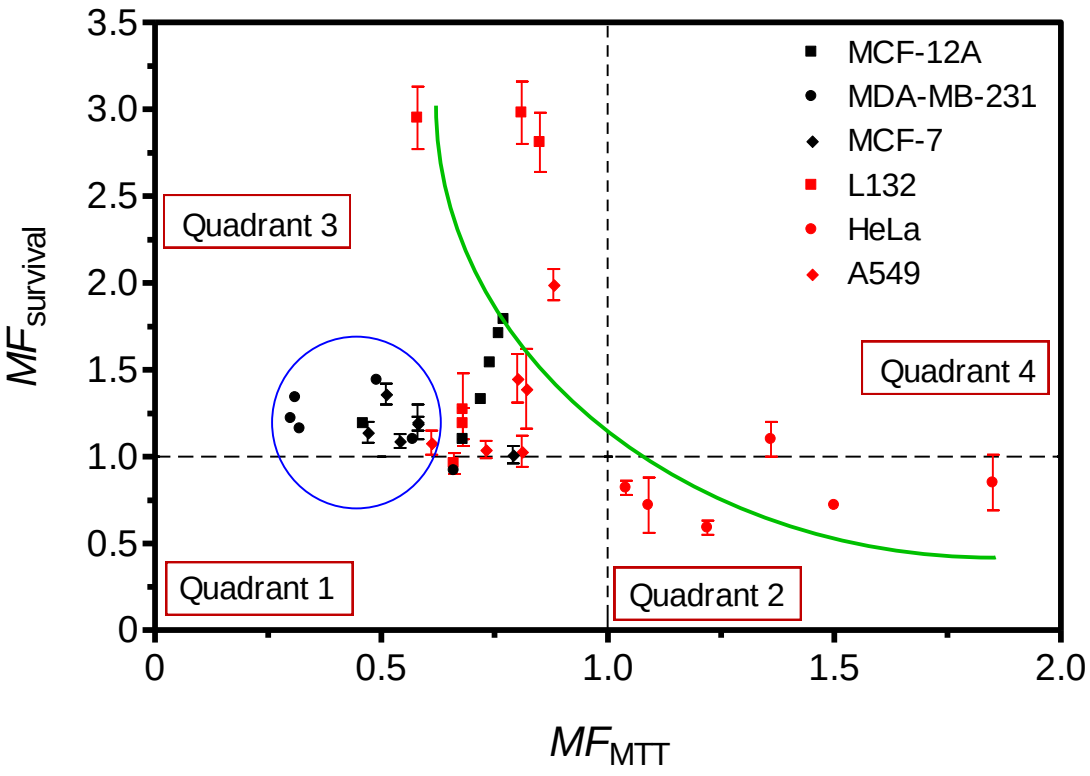

Figure 3.21: A summary plot of modifying factors from clonogenic cell survival as a function of modifying factors from metabolic activity (measured 0.5 hours after treatment) for six human cell lines irradiated in the presence of specific inhibitors of EGFR, PI3K and mTOR, and Bcl-2. Quadrants 1 and 3: increased metabolic activity; Quadrants 2 and 4: decreased metabolic activity; Quadrants 1 and 2: radioprotection; Quadrants 2 and 4: radiosensitisation. Dashed lines represent no treatment-induced effect.

The area of this scatter plot was divided into 4 quadrants by the lines representing MF_{MTT} and $MF_{survival}$ equal to 1.0, where pre-treatment with inhibitors have no effect. When the data points of the breast cancer cell lines (MDA-MB-231 and MCF-7) which tended to cluster at the lower edge of Quadrant 3 (minimal radiosensitisation with increased metabolic activity; blue ring), a high level of radiosensitisation appeared to be linked to enhanced metabolic activity ($MF_{MTT} < 1.0$). On the other hand, a reduction in metabolic activity ($MF_{MTT} < 1.0$) corresponds to enhanced radioresistance as seen for the HeLa cell line (Quadrant 2). Quadrants 1 and 4 are mostly devoid of data points, suggesting a potential link between metabolic changes and radiosensitisation may be represented by the solid green curve (Figure 3.21).

CHAPTER 4

4. DISCUSSION

Radiotherapy is a standard form of cancer patient care, as it provides tumour control and is a complementary therapeutic option for surgery and chemotherapy. Despite these essential roles and the enhancement in the efficiency of radiotherapy over the past decades, tumour radioresistance and normal tissue toxicity remain clinical obstacles. The development of novel treatment protocols, which maximise the effect of radiation by reducing tumour radioresistance and limiting adverse normal tissue effects, are thus warranted.

This study investigated the effect that inhibiting survival proteins (EGFR, PI3K/mTOR, Bcl-2) would have on the radiosensitivity of cancer cell lines (MDA-MB-231, MCF-7, HeLa, A549) and apparently normal cell lines (MCF-12A and L132) (non-cancerous cells derived from human breast and lung tissue that have been transformed for cell culture research). The development of novel treatment strategies that may broaden the therapeutic window of radiotherapy for cancers of the breast, lung and cervix was also assessed. The effect of concurrent inhibitor and radiation therapy on the metabolic activity of these cells was also evaluated, to determine whether a correlation exists between cellular radiosensitivity and metabolic activity. The outcomes of this study were derived from evaluating experimental protocols, described in Sections 2.1-2.12, in cell lines derived from humans. This may warrant further investigation in a clinical setting to determine the effect of a combined inhibitor and X-ray treatment modalities would have on cancer patients.

4.1. Intrinsic Radiosensitivity

The intrinsic radiosensitivity of the triple negative breast cancer cell line (MDA-MB-231), the subluminal A subtype of breast cancer cell line (MCF-7), the apparently normal breast cell line (MCF-12A), the cervical cancer cell line (HeLa), the lung carcinoma cell line (A549), and the apparently normal lung cell line (L132), was determined, using the colony forming assay (Figures 3.1 and 3.2). The overall rank order of increasing radiosensitivity was found to be L132 → A549 → MCF-12A → HeLa → MDA-MB-231 → MCF-7. Based on the surviving fraction at 2 Gy, the lung cancer cell line emerged as ~1.6 to 3-fold more radioresistant than the other cancer cell lines, with breast cancer cell lines being the most radiosensitive. A similar trend in radiosensitivity of the breast cell lines was also previously demonstrated (Hamunyela et al., 2015). The finding that the normal lung cell line (L132) is relatively more radioresistant than its malignant counterpart (A549) suggests that radiotherapy of lung cancers with features similar to those of A549 cells might have therapeutic benefit. It is also conceivable that a larger benefit can be derived from radiotherapy of breast cancers akin to the cell lines used here, considering the lung as a critical organ of interest.

Radiation targets cellular DNA and may induce lesions which lead to programmed cell death (apoptosis), if these DNA lesions are not efficiently repaired (Roos et al., 2016). In the presence of DNA damage, the activation of the p53 gene occurs to promote DNA repair, cell cycle arrest, and apoptosis (Shen et al., 2014). The MCF-7 and MCF-12A cell lines express wild-type p53 (Berglind et al., 2008; Synnott et al., 2017). However, the p53 gene has been reported to be mutated in the MDA-MB-231

cell line (Berglind et al., 2008). Despite the critical role that the p53 gene may play in the response of these cell lines to DNA damage, the current trend in radiosensitivity of these breast cell lines cannot be attributed to its status. However, it was suggested that the disparity in radiosensitivity of this panel of breast cell lines may be due to differences in PI3K expression (Hamunyela et al., 2015). While the relatively more radioresistant MDA-MB-231 and MCF-12A cell lines express wild-type PI3K, PI3K is mutated in the MCF-7 cell line (Vasudevan et al., 2009; Carlson et al., 2010). The mutation of PI3K in MCF-7 may reduce PI3K/mTOR signalling and affect their ability of these cells to recover from radiation-induced damage (Hamunyela et al., 2015).

The HeLa cell line has been reported to have a wild-type p53 gene that has been degraded by the E6 protein of the human papilloma virus (HPV) (Kralj et al., 2003, Marinez-Zapien et al., 2016, Fischer et al., 2017). The destruction of the p53 gene could inhibit the ability of the infected cervical cell line to initiate DNA repair or apoptotic pathways as a response to genotoxic agents like ionising radiation. These DNA repair aberrant cells may continue to proliferate, even after exposure to X-ray irradiation, and emerging relatively more radioresistant.

The A549 and L132 cell lines have been reported to be p53 wild-type (Takeyama et al., 2004; Berglind et al., 2008). This may explain the relatively higher radioresistance observed in these cell lines. The SF_2 found in this study for the A549 is similar to that reported by Wouters and colleagues when the cells were irradiated with Linear Accelerator (LINAC) generated X-rays (Wouters et al., 2010). Also, the mean inactivation doses for the L132 and A549 cell lines obtained in this study are

comparable to those obtained Verheye-Dua and Böhm in this laboratory over two decades ago when the cells were irradiated with ^{60}Co γ-rays (Verheye-Dua and Böhm, 1998). This indicates that when L132 and A549 is exposed to ^{60}Co γ-rays or X-rays the relative biological effectiveness would be approximately 1.0, suggesting that similar dose of each form radiation would be required to achieve the same biological effect.

4.2. Therapeutic Potential of X-rays

The clonogenic data, presented in Figures 3.1 - 3.2 and summarised in Table 3.1, was also used to evaluate the relative sensitivity of each cancer cell line to X-rays. For this, the D_{50} values of the cancer cell lines were compared to those of the normal cells lines, to determine whether potential therapeutic benefit may be derived in a radiotherapy setting for cancers with features similar those of the panel of cells used here.

These data demonstrated that a significant potential for therapeutic benefit may be derived from treating breast tumour cell lines (MDA-MB-231, MCF-7) with X-ray radiation. Subik and colleagues studied the molecular classification of 17 commonly used breast cell lines for studies, and showed that MDA-MB-231 and MCF-7 cell lines expressed the epidermal growth factor receptor (EGFR) at lower levels, while the apparently normal cell line (MCF-12A) had an approximately 2-fold higher expression (Subik et al., 2010). However, this may not be a sufficient rationale for the almost 3-fold relative sensitivity to X-rays seen in the MCF-7 cell line. A study by Toulany and colleagues has provided evidence that EGFR may activate PI3K to

stimulate the survival and proliferation pathways, particularly after exposure to radiation (Toulany et al., 2007). The mutation in the PI3K gene in the MCF-7 cell line, as previously mentioned may prevent this activating signal from being carried down the pathway to affect the ability of cells to repair DNA damage, proliferate, and survive. This could provide an opportunity for the wild-type p53 gene to initiate the apoptotic pathway, and lead to the relatively high radiosensitivity in the MCF-7 cell line.

Studies have reported that HPV-positive cell lines are more radiosensitive than their HPV-negative counterparts (Vozenin et al., 2010; Pang et al., 2011; Datta et al., 2015). Thus, a molecular component may be uniquely regulating the radiosensitivity of the HeLa cell line. These cells express a non-mutated EGFR at attenuated levels (Lida et al., 2011; Zhang et al., 2015). The difference in radiosensitivity of HeLa and MCF-12A may, thus, be attributed to their respective levels of EGFR expression. This may provide a rationale for the observed relative sensitivity and potential therapeutic advantage of treating HeLa cells with X-ray irradiation.

No statistically significant therapeutic advantage was demonstrated when the lung carcinoma cell line (A549) relative to the apparently normal cell line (L132). This may be attributed to the fact that these cell lines are p53 wild-type and may be responding to X-ray irradiation similarly. Also, the absence of a significant difference in the radiosensitivity of these cell lines cannot be justified by EGFR expression. While the A549 cell line is known to express high surface levels of EGFR (Jaramillo et al., 2006), the L132 cell line expresses lower levels of this essential survival protein (Sundarraj et al., 2014). EGFR is the activating component for a variety of

signalling pathways, including the MAPK-Erk, PI3K-Akt and STAT pathways (Cortas et al., 2007; Ai et al., 2017). The signal transducers and activators of transcription (STAT) pathway consists of a family of proteins, which play a crucial role in cell proliferation and apoptosis (Haricharan and Li, 2014). A study by Yoon and colleagues reported that A549 cells express a higher level of STAT4, while L132 cells expresses similar or slightly higher levels of other STAT proteins (Yoon et al., 2019). This may provide DNA repair and growth advantages for the L132 cell line, and explain the slightly higher sensitivity of the A549 cell line. These cell lines have been shown to be generally DNA repair proficient (Roos et al., 2000; Dittmann et al., 2005; Shin et al., 2009; Kim et al., 2012), a possible feature supporting their higher radioresistance in comparison with the breast and cervical cell lines.

4.3. Inhibitor Cytotoxicity

Clonogenic survival demonstrated that, for MDA-MB-231, MCF-7, MCF-12A, HeLa, A549 and L132, the NVP-BEZ235 treatment had the most potency (highest cell kill) (molar per molar), followed by ABT-263, and AG-1478 being the least potent. This trend seems to indicate that the survival of the cancer and apparently normal cell lines, used in this study, largely depends on the signalling of PI3K and mTOR. It can also be deduced from this trend that targeting multiple proteins may be more effective in managing cancer.

Of the breast cell lines, the MCF-7 cell line required the lowest concentration of the PI3K/mTOR inhibitor (NVP-BEZ235) for 50% of its cell population to die. This NVP-BEZ235-induced cell death may be attributed to an ER-mediation of PI3K activity

(Pozo-Guisado et al., 2002), as the MCF-12A and MDA-MB-231 cell lines are ER-negative (Subik et al., 2010) and may not be susceptible to ER-mediation. MDA-MB-231 required the highest concentration of the Bcl-2 inhibitor (ABT-263) for these levels of cell death, indicating that a p53 mutation may confer Bcl-2 inhibitor resistance as the MCF-7 and MCF-12A cell lines possess wild-type p53 (Berglind et al., 2008; Synnott et al., 2017). A greater resistance to EGFR inhibition was observed in the MCF-12A cell line. This was expected, as these cells are reported to have a higher expression of EGFR by Subik and colleagues (Subik et al., 2010).

Of all the cell lines used in this study, the HeLa cell line required the lowest concentration of NVP-BEZ235 for a 50% cell killing, indicating that the PI3K/mTOR may play a major role in its cell survival. This could also indicate that inhibiting more than one protein of the same pathway may have a greater effect on cell inactivation than when a single survival protein is inhibited. The low expression of EGFR by HeLa cells, as reported by Lida and colleagues (Lida et al., 2011), could have resulted in these cells requiring a lower concentration of the EGFR inhibitor (AG-1478) than the other cell lines in this study. Maldonado and colleagues reported that the low Bcl-2 expression observed in HeLa cells may not be solely due to the corrupted p53 gene (Maldonado et al., 1997). This low Bcl-2 expression may have impacted the concentration of ABT-263 needed to achieve a 50% killing, as the number of binding sites for the inhibitor would be expected to be low.

Despite the observation that the A549 cell line has a high surface expression of EGFR and exhibits low to intermediate sensitivity to EGFR inhibition (Jaramillo et al., 2006; 2008), these cells required less AG-1478 than the apparently normal lung cell line (L132) to reach 50% toxicity. The L132 cell line has a lower expression of EGFR,

and yet required a higher concentration of AG-1478 to reach 50% cell killing. This indicates that these cells are resistant to AG-1478 inhibition. This may be linked to resistance to PI3K/mTOR inhibition seen in the L132 cells, as EGFR is an activating protein for the PI3K/mTOR pathway (Maira et al., 2008). It is also likely that NVP-BEZ235 may have been required in lower concentrations than AG-1478 and ABT 263 in the A549 and L132 cell lines, as it is a dual inhibitor. A relatively lower to undetectable expression of Bcl-2 has been suggested for the A549 cell line which has been reported to be resistant to ABT-263 (Han et al., 2015). In this study, the higher EC_{50}-value of ABT-263 for the A549 cell line (Table 3.5) indicates that these cells are more resistant to Bcl-2 inhibition than the L132 cells. A study by Pezzella and colleagues reported detectable Bcl-2 expression levels in tumour samples from cancer patients and basal cells of normal lung tissue (Pezzella et al., 1993). This may provide a rationale for the observed difference in ABT-263 sensitivity between A549 and L132.

4.4. Therapeutic potential of AG-1478, NVP-BEZ235 and ABT-263

The cytotoxic effects of AG-1478, NVP-BEZ235 and ABT-263 are concentration dependent (Figure 3.4 - 3.8). The corresponding EC_{50}-values for MDA-MB-231 for each inhibitor produced relative sensitivities ranging from 0.24 - 1.04 (Table 3.6), suggesting that no potential therapeutic benefit may be derived from treating MDA-MB-231 cells with EC_{50} concentrations of AG-1478, NVP-BEZ235 or ABT-263, as these levels of inhibitors might adversely affect the apparently normal cells (MCF-12A), were there to represent normal tissue. A ~2-fold enhancement in the relative sensitivity was observed in the MCF-7 cell line, when cells were treated with the

EGFR inhibitor (AG-1478). This was expected, as the apparently normal cell line (MCF-12A) is shown to have a 2-fold higher expression of EGFR than the MCF-7 cells (Subik et al., 2010). A higher expression of the target protein would require a higher concentration of the corresponding inhibitor to inactivate it to a given extent. Inhibition of EGFR in breast cancers with characteristics similar to those of the MCF-7 cell line may yield a therapeutic benefit.

On average, the HeLa cells were 7- and 52-fold more sensitive to AG-1478 and NVP-BEZ235 treatment, compared to MCF-12A cells, indicating a potential therapeutic benefit for EGFR and PI3K/mTOR inhibition in cervical cancer. This may be attributed to the expression of EGFR in the MCF-12A and HeLa cell lines being high and low, respectively.

The approximately 7-fold higher sensitivity of the A549 cell line to NVP-BEZ235 treatment than the apparently normal cells (L132), also indicates a potential therapeutic benefit in inhibiting PI3K and mTOR in lung cancer. The high sensitivity of the A549 cells to PI3K and mTOR inhibition may be due to the higher expression of EGFR, which might lead to an increase in PI3K/mTOR signalling in the cells, making them vulnerable to NVP-BEZ235.

4.5. Inhibitor Interaction

The combination indices (*CI*) for the AG-1478/NVP-BEZ235, AG-1478/ABT-263 and ABT-263/NVP-BEZ235 cocktails for all breast cell lines ranged between 0.0237 and 0.4683 (Table 3.8), indicating that the inhibitor-inhibitor interaction varied from very

strong synergism to synergism for each inhibitor combination (Chou, 2006). The rank order of increasing synergism for all three cocktails in the breast cell lines emerged to be MCF-12A → MCF-7 → MDA-MB-231. Specifically, the findings for the ABT-263/NVP-BEZ235 cocktail are consistent with those reported by Hamunyela and colleagues (Hamunyela et al., 2017).

The combination indices for the same inhibitor cocktails for the HeLa cell line ranged from 0.0100 to 4.0835 (Table 3.10), indicating a very strong synergism in all cases, except for the cervical cell line (HeLa) in which cocktails containing NVP-BEZ235 showed strong antagonism. The reason for this antagonism is not clear, but a multi-target inhibition in cervical cancer might not yield desirable results. The very strong synergistic interaction between inhibitors of all cocktails in the A549 and L132 cell lines (Table 3.10), seems to suggest that although multiple inhibition of EGFR, PI3K/mTOR, and Bcl-2 in in lung cancer might be beneficial, the potential for inducing a significant level of normal tissue toxicity exists.

4.6. Radiomodulation by Inhibitors

In this study, pre-treating MCF-12A cells with NVP-BEZ235 or ABT-263 before to X-ray irradiation significantly enhanced the radiosensitivity. These cells have been reported to show a high level of EGFR expression (Subik et al., 2010). As EGFR is the activating protein for the PI3K/Akt/mTOR pathway (Cortas et al, 2007; Ai et al., 2017), it is conceivable that the level of intrinsic PI3K/mTOR activity would be high in the MCF-12A cell line. Inhibition of this increased signal before X-ray exposure could increase the susceptibility of the cells to undergo radiation-induced death, hence the

enhancement in radiosensitivty observed after NVP-BEZ235 pre-treatment. Ionising radiation may induce the activation of an apoptotic process, which is regulated by Bcl-2 family (Maier et al., 2016). Inhibiting Bcl-2 may hinder it from performing its regulatory function, and enhance apoptotic cell death. This may provide the rationale for an increase in radiosensitivity of ABT-263 pre-treated MCF-12A cells. A significant enhancement in radiosensitivity was also observed, when the MCF-12A cells were pre-treated with an inhibitor cocktail of AG-1478 and NVP-BEZ235. This could be a reflection of the synergistic interaction between the inhibitor components (Table 3.8). Similarly, a significant radiosensitisation occurred when MDA-MB-231 cells were pre-treated with the AG-1478/NVP-BEZ235 and NVP-BEZ235/ABT-263 cocktails. The strong synergism between the inhibitors of these cocktails may also have potentiated radiation-induced cell killing.

The ER-positive breast carcinoma cell line (MCF-7) showed a 36% enhancement in radiosensitivity, when pre-treated with an NVP-BEZ235/ABT-263 cocktail, and a 19% enhancement when pre-treated with an ABT-263/AG-1478 cocktail. The increase in radiosensitivity may be attributed to the very strong synergism between the inhibitors that constitute these cocktails.

A ~3-fold enhancement in radiosensitivity was observed when the apparently normal lung cell line (L132) was pre-treated with NVP-BEZ235. A similar enhancement in radiosensitivity was seen when these cells were pre-treated with the AG-1478/NVP-BEZ235 and NVP-BEZ235/ABT-263 cocktails. By comparison, the lung carcinoma cell line (A549) only showed a 45% enhancement in radiosensitivity, when pre-treated with NVP-BEZ235 alone and a 2-fold enhancement when pre-treated with a

cocktail of NVP-BEZ235 and ABT-263. The very strong synergy seen in the inhibitor cocktails (Table 3.10) is not correlated with a high level of radiosensitisation in these cells. Therefore, these treatment modalities may not be optimal for the management of lung cancer.

A significant reduction in radiosensitivity was seen in the HeLa cell line following pre-treated with ABT-263 alone, an NVP-BEZ235/ABT-263 cocktail, or an ABT-263/AG-1478 cocktail. This may be due to the HPV infection of these cells, especially for the ABT-263. In these cells, the p53 gene is degraded by the E6 protein of the human papillomavirus (Kralj et al., 2003; Marinez-Zapien et al., 2016, Fischer et al., 2017). This degradation may render p53 incapable of initiating the pro-apoptotic pathway and unable to maintain the Bcl-2/Bax balance, thereby, making the cells evade radiation-induced p53-mediated cell death. The strong antagonism between the inhibitors of the cocktails might be the reason for the radioprotection of HeLa cells (Tables 3.10 and 3.12).

4.7. Treatment-Induced Changes in Metabolic Activity

The metabolic activity of the MDA-MB-231, MCF-7, MCF-12, HeLa, A549 and L-132 cell lines was examined at various time points after treatment with inhibitors and 2 Gy of X-rays. The 30-minute data were chosen for further evaluation as they were the most consistent across treatments (Table 3.13A). These data indicated that for the breast cell lines, all treatment strategies resulted in an enhancement ($MF < 1$) in metabolic activity. The same trend was observed for the lung cell lines (Figure 3.21). From these data, it appeared that a synergistic inhibitor-inhibitor interaction coincides

with an enhancement in metabolic activity. This notion can be supported by the observation that the cervical cancer cell line (HeLa), in which inhibitor antagonism was exhibited, showed a reduction in metabolic activity for most all treatments.

Put together, increased metabolic activity appeared to be correlated with enhanced radiosensitisation, and *vice versa* (Figure 3.21). This finding concurs with the suggestion that reduced metabolic rates lead to radioresistance (Luk and Sutherland, 1987; Heller and Raaphorst, 1993; Moeller et al., 2005). The increase in metabolic activity, shortly after radiation treatment, may be due to cells attempting to provide energy and vital components for the DNA repair process, as cellular manipulation metabolism has been suggested as a hallmark of cancer (Wellen and Thompson, 2010; Hanahan and Weinberg, 2011; Anastasiou, 2017; Muir et al., 2017). The increased metabolic activity in the apparently normal lung cell line (L132) is not unexpected, as immortalised normal cells can be expected to acquire some survival traits of cancer cells. From the current findings, it can be deduced that therapeutic strategies that lead to increased metabolic activity in cancer cells might be beneficial as adjuvants to radiotherapy.

It may also be deduced from change in metabolic activity, 30 minutes after treatment, that non-proliferating cell are not necessarily non-metabolising. Although, a cell cycle arrest may occur after radiation-induced DNA damage (Tang et al., 2018), tumour cells may continue to repair DNA damage, which requires vital metabolites provided by an active metabolism. Thus, using an MTT assay, which

requires cells to metabolise MTT into formazan, may provide a reliable indication of treatment-induced changes in cellular metabolic activity over the short term.

CHAPTER 5

5. CONCLUSION

This study demonstrated that the breast cancer cell lines were relatively more sensitive to X-ray irradiation. While the cervical cancer cell line (HeLa) was relatively more sensitive to PI3K/mTOR and EGFR inhibition, the lung cancer cell line (A549) was more sensitive to only PI3K/mTOR and EGFR inhibition. An enhancement in radiosensitivity was demonstrated in the triple negative breast cancer cell line (MDA-MB-231) when cells were pre-treated with AG-1478/NVP-BEZ235 and NVP-BEZ235/ABT-263 cocktails. Patients presenting with cancers with characteristics akin to those of the MDA-MB-231 cell line may derive a therapeutic benefit when treated with these cocktails prior to radiotherapy. An enhancement in radiosensitivity was also seen in the ER-positive breast cancer cell line (MCF-7) when cells were pre-treated with an NVP-BEZ235/ABT-263 or ABT-263/AG-1478 cocktail. Cancers with characteristics similar to those of the MCF-7 cell line may be effectively managed with a combination of these inhibitor cocktails and radiotherapy. No potential therapeutic benefit could be demonstrate with any of the treatment strategies evaluated here for cervical cancer patients. Patients presenting with lung cancers, with characteristics similar to those of the A549 cell line, may experience an effective tumour control from the various treatment strategies, but with a potentially high level of normal tissue toxicity. Therapeutic strategies that enhance short-term metabolic activity may potentiate the efficacy of radiotherapy.

6. Possible Future Research Avenues

1. It may be interesting to validate the apparent radiosensitisation of the cancer cell lines, using lower concentrations of target inhibitors. This may provide useful information on the optimum inhibitor concentrations that can be used without inducing normal tissue toxicity.

2. It has been reported that exposing cancer cells to fractionated radiotherapy may select for the cell subpopulations which contain radioresistance characteristics (McDermott et al., 2016). This study found that breast, lung and cervical cancer cell radiosensitivity may be manipulated by pre-treating these cells with EGFR, PI3K/mTOR, and Bcl-2 inhibitors prior to exposure to X-rays. A study exposing these cells to inhibitors pre-treatment and a fractionated schedule of X-rays will assist in elucidating the true therapeutic potential of these inhibitors.

3. This study investigated the radiomodulatory effects of pre-treating breast, lung and cervical cancer cells with EGFR, PI3K/mTOR, BcL-2 inhibitors, 30 minutes prior to X-ray irradiation. It may be interesting to evaluate the radiomodulatory effects of administering these inhibitors at much earlier time points. Inhibition of targets at time points within the DNA repair window could also provide information on the potential role of the pathways of interest in the repair of radiation-induced damage.

4. Novel treatment strategies may be developed by evaluating the radiomodulatory effects of inhibiting alternative survival proteins such as, Poly(ADP-ribose) polymerase (PARP-1) (Dungey et al., 2009), heat shock protein 90 (Hsp90) (Dungey et al., 2009; Kabakov et al., 2010), insulin growth factor 1 receptor (IGF-1R) (Chitnis et al., 2014). These pathways could also be evaluated in the cellular systems used in this study.

5. This study evaluated the modulatory effects of a combination of EGFR, PI3K/mTOR, and BCl-2 inhibitors and 2-Gy dose of X-rays on the metabolic activity of cancer and normal cell lines. A study investigating the effect of inhibitor pre-treatment and doses ranging from 4-10 Gy cellular metabolic activity may provide insight into the metabolic changes that may occur at higher doses of X-ray irradiation.

6. Cytotoxic validation may be derived by using molecular protocols, such as Western blotting and flow cytometry techniques to evaluate the action of inhibitors and the preferred mode of death used by the cells.

7. The micronucleus assay may be used to assess the role of DNA damage repair in the radiomodulatory effects determined in this study.

8. A study by Patruno and colleagues found an increase in PI3K and mTOR activation after exposing human keratinocytes to an extremely low frequency electromagnetic field (ELF-EMF) (Patruno et al., 2015). Evaluating the effect of an ELF-EMF and appropriate inhibitor treatment on cancer and normal cells may

provide insight into the development of a novel treatment strategies which enhance tumour control, but limit normal tissue toxicity.

7. References

Aguirre-Ghiso JA. Models, mechanisms and clinical evidence for cancer dormancy. Nature Reviews Cancer, 2007;7:834-846.

Ai G, Shao X, Meng M, Song L, Qiu J, Wu Y, Zhou J, Cheng J, Tong X. Epidermal growth factor promotes proliferation and maintains multipotency of continuous cultured adipose stem cells via activating STAT signal pathway in vitro. Medicine, 2017;96:30 1-7.

Akudugu JM, Howell RW. A method to predict response of cell populations to cocktails of chemotherapeutics and radiopharmaceuticals: Validation with daunomycin, doxorubicin, and the alpha particle emitter ^{210}Po. Nuclear Medicine and Biology, 2012,a;39:954-961.

Akudugu JM, Howell RW. Flow cytometry-assisted Monte Carlo simulation predicts clonogenic survival of cell populations with lognormal distributions of radiopharmaceuticals and anticancer drugs. International Journal of Radiation Biology, 2012, b, 88:286-293.

Akudugu JM, Neti PVSV, Howell RW. Changes in lognormal shape parameter guide design of patient-specific radiochemotherapy cocktails. Journal of Nuclear Medicine, 2011;52:64-649.

Alessi DR, James SR, Downes CP, Holmes AB, Gaffney PR, Reese CB, Cohen P. Characterization of a 3-phosphoinositide-dependent protein kinase which phosphorylates and activates protein kinase B alpha. Current Biology, 1997;7(4): 261-269.

Allemani C, Dvaladze A, Gralow J, Yeates K, Taylor C, Oomman N, Krishnan S, Sullivan R, Kombe D, Blas MM, Parham G, Kassami N, Conteh L. Health, equity, and women's cancers 1: The global burden of women's cancers: a grand challenge in global health. The Lancet, 2017;389:847-860.

Anastasiou D. Tumour microenvironment factors shaping the cancer metabolism landscape. British Journal of Cancer, 2017;116(3):277-286.

Auger KR, Serunian LA, Soltoff SP, Libby P, Cantley LC. PDGF-dependent tyrosine phosphorylation stimulates production of novel polyphosphoinositides in intact cells. Cell, 1989;57:167-175.

Azpiazu I, Saltiel AR, DePaoli-Roach AA, Lawrence JC. Regulation of both glycogen synthase and PHAS-I by insulin in rat skeletal muscle involves mitogen-activated protein kinase-independent and rapamycin-sensitive pathways. The Journal of Biological Chemistry, 1996;271:5033-5039.

Bacus SS, Ruby SG, Weinberg DS, Chin D, Ortiz R, Bacus JW. HER-2/neu oncogene expression and proliferation in breast cancers. American Journal of Pathology, 1990;137(1):103-111.

Bajwa N, Liao C, Nikolovska-Coleska Z. Inhibitors of the anti-apoptotic Bcl-2 proteins: a patent review. Expert Opinion on Therapeutic Patents, 2012;22(1):37-55.

Bamford S, Dawson E, Forbes S, Clement J, Pettett R, Dogan A, Flanagan A, Teague J, Futreal PA, Stratton MR, Wooster R. The COSMIC (Catalogue of Somatic Mutations in Cancer) database and website. British Journal of Cancer, 2004;(91):335-358.

Baskar R, Lee KA, Yeo R, Yeoh KW. Cancer and radiation therapy: Current advances and future directions. International Journal of Medical Sciences, 2012;9(3):193-199.

Beasley M, Driver D, Dobbs HJ. Complications of radiotherapy: improving the therapeutic index. Cancer imaging, 2005; 5(1):78-84.

Begg AC, Stewart FA, Vens C. Strategies to improve radiotherapy with targeted drugs. Nature Reviews Cancer, 2011;11:239-253.

Ben-Sahra I, Howell JJ, Asara JM, Manning BD. Stimulation of de novo pyrimidine synthesis by growth signaling through mTOR and S6K1. Science, 2013;339(6125):1323-1328.

Ben-Sahra I, Hoxhaj G, Ricoult SJH, Asara JM, Manning BD. mTORC1 induces purine synthesis through control of the mitochondrial tetrahydrofolate cycle. Science, 2016;351(6274):728-733.

Ben-Sahra I, Manning BD. mTORC1 signaling and the metabolic control of cell growth. Current Opinion in Cell Biology, 2017;45:72-82.

Bentzen SM. Preventing or reducing late side effects of radiation therapy: radiobiology meets molecular pathology. Nature Reviews Cancer, 2006;6:702-713.

Berglind H, Pawitan Y, Kato S, Ishioka C, Soussi T. Analysis of p53 mutation status in human cancer cell lines: a paradigm for cell line cross-contamination. Cancer Biology and Therapy, 2008;7(5):699-708.

Bertotti A, Papp E, Jones S, Adleff V, Anagnostou V, Lupo B, Sausen M, Phallen J, Hruban CA, Tokheim C, Niknafs N, Nesselbush M, Lytle K, Sassi F, Cottino F, Migliardi G, Zanella ER, Ribero D, Russolillo N, Mellano A, Muratore A, Paraluppi G, Salizzoni M, Marsoni S, Kragh M, Lantto J, Cassingena A, Li QK, Karchin R, Scharpf R, Sartore-Bianchi A, Siena S, Diaz LA, Trusolino L, Velculescu VE. The genomic landscape of the response to EGFR blockade in colorectal cancer. Nature, 2015;526(7572):263-267.

Bjorge JD, Chan TO, Antczak M, Kung HJ, Fujita DJ. Activated type I phosphatidylinositol kinase is associated with the epidermal growth factor (EGF)

receptor following EGF stimulation. Proceedings of the National Academy of Sciences of the United States of America, 1990;87:3816-3820.

Black PC, Dinney CP. Growth factors and receptors as prognostic markers in urothelial carcinoma. Current Urology Reports, 2008, (9):55-61.

Boss MK, Bristow R, Dewhurst MW. Linking the History of Radiation Biology to the Hallmarks of Cancer. Radiation Research, 2014;181:561-577

Bray F, Ferlay J, Soerjomataram I, Siegel RL, Torre LA, Jemal A. Global cancer statistics 2018: GLOBOCAN estimates of incidence and mortality worldwide for 36 cancers in 185 countries. CA: A Cancer Journal for Clinicians, 2018;68:394-398.

Brown JM, Carlson DJ, Brenner DJ. The Tumour Radiobiology of SRS and SBRT:Are More Than the 5Rs involved?. Internation Journal of Radiation Oncology Biology Physics, 2014;88(2):254-262.

Bubici C, Papa S, Dean K, Franzoso G. Mutual cross-talk between reactive oxygen species and nuclear factor-kappa B: Molecular basis and biological significance. Oncogene, 2006;25:6731-6748.

Buchholz TA. Radiation therapy for early-stage breast cancer after breast-conserving surgery. The New England Journal of Medicine, 2009;360:63-70.

Burris HA. Overcoming acquired resistance to anticancer therapy: focus on the PI3K/AKT/mTOR pathway. Cancer Chemotherapy Pharmacology, 2013;71:829-842.

Cantley LC. The phosphoinositide 3-kinase pathway. Science, 2002;296:(5573):1655-1657.

Carey LA, Dees EC, Sawyer L, Gatti L, Moore DT,Collichio F, Ollila DW, Sartor CI, Graham ML, Perou CM. The triple negative paradox: primary tumor chemosensitivity of breast cancer subtypes. Clinical Cancer Research 2007;13:2329-2334.

Carlson CB, Mashock MJ, Bi K. BacMamenabled LanthaScreen® cellular assays for PI3K/Akt pathway compound profiling in disease-relevant cell backgrounds. Journal of Biomolecular Screening, 2010;15:327-334.

Carpenter G, Cohen S. Epidermal growth factor. Annual Review of Biochemistry, 1979;48:193-216.

Carpenter CL, Duckworth BC, Auger KR, Cohen B, Schaffhausen BS, Cantley LC. Purification and characterization of phosphoinositide 3-kinase from rat liver. The Journal of Biological Chemistry, 1990;265(32):19704-19711.

Castellano E, Downward J. RAS interaction with PI3K: more than just another effector pathway. Genes Cancer, 2011;(3):261-274.

Chandarlapaty S, Sakr RA, Giri D, Patil S, Heguy A, Morrow M, Modi S, Norton L, Rosen N, Hudis C, King TA. Frequent mutational activation of the PI3K-AKT pathway in trastuzumab-resistant breast cancer. Clinical Cancer Research, 2012;18:6784-6791.

Chargari C, Magne N, Guy JB, Rancoule C, Levy A, Goodman KA, Deutsch E. Optimize and refine therapeutic index in radiation therapy:Overview of a century. Cancer treatment Reviews, 2016;45:58-67.

Cheang MCU, Voduc D, Bajdik C, Leung S, McKinney S, Chia SK, Perou CM, Nielsen TO. Basal-like breast cancer defined by five biomarkers has superior prognostic value than triple-negative phenotype. Clinical Cancer Research, 2008;14(5):1368-1376.

Chen J, Almo SC, Wu Y. General principles of binding between cell surface receptors and multi-specific ligands: A computational study. PLOS Computational Biology, 2017;13(10):e1005805:1-19.

Chitnis MM, Lodhia KA, Aleksic T, Gao S, Protheroe AS, Macaulay VM. IGR-1R inhibition enhances radiosensitivity and delays double-strand break repair by both non-homologous end-joining and homologous recombination. Oncogene, 2014;33(45):5262-5273.

Chou TC. Theoretical basis, experimental design, and computerized simulation of synergism and antagonism in drug combination studies. Pharmacological Reviews, 2006;58(3):621-681.

Colombo N, Carinelli S, Columbo A, Marini C, Rollo D, Sessa C. Cervical cancer: ESMO Clinical Practice Guidelines for diagnosis, treatment and follow-up. Annals of Oncology, 2012;23(7):27-32.

Conciatori F, Ciuffreda L, Bazzichetto C, Falcone I, Pilotto S, Bria E, Cognetti F, Milella M. mTOR cross-talk in cancer and potential for combination therapy. Cancers, 2018;10(1):1-30.

Conte A, Sigismund S. Chapter Six- The Ubiquitin Network in the Control of EGFR Endocytosis and Signalling. Progress in molecular biology and translational science, 2016;141:225-276.

Contessa JN, Hampton J, Lammering G, Mikkelsen RB, Dent P, Valerie K, Schmidt-Ullrich RK. Ionizing radiation activates Erb-B receptor dependent Akt and p70 S6 kinase signalling in carcinoma cells. Oncogene, 2002;21:4032-4041.

Cornforth MN, Loucas BD. A cytogenetic profile of radiation damage. Radiation Research, 2019;191:1-19.

Cortas T, Eisenberg R, Fu P, Kern J, Patrick L, Dowlati A. Activation state egfr and STAT-3 as prognostic markers in resected non-small cell lung cancer. Lung Cancer, 2007; 55:349-355.

Czabotar PE, Lessene G, Strasser A, Adams JM. Control of apoptosis by the BCL-2 protein family: implications for physiology and therapy. Nature Reviews Molecular Cell Biology, 2014;15(1):49-63.

Datta NR, Singh S, Kumar P, Gupta D. Human papillomavirus confers radiosensitivity in cancer cervix: a hypothesis toward a possible restoration of apoptotic pathways based on clinical outcomes. Future Oncology, 2015;11(9):1-9.

DeBerardinis RJ, Thompson CB. Cellular metabolism and disease: what do metabolic outliers teach us? Cell, 2012;148(6):1132-1144.

Desouky O, Ding N, Zhou G. Target and non-target effects of ionizing radiation. Journal of Radiation and Applied Sciences, 2015;8:247-254.

Deurs B. Differential effects of EGFR ligands on endocytic sorting of the receptor. Traffic, 2009;10:1115-1127.

Dittmann K, Mayer C, Rodemann H-P. Inhibition of radiation-induced EGFR nuclear import by C225 (Cetuximab) suppresses DNA-PK activity. Radiotherapy and Oncology, 2005;76:157-161.

Dowling RJ, Topisirovic I, Alain T, Bidinosti M, Fonseca BD, Petroulakis E, Wang X, Larsson O, Selvaraj A, Liu Y, Kozma SC, Thomas G, Sonenberg N. mTORC1-mediated cell proliferation, but not cell growth, controlled by the 4E-BPs. Science, 2010;328(5982):1172-1176.

Dungey FA, Caldecott KW, Chalmers AJ. Enhanced radiosensitization of human glioma cells by combining inhibition of poly(ADP-ribose) polymerase with inhibition of heat shock protein 90. Molecular Cancer Therapeutics, 2009;8(8):2243-2254.

Durante M, Loeffler JS. Charged particles in radiation oncology. Nature Reviews Clinical Oncology, 2010;7:37-43.

Duru N, Fan M, Candar D, Menad C, Liu HC, Nantajit D, Wen Y, Xiao K, Eldridge A, Chromy BA, Li S, Spits DR, Lam KS, Wicha MS, Li JJ. HER-2-associated radioresistance of breast cancer stem cells isolated from HER-2-negative breast cancer cells. Clinical Cancer Research, 2012;18:6634-6647.

Duvel K, Yecies JL, Menon, S, Raman P, Lipovsky AI, Souza AL, Triantafellow E, Ma Q, Gorski R, Cleaver S, Vander Heiden MG, MacKeigan JP, Finan PM, Clish CB, Murphy LO, Manning BD. Activation of a metabolic gene regulatory network downstream of mTOR complex 1. Molecular Cell, 2010;39(2):171-183.

Earnshaw WC, Martins LM, Kaufmann SH. Mammalian caspases: structure, activation, substrates and functions during apoptosis, Annual Review of Biochemistry, 1999;68:383-424.

Eccles SA. The epidermal growth factor receptor/Erb-B/HER family in normal and malignant breast biology. International Journal of Developmental Biology, 2011;55:685-96.

Elstrom RL, Bauer DE, Buzzai M, Karnauskas R, Harris MH, Plas DR, Zhuang H, Cinalli RM, Alavi A, Rudin CM, Thompson CB. Akt stimulates aerobic glycolysis in cancer cells. Cancer Research, 2004;64(11):3892-3899.

Engelman JA. Targeting PI3K signalling in cancer: opportunities, challenges and limitations. Nature Reviews Cancer, 2009;9:550-562.

Escriva M, Peiro S, Herranz N, Villagrasa P, Dave N, Montserrat-Sentis B, Murray SA, Franci C, Gridley T, Virtanen I, De Herreros AG. Repression of PTEN phosphatase by snail1 transcriptional factor during gamma radiation-induced apoptosis. Molecular and Cellular Biology, 2008;28:1528-1540.

Feng Z, Zhang H, Levine AJ, Jin S. The coordinate regulation of the p53 and mTOR pathways in cells. Proceedings of the National Academy of Sciences of the United States of America, 2005;102(23):8204-8209.

Fernandez-de-Cossio-Diaz J, Vazquez A. A physical model of cell metabolism. Scientific Reports, 2018;8(1):8349.

Fertil B, Dertinger H, Course A, Malaise EP. Mean inactivation dose: a useful concept for intercomparison of human cell survival curves. Radiation Research, 1984;99:73-84.

Fingar DC, Salama S, Tsou C, Harlow E, Blenis J. Mammalian cell size is controlled by mTOR and its downstream targets S6K1 and 4EBP1/eIF4E. Genes and Development, 2002;16(12):1472-1487.

Fischer M, Uxa S, Stanko C, Magin TM, Engeland K. Human papilloma virus E7 oncoprotein abrogates the p53- p21-DREAM pathway. Scientific Reports, 2017;7(2603):1-11.

French AR, Tadaki DK, Niyogi SK, Lauffenburger DA. Intracellular trafficking of epidermal growth factor family ligands is directly influenced by the pH sensitivity of the receptor/ligand interaction. Journal of Biological Chemistry, 1995;270:4334-4340.

Fruman DA, Rommel C. PI3K and cancer: Lessons, challenges and opportunities. Nature Reviews Drug Discovery, 2014;13(2):140-156.

Fruman DA, Cantley LC. Phosphoinositide 3-kinase in immunological systems. Seminars in Immunology, 2002;14:7-18.

Gallo O, Chiarelli I, Boddi V, Bocciolini C, Bruschini L, Porfirio B. Cumulative prognostic value of p53 mutations and bcl-2 protein expression in head-and-neck cancer treated by radiotherapy. International Journal of Cancer, 1999;84(6):573-579.

Gan X, Wang J, Wang C, Sommer E, Kozasa T, Srinivasula S, Alessi D, Offermanns S, Simon MI, Wu D. PRR5L degradation promotes mTORC2-mediated PKC-delta phosphorylation and cell migration downstream of Galpha12. Nature Cell Biology. 2012;14(7):686-696.

Ginsburg O, Bray F, Coleman MP, Vanderpuye V, Eniu A, Kotha SR, Sarker M, Huong TT, Allemani C, Dvaladze A, Gralow J, Yeates K, Taylor C, Oomman N, Krishnan S, Sullivan R, Kombe D, Blas M, Parham G, Kassami N, Conteh L. The global burden of women's cancer: an unmet grand challenge in global health. The Lancet, 2017;389(10071):847-860.

Ginsberg MS, Grewal RK, Heelan RT. Lung cancer. Radiologic Clinics of North America, 2007;45(1):21-43.

Goh LK, Huang F, Woong K, Gygi S, Sorkin A. Multiple mechanisms collectively regulate clathrin-mediated endocytosis of the epidermal growth factor receptor. Journal of Cell Biology, 2015;189(5):871-883.

Goldhirsch A, Wood WC, Coates AS, Gelber RD, Thurlimann B, Senn HJ, Panel members. Strategies for subtypes—dealing with the diversity of breast cancer: highlights of the St Gallen International Expert Consensus on the Primary Therapy of Early Breast Cancer 2011. Annals of Oncology, 2011;22(8):1736-1747.

Gomes AP, Blenis J. A nexus for cellular homeostasis: the interplay between metabolic and signal pathways. Current Opinion in Biotechnology, 2015;34:110-117.

Gordan JD, Thompson CB, Simon MC. HIF and c-Myc: Sibling rivals for control of cancer cell metabolism and proliferation. Cancer Cell, 2007;12(2):108-113.

Grabiner BC, Nardi V, Birsoy K, Possemato R, Shen K, Sinha S, Jordan A, Beck AH, Sabatini DM. A diverse array of cancer-associated MTOR mutations are hyperactivating and can predict rapamycin sensitivity. Cancer Discovery, 2014;4(5):554-563.

Graus-Porta D, Beerli RR, Daly JM, Hynes NE. ErbB-2, the preferred heterodimerization partner of all ErbB receptors, is a mediator of lateral signaling. EMBO Journal, 1997;16:1647-1655.

Guadagnolo BA, Liao K-P, Elting L, Giordano S, Buchholz TA, Shih Y-CT. Use of radiation therapy in the last 30 days of life among a large population-based cohort of elderly patients in the United States. Journal of Clinical Oncology, 2013;31:80-87.

Guertin DA, Sabatini DM. Defining the role of mTOR in cancer. Cancer Cell, 2007;12:9-22.

Guertin DA, Stevens DM, Saitoh M, Kinkel S, Crosby K, Sheen JH, Mullholland DJ, Magnuson MA, Wu H, Sabatini DM. mTOR complex 2 is required for the development of prostate cancer induced by Pten loss in mice. Cancer Cell, 2009;15(2):148-159.

Hall EJ, Giaccia AJ. Radiobiology for the Radiologist. Lippincott Williams and Wilkins 2006, 6(546):85-180.

Han B, Park D, Li R, Xie T, Owonikoko TK, Zhang G, Sica GL, Ding C, Zhou J, Magis AT, Chen ZG, Shin DM, Ramalingam SS, Khuri FR, Curran WJ, Deng X. Small-molecule Bcl-2 BH4 antagonist for lung cancer therapy. Cancer Cell, 2015;27(6):852-863.

Hanahan D, Weinberg RA. Hallmarks of cancer: The next generation. Cell, 2011;144:646-674.

Hanahan D, Weinberg RA. The hallmarks of cancer. Cell, 2000;100:57-70.

Hamunyela RH, Serafin AM, Akudugu JM. Strong synergism between small molecule inhibitors of HER2 , PI3K , mTOR and Bcl-2 in human breast cancer cells. Toxicology In Vitro, 2017;38:117-123.

Hamunyela R, Serafin A, Hamid MB, Maleka S, Achel D, Akudugu J. A cocktail of specific inhibitors of HER-2, PI3K, and mTOR radiosensitises human breast cancer cells. Gratis Journal of Cancer Biology and Therapeutics, 2015;1(1):46-56.

Harachi M, Masui K, Okamura Y, Tsukui R, Mischel PS, Shibata N. mTOR complexes as a nutrient sensor for driving cancer progression. International Journal of Molecular Sciences, 2018;19(10):3267.

Harandi A, Zaidi AS, Stocker AM, Laber DA. Clinical efficacy and toxicity of anti-EGFR therapy in common cancers. Journal of Oncology, 2009;1-14.

Haricharan S, Li Y. STAT signaling in mammary gland differentiation, cell survival and tumorigenesis. Molecular and Cellular Endocrinology, 2014;382:560-569.

Hashmi AA, Aijaz S, Khan SM, Mahboob R, Irfan M, Zafar NI, Nisar M, Siddiqui M, Edhi MM, Faridi N, Khan A. Prognostic parameters of luminal A and luminal B intrinsic breast cancer subtypes of Pakistani patients. World Journal of Surgical Oncology, 2018;16(1):1.

Heller DP, Raaphorst GP. Inhibition of potentially lethal damage recovery by altered pH, glucose utilization and proliferation in plateau growth phase human glioma cells. International Journal of Radiation Biology, 1993;66(1):41-47.

Hengartner O. The biochemistry of apoptosis. Nature, 2000;407:770-776.

Higashiyama S, Iwabuki H, Morimoto C, Hieda M, Inoue H, Matsushita N. Membrane-anchored growth factors, the epidermal growth factor family: beyond receptor ligands. Cancer Science, 2008;99:214-220.

Higgins MJ, Baselga J. Targeted therapies for breast cancer. The Journal of Clinical Investigation, 2011;121:3797-3802.

Huang L, Fu L. Mechanisms of resistance to EGFR tyrosine kinase inhibitors. Acta Pharmaceutica Sinica B. 2005;5(5):390-401.

Huang SM, Harari PM. Modulation of radiation response after epidermal growth factor receptor blockade in squamous cell carcinomas: inhibition of damage repair, cell cycle kinetics, and tumor angiogenesis. Clinical Cancer Research, 2000;6:2166-2174.

Hudson CC, Liu M, Chiang GG, Otterness DM, Loomis DC, Kaper F, Giaccia AJ, Abraham RT. Regulation of hypoxia-inducible factor 1alpha expression and function by the mammalian target of rapamycin. Molecular and Cell Biology, 2002;22(20):7004-7014.

Huffman TA, Mothe-Satney I, Lawrence Jr JC. Insulin-stimulated phosphorylation of lipin mediated by the mammalian target of rapamycin. Proceedings of the National Academy of Sciences of the United States of America, 2002;99(2):1047-1052.

Hurvitz AA, Hu Y, O'Brien N, Finn RS. Current approaches and future directions in the treatment of HER2-positive breast cancer. Cancer Treatment Reviews, 2013;9:219-229.

Hutchinson F. The molecular basis for radiation effects on cells. Cancer Research, 1966;26:2045-2052.

Indran IR, Tufo G, Pervaiz S, Brenner C. Recent advances in apoptosis, mitochondria and drug resistance in cancer cells. Biochimica et Biophysica Acta (BBA)-Bioenergetics, 2011;1807(6):735-745.

Jacinto E, Loewith R, Schmidt A, Lin S, Ruegg MA, Hall A, Hall MN. Mammalian TOR complex 2 controls the actin cytoskeleton and is rapamycin insensitive. Nature Cell Biology, 2004;6(11):1122-1128.

Jaramillo ML, Banville M, Collins C, Paul-Roc B, Bourget L, O'Connor-McCourt M. Differential sensitivity of A549 non-small lung carcinoma cell responses to epidermal growth factor receptor pathway inhibitors. Cancer Biology and Therapy, 2008;7(4):557-568.

Jaramillo ML, Leon Z, Grothe S, Paul-Roc B, Abulrob A, O'Connor McCourt M. Effect of the anti-receptor ligand-blocking 225 monoclonal antibody on EGF receptor endocytosis and sorting. Experimental cell research 2006; 312:2778-90.

Jemal A, Bray F, Center M, Ferlay J, Ward E, Forman D. Global cancer statistics. CA: A Cancer Journal for Clinicians, 2011, 61:69-90.

Jiang X, Wang X. Cytochrome C-mediated apoptosis. Annual Review of Biochemistry, 2004;73:87-106.

Jin H, Kang GY, Jeon S, Kim JM, Park YN, Cho J, Lee YS. Identification of molecular signatures involved in radiation-induced lung fibrosis. Journal of Molecular Medicine, 2019;97(1):37-74.

Jonathan EC, Bernhard EJ, McKenna WG. How does radiation kill cells? Current Opinion in Chemical Biology, 1999;3:77-83.

Kabakov AE, Kudryavtsev VA, Gabai VL. Hsp90 inhibitors as promising agents for radiotherapy. Journal of Molecular Medicine, 2010;88:241-247.

Karrison TG, Ferguson DJ, Meier P. Dormancy of mammary carcinoma after mastectomy. Journal of the National Cancer Institute, 1999;91:80-85.

Kim HJ, Kim JH, Chie EK, Young PD, Kim IA, Kim IH. DNMT (DNA methyltransferase) inhibitors radiosensitize human cancer cells by suppressing DNA repair activity. Radiation Oncology, 2012;7:39.

Kondov B, Milenkovikj Z, Kondov G, Petrushevska G, Basheska N, Bogdanovska-Todorovska M, Tolevska N, Ivkovski L. Presentation of the molecular subtypes of breast cancer detected by immunohistochemistry in surgically treated patients. Open Access Macedonia Journal of Medical Sciences, 2018;6(6):961-967.

Korch C, Varella-Garcia M. Tackling the human cell line and tissue misidentification problem is needed for reproducible biomedical research. Advances in Molecular Pathology, 2018;1(1):209-264.e36

Krajewski S, Krajewska M, Ehrmann J, Sikorska M, Lach B, Chatten J, Reed JC. Immunohistochemical analysis of Bcl-2, Bcl-X, Mcl-1, and Bax in tumors of central and peripheral nervous system origin. The American Journal of Pathology, 1997;150(3):805-814.

Kralj M, Husnjak K, Körbler T, Paveli J. Endogenous p21WAF1/CIP1 status predicts the response of human tumor cells to wild-type p53 and p21WAF1/CIP1 overexpression. Cancer Gene Therapy, 2003;10:457-467.

Kumar A, Dangi V. Electromagnetic spectrum and its impact on human life. International Journal of All Research Education and Scientific Methods, 2016;4(8):67-72.

Kvinnsland Y, Stokke T, Aurlien E. Radioimmunotherapy with alpha-particle emitters: microdosimetry of cells with a heterogeneous antigen expression and with various diameters of cells and nuclei. Radiation Research, 2001;155:288-296.

Laplante M, Sabatini DM. mTOR signaling in growth control and disease. Cell, 2012;149:274-293.

Lee JH, Nan A. Combination drug delivery approaches in metastatic breast cancer. Journal of Drug Delivery, 2012;Article ID 915375:17 pages.

Leidy J, Khan A, Kandil D. Basal-like breast cancer; update on clinicopathologic, immunohistochemical, and molecular features. The Archives of Pathology and Laboratory Medicine, 2014;138:37-43.

Lemjabbar-Alaoui H, Hassan O, Yanga Y, Buchanan P. Lung cancer: biology and treatment options. Biochimica et Biophysica Acta, 2015;1856(2):189-210.

Lemmon MA, Schlessinger J. Cell signaling by receptor tyrosine kinases. Cell, 2010;141:1117-1134.

Levitzki A, Gazit A. Tyrosine kinase inhibition: an approach to drug development. Science, 1995;267:1782-1788.

Levkowitz G, Waterman H, Ettenberg SA, Katz M, Tsygankov AY, Alroy I, Lavi S, Iwai K, Reiss Y, Ciechanover A, Lipkowitz S, Yarden Y. Ubiquitn Ligase Activity and Tyrosine Phosphorylation Underlie Suppression of growth factor Signaling by c-Cbl/Sli-1. Molecular Cell, 1999;4:1029-1040.

Li JY, Li Y, Jin W, Yang Q, Shao ZM, Tian XS. ABT-737 Reverses the acquired radioresistance of breast cancer cells by targeting Bcl-2 and Bcl-xL. Journal of Experimental and Clinical Cancer Research, 2012;31(102):1-8.

Liang K, Lu Y, Jin W, Ang KK, Milas L, Fan Z. Sensitization of breast cancer cells to radiation by Trastuzumab. Molecular Cancer Therapeutics, 2003;(2):1113-1120.

Liauw SL, Connell PP, Weichselbaum RR. New paradigms and future challenges in radiation oncology: an update of biological targets and technology. Science Translational Medicine, 2013;5:173sr2.

Lida K, Nakayama K, Rahman MT, Rahman M, Ishikawa M, Katagiri A, Yeasmin S, Otsuki Y, Kobayashi H, Nakayama S and Miyazaki K. EGFR gene amplification is related to adverse clinical outcomes in cervical squamous cell carcinoma, making the EGFR pathway a novel therapeutic target. British Journal of Cancer, 2011;105:420- 427.

Liu L, Zhu XD, Wang WQ, Shen Y, Qin Y, Ren ZG, Sun HC, Tang ZY. Activation of beta-catenin by hypoxia in hepatocellular carcinoma contributes to enhanced metastatic potential and poor prognosis. Clinical Cancer Research, 2010;16:2740-2750.

Liu P, Gan W, Chin YR, Ogura K, Guo J, Zhang J, Wang B, Blenis J, Cantley LC, Toker A, Su B, Wei W. PtdIns(3,4,5)P3-dependent activation of the mTORC2 kinase complex. Cancer Discovery, 2015;5(11):1194-1209.

Liu P, Cheng H, Roberts TM, Zhao JJ. Targeting the phosphoinositide 3-kinase pathway in cancer. Nature Reviews Drug Discovery, 2009;8:(8):627-644.

Liu X, Kim CN, Yang J, Jemmerson R, Wang X. Induction of apoptotic program in cell-free extracts: requirement for dATP and cytochrome C. Cell, 1996;86(1):147-157.

Lønning PE, Børresen-Dale AL, Brown PO, Botstein D. Molecular portraits of human breast tumours. Nature, 2000;406:747-752.

Lucey, BP, Nelson-Rees, WA, Hutchins GM. Henrietta Lacks, HeLa cells and cell culture contamination. Archives of Pathology and Laboratory Medicine, 2009;133:1463-1467.

Luk CK, Sutherland RM. Nutrient modification of proliferation and radiation response in EMT6/RO spheroids. International Journal of Radiation Oncology Biology Physics, 1987;13(6):885-895.

Madani SY, Naderi N, Dissanayake O, Tan, AS. A new era of cancer treatment: carbon nanotubes as drug delivery tools. International Journal of Nanomedicine, 2011;6:2963-2979.

Maier P, Hartmann L, Wenz F, Herskind C. Cellular pathways in response to ionizing radiation and their targetability for tumor radiosensitization. International Journal of Molecular Sciences, 2016;17(102):1-32.

Maira SM, Stauffer F, Brueggen J, Furet P, Schnell C, Fritsch C, Brachmann S, Chène P, De Pover A, Schoemaker K, Fabbro D, Gabriel D, Simone M, Murphy L, Finan P, Sellers W, García-Echeverría C. Identification and characterization of NVP-BEZ235, a new orally available dual phosphatidylinositol 3-kinase/mammalian target

of rapamycin inhibitor with potent in vivo antitumor activity. Molecular Cancer Therapy, 2008;7(7):1851-1863.

Majumder PK, Febbo PG, Bikoff R, Berger R, Xue Q, McMahon LM, Manola J, Brugarolas J, McDonnell TJ, Golub TR, Loda M, Lane HA, Sellers WR. mTOR inhibition reverses Akt-dependent prostate intraepithelial neoplasia through regulation of apoptotic and HIF-1-dependent pathways. Nature Medicine, 2004;10(6):594-601.

Maldonado V, Melendez-Zajgla J, Ortega A. Modulation of NF-κB, p53 and Bcl-2 in apoptosis induced by cisplatin in HeLa cells. Mutation Research, 1997;381:67-75.

Maleka S, Serafin AM, Akudugu JM. PI3K and mTOR inhibitor, NVP-BEZ235, is more toxic than X-rays in prostate cancer cells. International Journal of Radiation Research, 2019;17(1):37-45.

Maleka S, Serafin A, Hamunyela R, Hamid M, Achel D, Akudugu J. NVP-BEZ235 enhances radiosensitivity of human prostate cancer but acts as a radioprotector to normal prostate cells. Gratis Journal of Cancer Biology and Therapeutics, 2015;1(1):38-45.

Mangelberger D, Kern D, Loipetzberger A, Eberl M, Aberger F. Cooperative Hedgehog-EGFR signaling. Frontiers in Bioscience, 2012;17:90-99.

Manning BD, Cantley LC. Rheb fills a GAP between TSC and TOR. Trends in Biochemical Sciences, 2003;28(11):573-576.

Martinelli E, De Palma R, Orditura M. Anti-epidermal growth factor receptor monoclonal antibodies in cancer therapy. The Journal of Transitional Immunology, 2009; 158:1-9.

Martinez-Zapien D, Ruiz FX, Poirson J, Mitschler A, Ramirez-Ramos J, Forster A, Cousido-Siah A, Masson M, Vande Pol S, Podjarny A, Travé G, Zanier K. Structure of the E6/E6AP/p53 complex required for HPV-mediated degradation of p53. Nature, 2016;529(7587):541-545.

Masood S. Breast cancer subtypes: morphologic and biologic characterization. Women's Health, 2016;12(1):103-119.

Massague J and Pandiella A. Membrane-anchored growth factors. Annual Review of Biochemistry, 1993; 62:515:541

Mayer IA, Arteaga CL. The PI3K/AKT pathway as a target for cancer treatment. Annual Review of Medicine, 2016;67:11-28.

McDermott N, Meunier A, Mooney B, Nortey G, Hernandez C, Hurley S, Lynam-Lennon N, Barsoom SH, Bowman KJ, Marples B, Jones GDD, Marignol L. Fractionated radiation exposure amplifies the radioresistant nature of prostate cancer cells. Scientific Report, 2016; 6:34796. doi: 10.1038/srep34796

Meng XW, Lee SH, Kaufmann SH. Apoptosis in the treatment of cancer: a promise kept? Current Opinion in Cell Biology, 2006;18(6):668-676.

Metallo, CM and Vander Heiden, MG. Understanding metabolic regulation and it influence on the physiology. Molecular Cell, 2013;49(3):388-398.

Mestre-Escorihuela C, Rubio-Moscardo F, Richter JA, Siebert R, Climent J, Fresquet V, Beltran E, Agirre X, Marugan I, Marín M, Rosenwald A, Sugimoto KJ, Wheat LM, Karran EL, García JF, Sanchez L, Prosper F, Staudt LM, Pinkel D, Dyer MJ, Martinez-Climent JA. Homozygous deletions localize novel tumor suppressor genes in B-cell lymphomas. Blood, 2007;109(1):271-280.

Minn AJ, Rudin CM, Boise LH, Thompson CB. Expression of bcl-xL can confer a multidrug resistance phenotype. Blood, 1995;86:1903-1910.

Misra R, Acharya S, Sahoo SK. Cancer nanotechnology: application of nanotechnology in cancer therapy. Drug Discovery Today, 2012;15:842-850.

Moding EJ, Kastan MB, Kirsch DG. Strategies for optimizing the response of cancer and normal tissues to radiation. Nature Reviews Drug Discovery, 2013;12:526-542.

Modjtahedi H and Essapen S. Epidermal growth factor receptor inhibitors in cancer treatment: advances, challenges and opportunities. Anti-Cancer Drugs, 2009;20:851-855.

Moeller BJ, Dreher MR, Rabbani ZN, Schroeder T, Cao Y, Li CY, Dewhirst MW. Pleiotropic effects of HIF-1 blockade on tumor radiosensitivity. Cancer Cell, 2005;8:99-110.

Moldoveanu T, Follis AV, Kriwacki RW, Green DR. Many players in BCL-2 family Affairs. Trends in Biochemical Sciences, 2014;39(3):101-111.

Mohseni-Meybodi A, Mozdarani H, Mozdarani S. DNA damage and repair of leukocytes from Fanconi anaemia patients, carriers and healthy individuals as measured by the alkaline comet assay. Mutagenesis, 2009;24:67-73.

Mossmann D, Park S, Hall MN. mTOR signalling and cellular metabolism are mutual determinants in cancer. Nature Reviews Cancer, 2018;18(12):744-757.

Muir A, Danai LV, Gui DY, Waingarten CY, Lewis CA, Vander Heiden MG. Environmental cystine drives glutamine anaplerosis and sensitizes cancer cells to glutaminase inhibition. Elife, 2017;6:27713.

Naumov S, von Sonntag C. The energetics of rearrangement and water elimination reactions in the radiolysis of the DNA bases in aqueous solution (eaq- and *OH Attack): DFT calculations. Radiation Research, 2008;169:355-363

No M, Choi EJ, Kim IA. Targeting HER2 signaling pathway for radiosensitization. Cancer Biology and Therapy, 2009;24:2351-2361.

Nobes CD, Hall A. Rho GTPases control polarity, protrusion, and adhesion during cell movement. The Journal of Cell Biology, 1999;144(6):1235-1244.

Normanno N, Morabito A, De Luca A, Piccirillo MC, Gallo M, Maiello MR, Perrone F. Target-based therapies in breast cancer: current status and future perspectives. Endocrine-Related Cancer, 2009;16:675-702.

Normanno N, De Luca A, Bianco C, Strizzi L, Mancino M, Maiello MR, Carotenuto A, De Feo G, Caponigro F, Salomon DS. Epidermal growth factor receptor (EGFR) signaling in cancer. Gene, 2006;366:2-16.

Novaes FT, Cataneo DC, Ruiz Junior RL, Defaveri J, Michelin OC, Cataneo AJ. Lung cancer: histology, staging, treatment and survival. Jornal Brasileiro de Pneumologia, 2008;34(8):595-600.

Nyati MK, Morgan MA, Feng FY, Lawrence TS. Integration of EGFR inhibitors with radiochemotherapy. Nature Reviews Cancer, 2006;6:876-885.

Oda K, Matsuoka Y, Funahashi A, Kitano H. A comprehensive pathway map of epidermal growth factor receptor signaling. Molecular Systems Biology, 2005;1:2005.0010.

Olopade OI, Adeyanju MO, Safa AR, Hagos F, Mick R, Thompson CB, Recant WM. Overexpression of BCL-x protein in primary breast cancer is associated with high

tumor grade and nodal metastases. The Cancer Journal from Scientific America, 1997;3(4):230-237.

Ong F, Moonen LMF, Gallee MPW, ten Bosch C, Zerp SF, Hart AAM, Bartelink H, Verheij M. Prognostic factors in transitional cell cancer of the bladder: an emerging role for Bcl-2 and p53. Radiotherapy and Oncology, 2001;61(2):169-175.

Paine TM, Soule HD, Pauley RJ, Dawson PJ. Characterization of epithelial phenotypes in mortal and immortal human breast cells. International Journal of Cancer, 1992;50:463-473.

Pang E, Delic NC, Hong A, Zhang M, Rose BR, Lyons JG. Radiosensitization of oropharyngeal squamous cell carcinoma cells by human papillomavirus 16 oncoprotein E6*I. International Journal of Radiation Oncology, Biology, Physics, 2011;79(3):860-865.

Paquette M, El-Houjeiri L, Pause A. mTOR pathways in cancer and autophagy. Cancers, 2018;10(1):E18.

Park S, Koo JS, Kim MS, Park HS, Lee JS, Lee JS, Kim SI, Park BW. Characteristics and outcomes according to molecular subtypes of breast cancer as classified by a panel of biomarkers using immunohistochemistry. The Breast, 2012;21:50-57.

Parshad R, Sanford KK, Jones GM. Chromatid damage after G2 phase x-irradiation of cells from cancer-prone individuals implicates deficiency in DNA repair. Proceedings of the National Academy of Sciences of the United States of America, 1993;80:5612-5616.

Patruno A, Pesce M, Grilli A, Speranza L , Franceschelli S, De Lutiis MA, Vianale G, Costantini E, Amerio P, Muraro R, Felaco M, Reale M. mTOR Activation by PI3K/Akt and ERK Signaling in Short ELF-EMF Exposed Human Keratinocytes. PLoS ONE, 2015;10(10):e0139644.

Paul MK and Mukhopadhyay AK. Tyrosine Kinase - Role and the significance in cancer. International Journal of Medical Sciences, 2004;1(2):101-115.

Pearce AG, Sergura TM, Rintala-Maki AC, Lee H. The generation and characterization of a radiation-resistant model system to study radioresistance in human breast cancer cells. Radiation Research, 2001;175:739-750.

Pena JC, Thompson CB, Recant W, Vokes EE, Rudin CM: Bcl-xL and Bcl-2 expression in squamous cell carcinoma of the head and neck. Cancer, 1999;85:164-170.

Perou CM, Sorlie T, Eisen MB, van de Rijin M, Jeffrey SS, Rees CA, Pollack JR, Ross DT, Johnsen H, Akslen LA, Fluge O, Pergamenschikov A, Williams C, Zhu SX, van Diest PJ, van der Wall E, Baak JPA. Molecular portraits of human breast tumours. Nature, 2000; 406(6797):747-752.

Peterson RT, Desai BN, Hardwick JS, Schreiber SL. Protein phosphatase 2A interacts with the 70-kDa S6 kinase and is activated by inhibition of FKBP12-rapamycin associated protein. Proceedings of the National Academy of Sciences of the United States of America, 1999;96(8):4438-4442.

Peterson TR, Sengupta SS, Harris TE, Carmack AE, Kang SA, Balderas E, Guertin DA, Madden KL, Carpenter AE, Finck BN, Sabatini DM. mTOR complex 1 regulates lipin 1 localization to control the SREBP pathway. Cell, 2011;146:408-420.

Pezzella F, Turley H, Kuzu I, Tungekar MF, Dunnill MS, Pierce CB, Harris A, Gatter KC, Mason DY. Bcl-2 protein in non-small-cell lung carcinoma. The New England Journal of Medicine, 1993;329:690-694.

Pfitzenmaier J, Ellis WJ, Arfman EW, Hawley S, McLaughlin PO, Lange PH, Robert VL. Telomerase activity in disseminated prostate cancer cells. British Journal of Urology International, 2006;97:1309-1313.

Pines G, Köstler WJ, Yarden Y. Oncogenic mutant forms of EGFR: Lessons in signal transduction and targets for cancer therapy. FEBS Letters, 2010;584:2699-2706.

Pollycove M, Feinendegen LE. Radiation-induced versus endogenous DNA damage: Possible effect of inducible protective responses in mitigating endogenous damage. Human and Experimental Toxicology, 2003;22:290-306.

Porstmann T, Santos CR, Griffiths B, Cully M, Wu M, Leevers S, Griffiths JR, Chung YL, Schulze A. SREBP activity is regulated by mTORC1 and contributes to Akt-dependent cell growth. Cell Metabolism, 2008;8(3):224-236.

Pozo-Guisado E, Alvarez-Barrientos A Mulero-Navarro S, Santiago-Josefat B, Fernandez-Salguero PM. The antiproliferative activity of resveratrol results in apoptosis in MCF-7 but not in MDA-MB-231 human breast cancer cells: cell-specific alteration of the cell cycle. Biochemical Pharmacology, 2002;4(9):1375-1386.

Prise KM. New advances in radiation biology. Occupational Medicine (London), 2006;56:156-161.

Puri N, Salgia R. Synergism of EGFR and c-Met pathways, cross-talk and inhibition, in non-small cell lung cancer. Journal of Carcinogenesis, 2008;7:9.

Reece C, Kumar R, Nienow D, Nehra A. Extending the rationale of combination therapy to unresponsive erectile dysfunction. Reviews in Urology, 2007;9:197-206.

Reed JC, Miyashita T, Takayama S, Wang HG, Sato T, Krajewski S, Aimé-Sempé C, Bodrug S, Kitada S, Hanada M. BCL-2 family proteins: regulators of cell death involved in the pathogenesis of cancer and resistance to therapy. Journal of Cellular Biochemistry, 1996;60(1):23-32.

Renault TT, Chipuk JE. Death upon a kiss: mitochondrial outer membrane composition and organelle communication govern sensitivity to BAK/BAX-dependent apoptosis. Chemical and Biology, 2014;21:114-123.

Reisterer O, Tenzer A, Zingg D, Hofstetter B, Vuong V, Pruschy M, Bodis S. Novel radiosensitizers for locally advanced epithelial tumor: inhibition of the PI3K/Akt pathway survival pathway in tumor cells and in tumor-associated endothelial cells as a novel treatment strategy. International Journal of Radiation Oncology Biology Physics, 2004;58:361-368.

Rhee SG, Chang TS, Bae YS, Lee SR, Kang SW. Cellular regulation by hydrogen peroxide. Journal of American Society of Nephrology, 2003;14:S211-S215.

Rhee SG. Redox signaling: Hydrogen peroxide as intracellular messenger. Experimental and Molecular Medicine, 1999;31:53-59.

Rodemann HP, Blaese MA. Responses of normal cells to ionizing radiation. Seminars in Radiation Oncology, 2007;17:81-88.

Rodemann HP, Dittmann K, Toulany M. Radiation-induced EGFR-signaling and control of DNA-damage repair. The International Journal of Radiation Biology, 2007;83:781-791.

Roos WP, Binder A, Böhm L. Determination of the initial DNA damage and residual DNA damage remaining after 12 hours of repair in eleven cell lines at low doses of irradiation. International Journal of Radiation Biology, 2000;76(11):1493-1500.

Roos WP, Thomas AD, Kaina B. DNA damage and the balance between survival and death in cancer biology. Nature Reviews Cancer, 2016;16:20-30.

Roskoski R. The ErbB/HER family of protein-tyrosine kinases and cancer. Pharmacological Research, 2014;79:34-74.

Rycaj K, Tang DG. Cancer stem cells and radioresistance. International Journal of Radiation Biology, 2014;90:615-21.

Sahin U, Weskamp G, Kelly K, Zhou HM, Higashiyama S, Peschon J, Hartmann D, Saftig P, Blobel CP. Distinct roles for ADAM10 and ADAM17 in ectodomain shedding of six EGFR ligands. The Journal of Cell Biology, 2004;164(5):769-779.

Sarbassov DD, Ali SM, Kim DH, Guertin DA, Latek RR, Erdjument-Bromage H, Tempst P, Sabatini DM. Rictor, a novel binding partner of mTOR, defines a rapamycin-insensitive and raptor-independent pathway that regulates the cytoskeleton. Current Biology, 2004;14(14):1296-1302.

Saxton RA, Sabatini DM. mTOR signaling in growth, metabolism, and disease. Cell, 2017;169:361-371.

Schneider HJ, Sampson SA, Cunningham D, Norman AR, Andreyev, HJ, Tilsed JV, Clarke PA. Bcl-2 expression and response to chemotherapy in colorectal adenocarcinomas. British Journal of Cancer, 1997;75:427-431.

Shahidi M, Mozdarani H, Mueller WU. Radiosensitivity and repair kinetics of gamma irradiated leukocytes from sporadic prostate cancer patients and healthy individuals assessed by alkaline comet assay. Iranian Biomedical Journal, 2010;14:67-75.

Shahidi M, Mozdarani H, Bryant PE. Radiation sensitivity of leukocytes from healthy individuals and breast cancer patients as measured by the alkaline and neutral comet assay. Cancer Letters, 2007;257:263-273.

Shen Y, Zhang S, Huang X, Chen K, Shen J, Wang Z. Involvement of p53 mutation and mismatch repair proteins dysregulation in NNK-induced malignant transformation of human bronchial epithelial cells. BioMed Research International, 2014;1-12.

Sundarraj S, Ramar Thangam R, Mohanan V. Sujitha MV, Vimala K, Kannan S. Ligand-conjugated mesoporous silica nanorattles based on enzyme targeted prodrug delivery system for effective lung cancer therapy. Toxicology and Applied Pharmacology, 2014;275:232-243.

Shi Y, Peng XH, Li X, Luo GP, Wu MF. Neuroprotective role of dexmedetomidine pretreatment in cerebral ischemia injury via ADRA2A-mediated phosphorylation of ERK1/2 in adult rats. Experimental and Therapeutic Medicine, 2018;16:5201-5209.

Shin S, Cha HJ, Lee E-M, Lee S-J, Seo S-K, Jin H-O, Park I-C, Jin Y-W, An S. Alteration of miRNA profiles by ionizing radiation in A549 human non-small cell lung cancer cells. International Journal of Oncology, 2009;35:81-86.

Singh B, Carpenter G, Coffey RJ. EGF receptor ligands: Recent advances. F1000 Research, 2016;5(2270):1-11.

Singh AB, Harris RC. Autocrine, paracrine and juxtacrine signaling by EGFR ligands. Cell Signal, 2005;17:1183-1193.

Simonian PL, Grillot DA, Nunez G. Bcl-2 and Bcl-XL can differentially block chemotherapy-induced cell death. Blood, 1997;90:1208-1216.

Sousa LP, Lax I, Shen H, Ferguson SM, De Camilli P, Schlessinger J. Suppression of EGFR endocytosis by dynamin depletion reveals that EGFR signaling occurs primarily at the plasma membrane. Proceedings of the National Academy of Sciences of the United States of America, 2012;109(12):4419-4424.

Strasser A, Cory S, Adams JM. Deciphering the rules of programmed cell death to improve therapy of cancer and other diseases. The EMBO Journal, 2011;30:3667-3683.

Subik K, Lee JF, Baxter L, Strzepek T, Costello D, Crowley P, Xing L, Hung MC, Bonfiglio T, Hicks DG, Tang P. The expression patterns of ER, PR, HER2, CK5/6,

EGFR, Ki-67 and AR by immunohistochemical analysis in breast cancer cell lines. Breast Cancer: Basic and Clinical Research, 2010;4:35-41.

Sweeny MF, Sonnenschein C, Soto AM. Characterization of MCF-12A cell phenotype, response to estrogens, and growth in 3D. Cancer Cell International, 2018;18(43):1-12.

Synnott NC, Murray A, McGowan PM, Kiely M, Kiely PA, O'Donovan N, O'Connor DP, Gallagher WM, Crown J, Duffy MJ. Mutant p53: a novel target for the treatment of patients with triple-negative breast cancer? International Journal of Cancer, 2017;140:234-246.

Tang L, Wei F, Wu Y, He Y, Shi L, Xiong F, Gong Z, Guo C, Li X, Deng H, Cao K, Zhou M, Xiang B, Li X, Li Y, Li G, Xiong W, Zeng Z. Role of metabolism in cancer cell radioresistance and radiosensitization methods. Journal of Experimental and Clinical Cancer research, 2018;37(87):1-15.

Takeyama N, Tanaka T, Yabuki T, Nakatani T. The involvement of p53 in paraquat-induced apoptosis in human lung epithelial-like cells. International Journal of Toxicology, 2004;23:33-40.

Taylor RC, Cullen SP, Martin SJ. Apoptosis: controlled demolition at the cellular level. Nature Reviews Molecular Cell Biology, 2008;9(3):231-241.

Thomanetz, V, Angliker N, Cloetta D, Lustenberger RM, Schweighauser M, Oliveri F, Suzuki N, Ruegg MA. Ablation of the mTORC2 component rictor in brain or Purkinje cells affects size and neuron morphology. The Journal of Cell Biology, 2013;201(2):293-308.

Thorpe LM, Yuzugullu H, Zhao JJ. PI3K in cancer: Divergent roles of isoforms, modes of activation and therapeutic targeting. Nature Reviews Cancer, 2015;15:7-24.

Toulany M, Baumann M, Rodemann HP. Stimulated PI3K-Akt signaling mediated through ligand or radiation-induced EGFR depends indirectly, but not directly, on constitutive K-Ras activity. Molecular Cancer Research, 2007;5(8):863-872.

Toulany M, Rodemann HP. Potential of Akt mediated DNA repair in radioresistance of solid tumors overexpressing erbB-PI3K-Akt pathway. Translational Cancer Research, 2013;2:190-202.

Trask DK, Wolf GT, Bradford CR, Fisher SG, Devaney K, Johnson M, Singleton T, Wicha M. Expression of Bcl-2 family proteins in advanced laryngeal squamous cell carcinoma: correlation with response to chemotherapy and organ preservation. Laryngoscope, 2002;112:638-644.

Tse C, Shoemaker AR, Adickes J, Anderson MG, Chen J, Jin S, Johnson EF, Marsh KC, Mitten MJ, Nimmer P, Roberts L, Tahir SK, Xiao Y, Yang X, Zhang H, Fesik S,

Rosenberg SH, Elmore SW. ABT-263: a potent and orally bioavailable Bcl-2 family inhibitor. Cancer, 2008;68(9):3421-3428.

Turgeon M, Perry NJS, Poulogiannis G. DNA Damage, Repair, and Cancer Metabolism. Frontiers in Oncology, 2018;8(15):1-8.

Uberall I, Kolar Z, Trojanec R, Berkovcova J, Hajduch M: The status and role of ErbB receptors in human cancer. Experimental and Molecular Pathway, 2008, 84, 79-89.

Vallejos CS, Gómez HL, Cruz WR, Pinto JA, Dyer RR, Velarde R, Suazo JF, Neciosup SP, León M, de la Cruz MA, Vigil CE. Breast cancer classification according to immunohistochemistry markers: subtypes and association with clinicopathologic variables in a peruvian hospital database. Clinical Breast Cancer, 2010;10(4):294-300.

van Delft MF, Huang DC. How the Bcl-2 family of proteins interact to regulate apoptosis. Cell Research, 2006;16(2):203-213.

van Diest PJ, van der Wall E, Baak JP .Prognostic value of proliferation in invasive breast cancer: a review. Journal of Clinical Pathology, 2004;57(7):675-681.

Vasudevan KM, Barbie DA, Davies MA, Rabinovsky R, McNear CJ, Kim JJ, Hennessy BT, Tseng H, Pochanard P, Kim SY, Dunn IF, Anna C. Schinzel AC, Sandy P, Hoersch S, Sheng Q, Gupta PB, Boehm JS, Reiling JH, Silver S, Lu Y, Stemke-Hale K, Dutta B, Joy C, Sahin AA, Gonzalez-Angulo AM, Lluch A, Rameh

LE, Jacks T, Root DE, Lander ES, Mills GB, Hahn WC, Sellers WR, Garraway LA. AKT-independent signaling downstream of oncogenic PIK3CA mutations in human cancer. Cancer Cell, 2009;16:21-32.

Verheye-Dua F, Böhm L. Na^+, K^+-ATPase inhibitor, ouabain accentuates irradiation damage in human tumour cell lines. Radiation Oncology Investigations, 1998;6:109-119.

Vozenin MC, Lord HK, Hartl D, Deutsch E. Unraveling the biology of human papillomavirus (HPV) related tumours to enhance their radiosensitivity. Cancer Treatment Reviews, 2010;36(8):629-636.

Wang C, Youle RJ. The role of mitochondria in apoptosis. Annual Review of Genetics, 2009;43:95-118.

Wang H, Jiang H, Van De Gucht M, Ridder M. Hypoxic Radioresistance: Can ROS be the key to overcome it?.Cancers(Basel), 2019;11(112):1-23.

Wang Q, Chen X, Wang Z. Dimerization drives EGFR endocytosis through two sets of compatible endocytic codes. Journal of Cell Science, 2015;128:935-950.

Weckermann D, Müller P, Wawroschek F, Harzmann R, Riethmüller G, Schlimok G. Disseminated cytokeratin positive tumor cells in the bone marrow of patients with prostate cancer: detection and prognostic value. Journal of Urology, 2001;166:699-703.

Weigelt B, Mackay A, A'hern R, Natrajan R, Tan DS, Dowsett M, Ashworth A, Rei-Filho JS. Breast cancer molecular profiling with single sample predictors: a retrospective analysis. Lancet Oncology, 2010;11: 339-349.

Wellen KE, Thompson CB. Cellular metabolic stress: considering how cells respond to nutrient excess. Molecular Cell, 2010;40(2):323-332.

White E. The role for autophagy in cancer. The Journal of Clinical Investigation, 2015;125(1):42-46.

Whitman M, Downes CP, Keeler M, Keller T, Cantley L. Type I phosphatidylinositol kinase makes a novel inositol phospholipid, phosphatidylinositol-3-phosphate. Nature, 1988;332(6165):644-666.

Wouters A, Pauwels B, Lardon F, Pattyn GG, Lambrechts HAJ, Baay M, Meijnders P, Vermorken JB. In vitro study on the schedule-dependency of the interaction between pemetrexed, gemcitabine and irradiation in non-small cell lung cancer and head and neck cancer cells. BioMed Central Cancer, 2010; 10(441):1-12.

Wullschleger S, Loewith R, Hall MN. TOR signaling in growth and metabolism. Cell, 2006;124(3):471-484.

Yamagata K, Izawa Y, Onodero D, Tagami M. Chlorogenic acid regulates apoptosis and stem cell marker-related gene expression in A549 human lung cancer cells. Molecular Cell Biochemistry, 2018;441:9-19.

Yersal O, Barutca S. Biological subtypes of breast cancer: Prognostic and therapeutic implications. World Journal of Clinical Oncology, 2014;5(3):412-423.

Yokogami K, Wakisaka S, Avruch J, Reeves SA. Serine phosphorylation and maximal activation of STAT3 during CNTF signaling is mediated by the rapamycin target mTOR. Current Biology, 2000;10(1):47-50.

Yoon YH, Hwang HJ, Sung HJ, Heo SH, Kim DS, Hong SH, Lee KH, Cho JY. Upregulation of complement factor H by SOCS-1/3-STAT4 in lung cancer. Cancers, 2019;11(471):1-16.

Youlden DR, Cramb SM, Baade PD. The international epidemiology of lung cancer: geographical distribution and secular trends. Journal of Thoracic Oncology, 2008;3(8):819-31.

Zagozdzon R, Gallagher WM, Crown J. Truncated HER2: implications for HER2-targeted therapeutics. Drug Discovery Today, 2011;16(17-18):810-816.

Zhang H, Bajraszewski N, Wu E, Wang H, Moseman AP, Dabora SL, Griffin JD, Kwiatkowski DJ. PDGFRs are critical for PI3K/Akt activation and negatively regulated by mTOR. The Journal of Clinical Investigation, 2007;117(3):730-738.

Zhang F, Wang S, Yin L, Yang Y, Guan Y, Wang W, Xu H,Tao N. Quantification of epidermal growth factor receptor expression level and binding kinetics on cell surfaces by surface plasmon resonance imaging. Analytical Chemistry, 2015;87(19):9960-9965.

Zhao L, Vogt PK. Class I PI3K in oncogenic cellular transformation. Oncogene, 2008;27(41):5486-5496.

Appendix A: Publications

Published Abstracts

1. Hamid MB, Serafin AM, Akudugu JM. Evaluation of the biological effectiveness of X-ray irradiation and epidermal growth factor receptor inhibition. *Physica Medica: Eur J Med Phys* 41: S9, 2017; DOI:10.1016/S1120-1797(17)30294-6

Conference Contributions

1. Hamid MB, Serafin AM, Akudugu JM. Changes in metabolic activity of cancer and normal cells after X-ray irradiation and inhibitor treatment. 63rd Academic Year Day, Faculty of Medicine and Health Sciences, University of Stellenbosch, Tygerberg, South Africa, August 2019 (oral).
2. Hamid MB, Serafin AM, Akudugu JM. Evaluating the metabolic activity of cancer and normal cells after X-ray irradiation and inhibitor treatment. 62nd Academic Year Day, Faculty of Medicine and Health Sciences, University of Stellenbosch, Tygerberg, South Africa, August 2018 (oral).
3. Hamid MB, Serafin AM, Akudugu JM. Evaluation of the biological effectiveness of X-ray irradiation and epidermal growth factor receptor inhibition. SAAPMB Congress, Durban, South Africa, September 2017 (oral).
4. Hamid MB, Serafin AM, Akudugu JM. Evaluation of the biological effectiveness of X-ray irradiation and epidermal growth factor receptor inhibition. 61st Academic Year Day, Faculty of Medicine and Health Sciences, University of Stellenbosch, Tygerberg, South Africa, August 2017 (oral).

5. Hamid MB, Serafin AM, Akudugu JM. Evaluation of the biological effectiveness of X-ray irradiation and epidermal growth factor receptor inhibition. 18th SASMO/SASCRO Congress, Johannesburg, South Africa, August 2017 (oral).
6. Hamid MB, Serafin AM, Akudugu JM. EGFR targeting in triple negative breast cancer. 60th Academic Year Day, Faculty of Medicine and Health Sciences, University of Stellenbosch, Tygerberg, South Africa, August 2016 (oral).
7. Hamid MB, Serafin AM, Hamunyela RH, Maleka S, Achel DG, Akudugu JM. Radiosensitisation of low HER-2 expressing human breast cancer cell lines. 17th SASMO/SASCRO Congress, Cape Town, South Africa, August 2015 (poster).

Appendix B: Ethics Letter

UNIVERSITEIT
STELLENBOSCH
UNIVERSITY

Approval Notice

New Application

16/04/2019

Project ID :7238

HREC Reference #: X19/02/003

Title: Novel treatment strategies for cancers of the breast, lung and cervix.

Dear Mr. Mogammad Hamid,

The **New Application** received on 13/02/2019 08:35 was reviewed by members of **Health Research Ethics Committee 2 (HREC2)** via **expedited** review procedures on 16/04/2019 and was approved.

Please note the following information about your approved research protocol:

Protocol Approval Period: This project has approval for 12 months from the date of this letter.

Please remember to use your **Project ID [7238]** on any documents or correspondence with the HREC concerning your research protocol.

Please note that the HREC has the prerogative and authority to ask further questions, seek additional information, require further modifications, or monitor the conduct of your research and the consent process.

After Ethical Review

Please note you can submit your progress report through the online ethics application process, available at: Links Application Form Direct Link and the application should be submitted to the HREC before the year has expired. Please see *Forms and Instructions* on our HREC website (www.sun.ac.za/healthresearchethics) for guidance on how to submit a progress report.

The HREC will then consider the continuation of the project for a further year (if necessary). Annually a number of projects may be selected randomly for an external audit.

Provincial and City of Cape Town Approval

Please note that for research at a primary or secondary healthcare facility, permission must still be obtained from the relevant authorities (Western Cape Departement of Health and/or City Health) to conduct the research as stated in the protocol. Please consult the Western Cape Government website for access to the online Health Research Approval Process, see: https://www.westerncape.gov.za/general-publication/health-research-approval-process. Research that will be conducted at any tertiary academic institution requires approval from the relevant hospital manager. Ethics approval is required BEFORE approval can be obtained from these health authorities.

We wish you the best as you conduct your research.

For standard HREC forms and instructions, please visit: Forms and Instructions on our HREC website https://applyethics.sun.ac.za/ProjectView/Index/7238

If you have any questions or need further assistance, please contact the HREC office at 021 938 9677.

Yours sincerely,

Mr. Francis Masiye,

HREC Coordinator,

Health Research Ethics Committee 2 (HREC2).

National Health Research Ethics Council (NHREC) Registration Number:

REC-130408-012 (HREC1)•REC-230208-010 (HREC2)

Federal Wide Assurance Number: 00001372

The Health Research Ethics Committee (HREC) complies with the SA National Health Act No. 61 of 2003 as it pertains to health research. The HREC abides by the ethical norms and principles for research, established by the World Medical Association (2013). Declaration of Helsinki: Ethical Principles for Medical Research Involving Human Subjects;the South African Department of Health (2006). Guidelines for Good Practice in the Conduct of Clinical Trials with Human Participants in South Africa (2nd edition); as well as the Department of Health (2015). Ethics in Health Research: Principles, Processes and Structures (2nd edition).

The Health Research Ethics Committee reviews research involving human subjects conducted or supported by the Department of Health and Human Services, or other federal departments or agencies that apply the Federal Policy for the Protection of Human Subjects to such research (United States Code of Federal Regulations Title 45 Part 46); and/or clinical investigations regulated by the Food and Drug Administration (FDA) of the Department of Health and Human Services.